3/4.4.6 PRESSURE/TEMPERATURE LIMITS

REACTOR COOLANT SYSTEM

LIMITING CONDITION FOR OPERATION

3.4.6.1 The reactor coolant system temperature and reactor vessel pressure shall be limited in accordance with the limit lines shown on (1) Figure 3.4.6.1-1 for heatup by non-nuclear means, cooldown following a nuclear shutdown and low power PHYSICS TESTS; (2) Figure 3.4.6.1-2 for operations with a critical core other than low power PHYSICS TESTS; and (3) Figure 3.4.6.1-3 for inservice hydrostatic or leak testing, with:

a. A maximum heatup of 100°F in any one hour period, and

b. A maximum cooldown of 100°F in any one hour period.

APPLICABILITY: At all times.

ACTION:

With any of the above limits exceeded, restore the temperature and/or pressure to within the limits within 30 minutes; perform an engineering evaluation to determine the effects of the out-of-limit condition on the fracture toughness properties of the reactor coolant system; determine that the reactor coolant system remains acceptable for continued operations or be in at least HOT SHUTDOWN within 12 hours and in COLD SHUTDOWN within the next 24 hours.

SURVEILLANCE REQUIREMENTS

4.4.6.1.1 The reactor coolant system temperature and reactor vessel pressure shall be determined to be within the limits at least once per 30 minutes during system heatup, cooldown and inservice leak and hydrostatic testing operations.

4.4.6.1.2 The reactor coolant system temperature and reactor vessel pressure shall be determined to be to the right of the criticality limit line of Figure 3.4.6.1-2 within 15 minutes prior to the withdrawal of control rods to bring the reactor to criticality.

4.4.6.1.3 The reactor material irradiation surveillance specimens shall be removed and examined to determine changes in material properties, as required by 10 CFR 50, Appendix H. The results of these examinations shall be used to update Figures 3.4.6.1-1, 3.4.6.1-2 and 3.4.6.1-3.

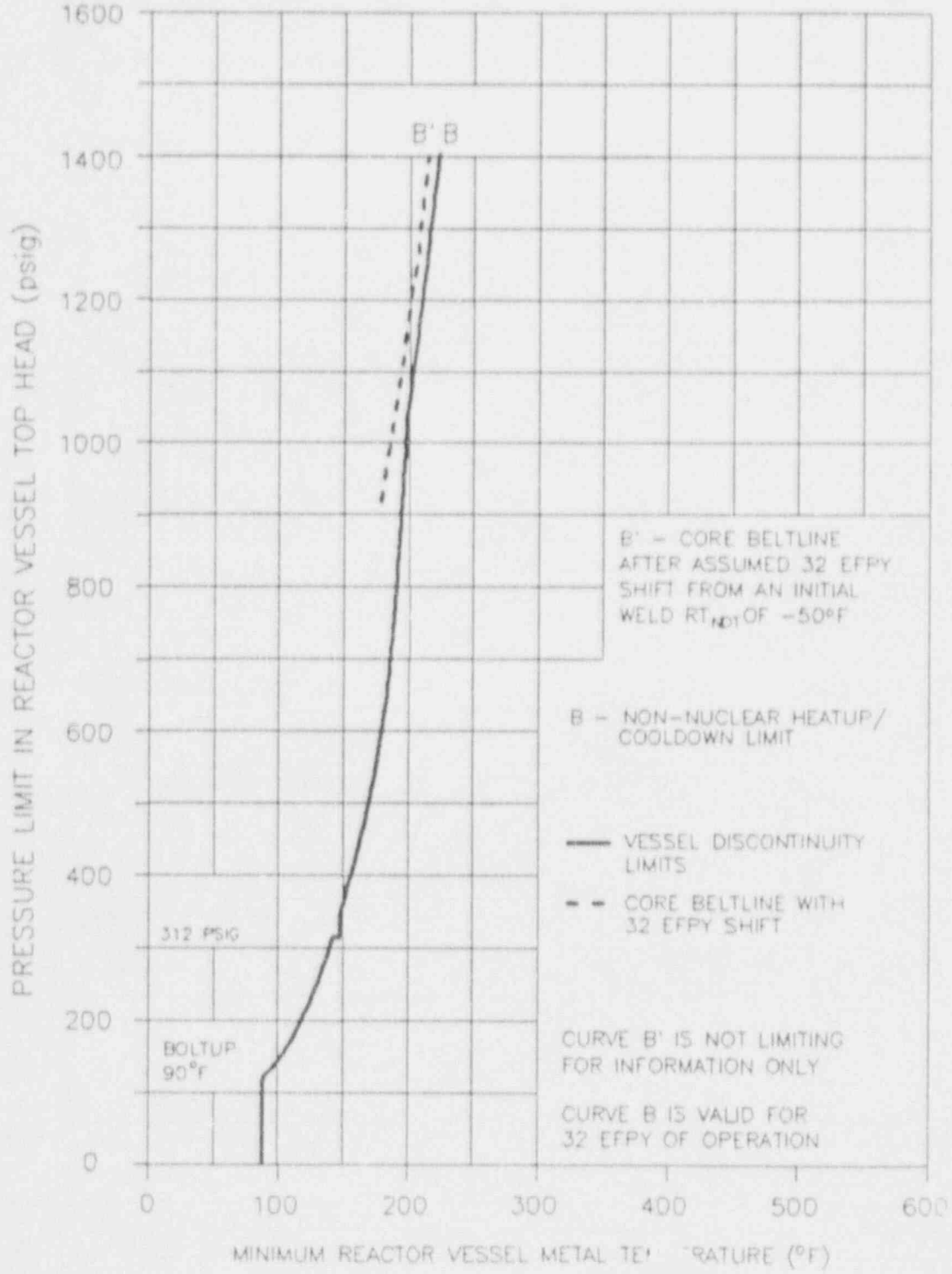

TEMPERATURE PRESSURE LIMITS FOR NON-NUCLEAR HEATUP, LOW POWER PHYSICS TESTS AND COOLDOWN FOLLOWING A SHUTDOWN
FIGURE 3.4.6.1-1

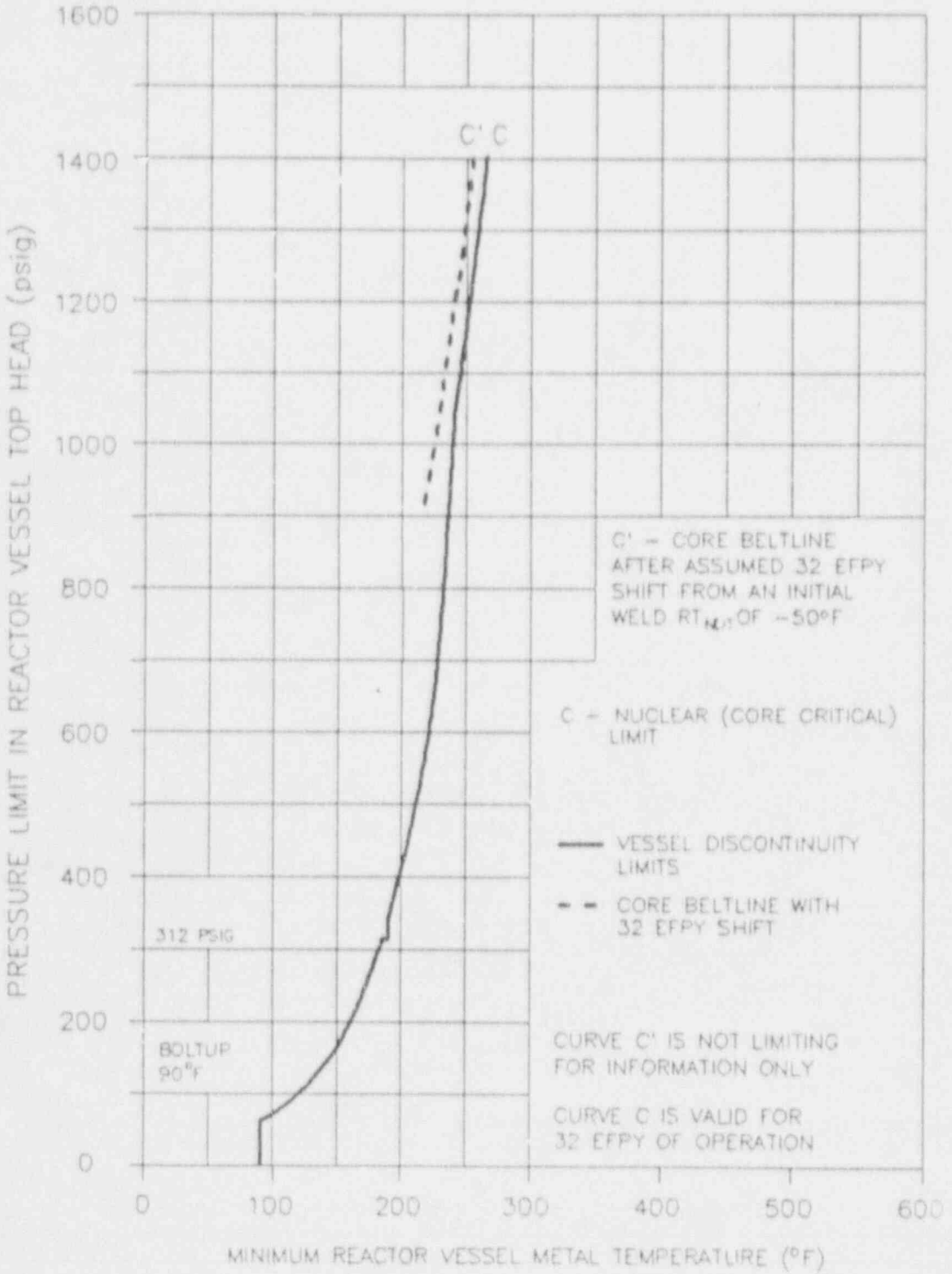

TEMPERATURE-PRESSURE LIMITS FOR CRITICALITY
(INCLUDES ADDITIONAL 40°F MARGIN
REQ'D BY 10CFR50, APP.G)
FIGURE 3.4.6.1-2

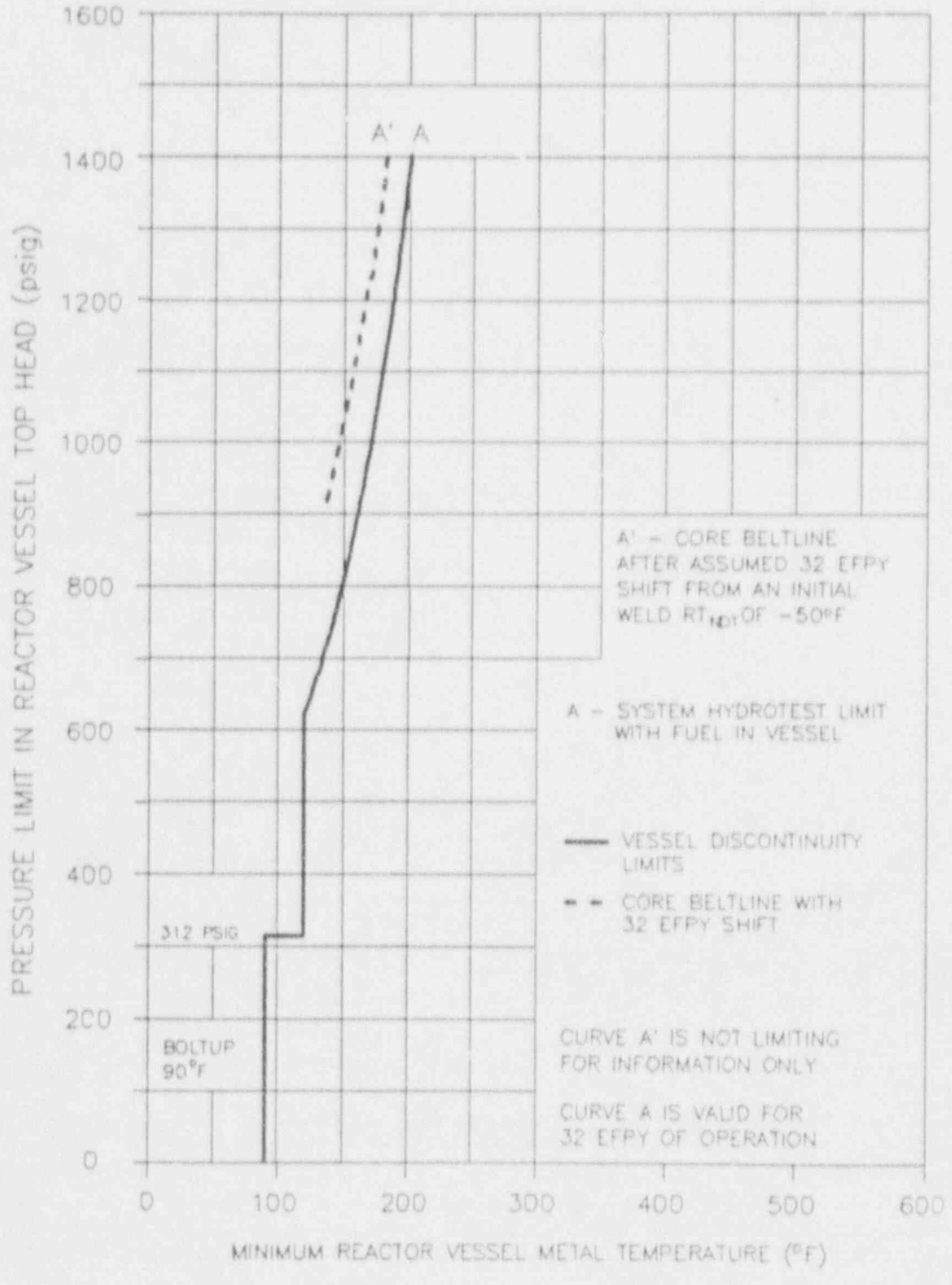

TEMPERATURE-PRESSURE LIMITS FOR
INSERVICE HYDROSTATIC TEST
FIGURE 3.4.6.1-3

TABLE 4.4.6.1.3-1

Deleted

3/4.4.6 PRESSURE/TEMPERATURE LIMITS

All components in the reactor coolant system are designed to withstand the effects of cyclic loads due to system temperature and pressure changes. These cyclic loads are introduced by normal load transients, reactor trips, and startup and shutdown operations. The various categories of load cycles used for design purposes are provided in Section 5.2 of the FSAR. During startup and shutdown, the rates of temperature and pressure changes are limited so that the maximum specified heatup and cooldown rates are consistent with the design assumptions and satisfy the stress limits for cyclic operation.

During heatup or cooldown, the thermal gradients in the reactor vessel wall produce thermal stresses. During heatup, the stresses are compressive in the inner wall and tensile in the outer wall. During cooldown, the opposite is the case. Thus, the one quarter of the material thickness (1/4 T) location is critical during cooldown and the 3/4 T location is critical during heatup. However, a conservative simplification is made by applying the absolute value of the thermal stress at the 1/4 T location, where the Reference Temperature-Nil-ductility temperature (RT_{NDT}) is the highest. In this manner, a single curve is generated for both the heatup and cooldown conditions.

The reactor vessel materials have been tested, and analyses performed to determine their initial RT_{NDT} values. Reactor operation and resultant fast neutron (E>1 MeV) irradiation will cause an increase in the RT_{NDT} values of the beltline materials. Adjusted reference temperatures, based upon the fluence, have been predicted using Regulatory Guide 1.99, Revision 2, and the beltline material test results. The adjusted reference temperature for the most limiting beltline material is plotted versus EFPY of operation in Bases Figure B 3/4.4.6-1. The pressure/temperature limit curves, shown in Figures 3.4.6.1-1 through 3.4.6.1-3, include predicted adjustments in RT_{NDT} for 32 EFPY of operation. Comparison with the nonbeltline curves shows the nonbeltline curves are limiting for 32 EFPY of operation.

During inservice hydrostatic or leak testing, Figure 3.4.6.1-1 is used for nonnuclear heatup until the test temperature is achieved. After the test temperature is reached, performance of the inservice hydrostatic or leak test is governed by Figure 3.4.6.1-3. After test completion, vessel cooldown is in accordance with Figure 3.4.6.1-1.

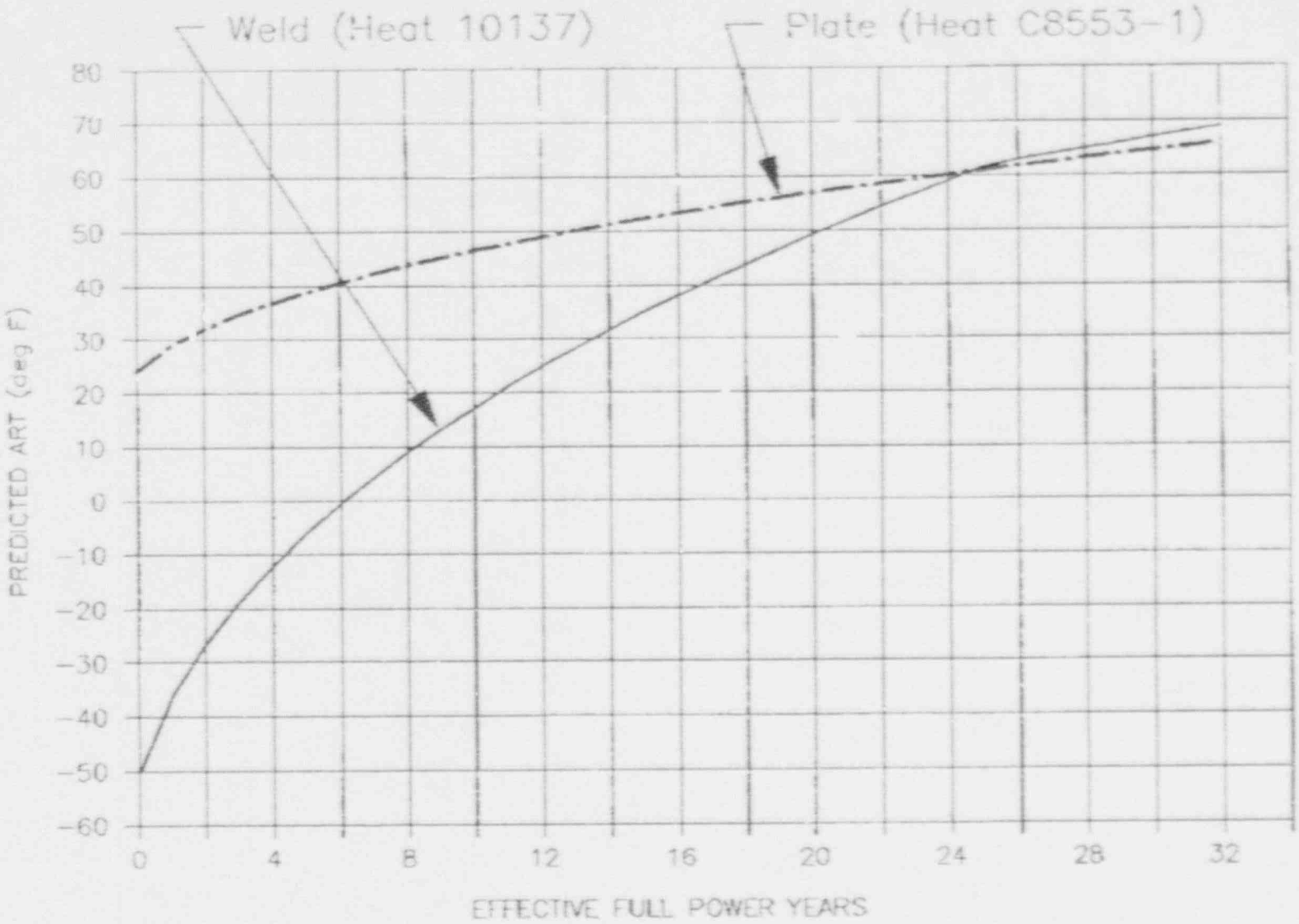

Bases Figure B 3/4.4.6-1
Adjusted Reference Temperature for Limiting Beltline Materials

PRESSURE/TEMPERATURE LIMITS (Continued)

The actual shift in RT_{NDT} of the vessel material will be established periodically during operation by removing and evaluating reactor vessel material irradiation surveillance specimens installed near the inside wall of the reactor vessel in the core area. Since the neutron spectra at the irradiation samples and vessel inside radius are essentially identical, the measured transition shift for a sample can be applied with confidence to the adjacent section of the reactor vessel. The heatup and cooldown curves must be recalculated when the ΔRT_{NDT} determined from the surveillance capsule is different from the calculated ΔRT_{NDT} for the equivalent capsule radiation exposure.

The pressure-temperature limit lines shown in Figures 3.4.6.1-2 and 3.4.6.1-3 for reactor criticality and for inservice leak and hydrostatic testing have been provided to assure compliance with the minimum temperature requirements of Appendix G to 10 CFR Part 50 for reactor criticality and for inservice leak and hydrostatic testing.

The number of reactor vessel irradiation surveillance specimens and the frequencies for removing and testing these specimens are provided in Unit 2 FSAR Section 5.2. The removal of the specimens meets the requirements of Appendix H to 10 CFR Part 50.

3/4.4.7 MAIN STEAM LINE ISOLATION VALVES

Double isolation valves are provided on each of the main steam lines to minimize the potential leakage paths from the containment in case of a line break. Only one valve in each line is required to maintain the integrity of the containment. The surveillance requirements are based on the operating history of this type valve. The maximum closure time has been selected to contain fission products and to ensure the core is not uncovered following line breaks.

3/4.4.8 STRUCTURAL INTEGRITY

The inspection programs for ASME Code Class 1, 2 and 3 components ensure that the structural integrity of these components will be maintained at an acceptable level throughout the life of the plant. To the extent applicable, the inspection program for these components is in compliance with Section XI of the ASME Boiler and Pressure Vessel Code.

Test pressures for inservice hydrostatic and leak testing required by the ASME B&PV Code, Section XI, are a function of testing temperature and component material. For the Hatch 1 reactor pressure vessel, the ISI hydrostatic test pressure would be approximately 1.1 times operating pressure, or about 1106 psig, depending on the reactor water temperature. The temperatures for pressures above 440 psig are determined by the RPV core beltline with a shift in RT_{NDT} of 123°F, appropriate for operation up to 16 effective full power years (EFPY).

Figure 3.6-2 provides appropriate limitations for plant heatup and cooldown when the reactor is not critical. Figure 3.6-2 is also applicable to low power physics tests. These curves assume heatup and cooldown rates up to 100°F per hour. Temperatures for pressures above 300 psig represent the limits of the RPV core beltline with a shift in RT_{NDT} of 123°F, appropriate for 16 EFPY of operation.

Figure 3.6-3 establishes operating limits when the core is critical. Figure 3.6-3 is not applicable to low power physics tests. These limits include a margin of 40°F as required by 10CFR50 Appendix G. In accordance with the May 1983 revision of 10CFR50 Appendix G, core critical operation may be initiated at temperatures at or above (RT_{NDT} + 60°F) of the closure flange region, or 76°F. Temperatures for pressures above 300 psig represent the limits of the RPV core beltline with a RT_{NDT} shift of 123°F, appropriate for 16 EFPY of operation.

During inservice hydrostatic or leak testing, Figure 3.6-2 is used for nonnuclear heatup until the test temperature is achieved. After the test temperature is reached, performance of the inservice hydrostatic or leak test is governed by Figure 3.6-1. After test completion, vessel cooldown is in accordance with Figure 3.6-2.

The fracture toughness of all ferritic steels gradually and uniformly decreases with exposure to fast neutrons above a threshold value, and it is prudent and conservative to account for this in the operation of the RPV. Two types of information are needed in this analysis: (a) a relationship between the change in fracture toughness of the RPV steel and the neutron fluence (integrated neutron flux); and (b) a measure of the neutron fluence at the point of interest in the RPV wall. A method of relating shift in RT_{NDT} to accumulated fast nuetron (>1 MeV) fluence is contained in Regulatory Guide 1.99, Revision 1. Experimental results of irradiated surveillance specimens taken from the RPV show a shift in RT_{NDT} greater than predicted by Regulatory Guide 1.99, so the surveillance results were used with the methods of 1.99 to establish the RT_{NDT} shift. The shift for 16 EFPY was added to the unirradiated RPV core beltline curves, resulting in the beltline being the limiting region in the vessel for higher pressure-temperature conditions.

REACTOR COOLANT SYSTEM

3/4.4.6 PRESSURE/TEMPERATURE LIMITS

REACTOR COOLANT SYSTEM

LIMITING CONDITION FOR OPERATION

3.4.6.1 The reactor coolant system temperature and reactor vessel pressure shall be limited in accordance with the limit lines shown on (1) Figure 3.4.6.1-1 for heatup by non-nuclear means, cooldown following a nuclear shutdown and low power PHYSICS TESTS; (2) Figure 3.4.6.1-2 for operations with a critical core other than low power PHYSICS TESTS; and (3) Figure 3.4.6.1-3 for inservice hydrostatic or leak testing, with:

a. A maximum heatup of 100°F in any one hour period, and

b. A maximum cooldown of 100°F in any one hour period.

APPLICABILITY: At all times.

ACTION:

With any of the above limits exceeded, restore the temperature and/or pressure to within the limits within 30 minutes; perform an engineering evaluation to determine the effects of the out-of-limit condition on the fracture toughness properties of the reactor coolant system; determine that the reactor coolant system remains acceptable for continued operations or be in at least HOT SHUTDOWN within 12 hours and in COLD SHUTDOWN within the next 24 hours.

SURVEILLANCE REQUIREMENTS

4.4.6.1.1 The reactor coolant system temperature and reactor vessel pressure shall be determined to be within the limits at least once per 30 minutes during system heatup, cooldown and inservice leak and hydrostatic testing operations.

4.4.6.1.2 The reactor coolant system temperature and reactor vessel pressure shall be determined to be to the right of the criticality limit line of Figure 3.4.6.1-2 within 15 minutes prior to the withdrawal of control rods to bring the reactor to criticality.

4.4.6.1.3 The reactor material irradiation surveillance specimens shall be removed and examined to determine changes in material properties ~~at the intervals shown in Table 4.4.6.1.3-1.~~ The results of these examinations shall be used to update Figures 3.4.6.1-1, 3.4.6.1-2 and 3.4.6.1-3.

, as required by 10 CFR 50, Appendix H.

REPLACE WITH NEW FIGURE
3.4.6.1-1

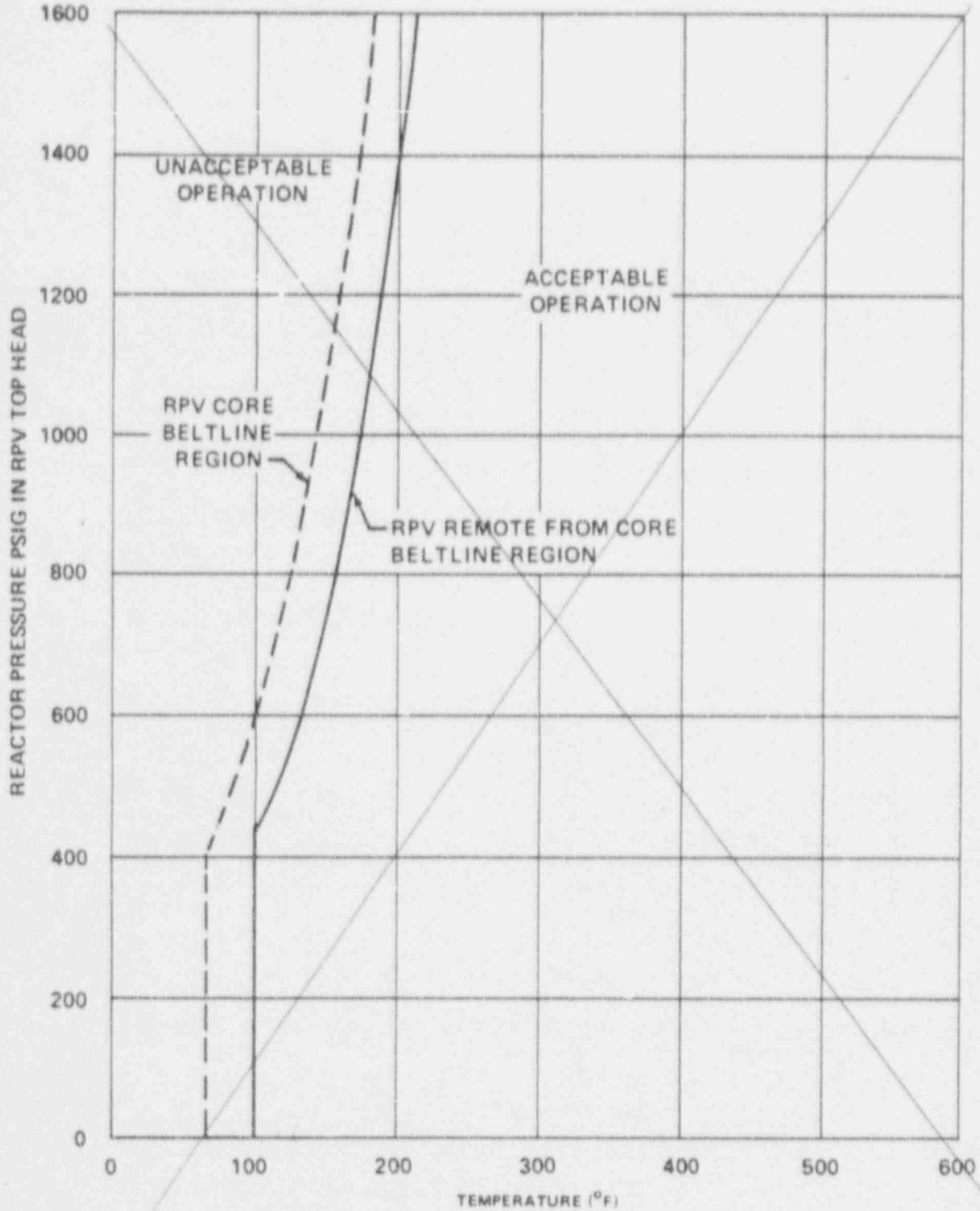

TEMPERATURE PRESSURE LIMITS FOR NON-NUCLEAR
HEATUP, LOW POWER PHYSICS TESTS AND
COOLDOWN FOLLOWING A SHUTDOWN
FIGURE 3.4.6.1-1

REPLACE WITH NEW FIGURE 3.4.6.1-2

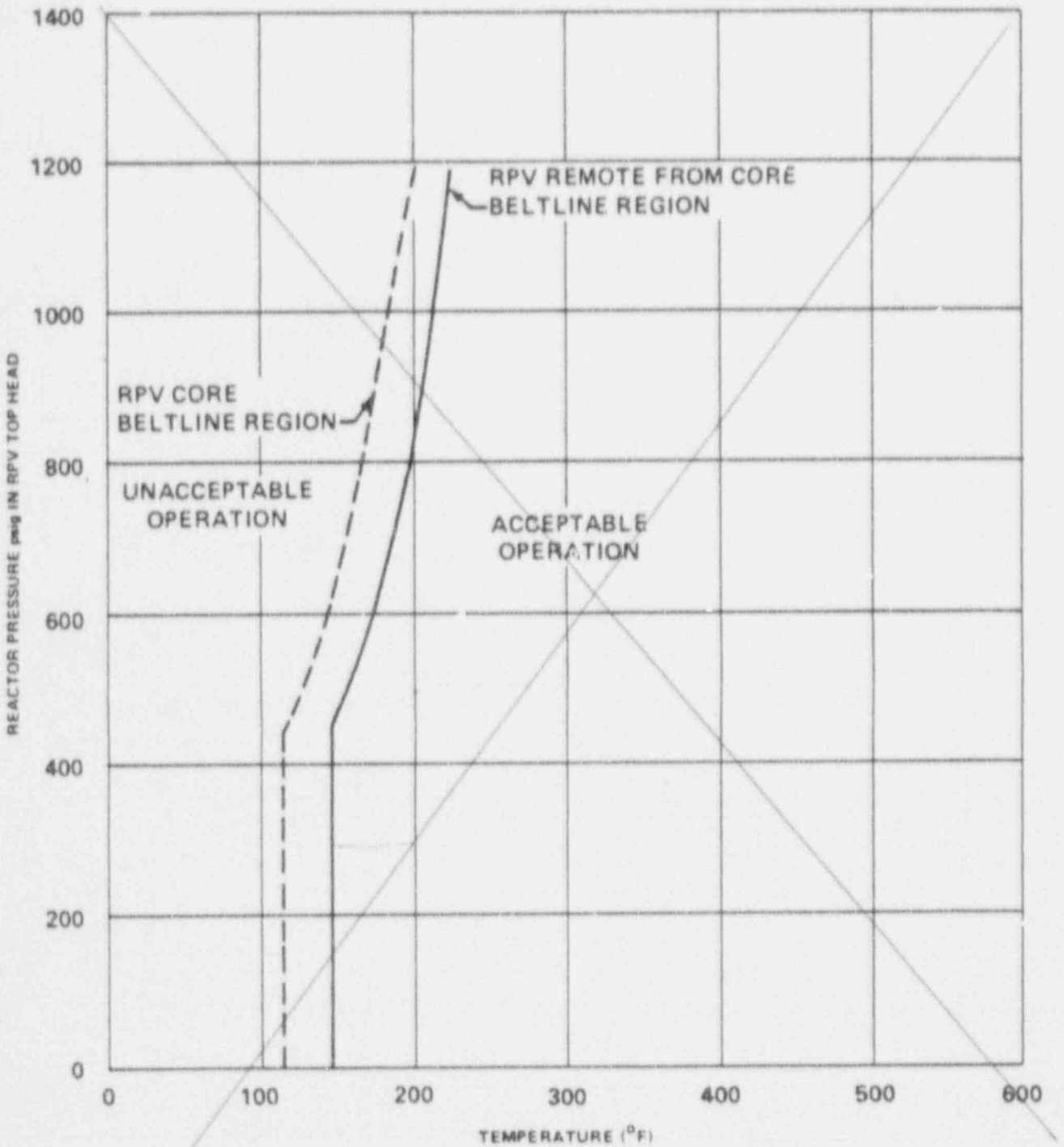

TEMPERATURE-PRESSURE LIMITS FOR CRITICALITY
(INCLUDES ADDITIONAL 40°F MARGIN
REQ'D BY 10CFR50, APP.G)
FIGURE 3.4.6.1-2

REPLACE WITH NEW FIGURE 3.4.6.1-3

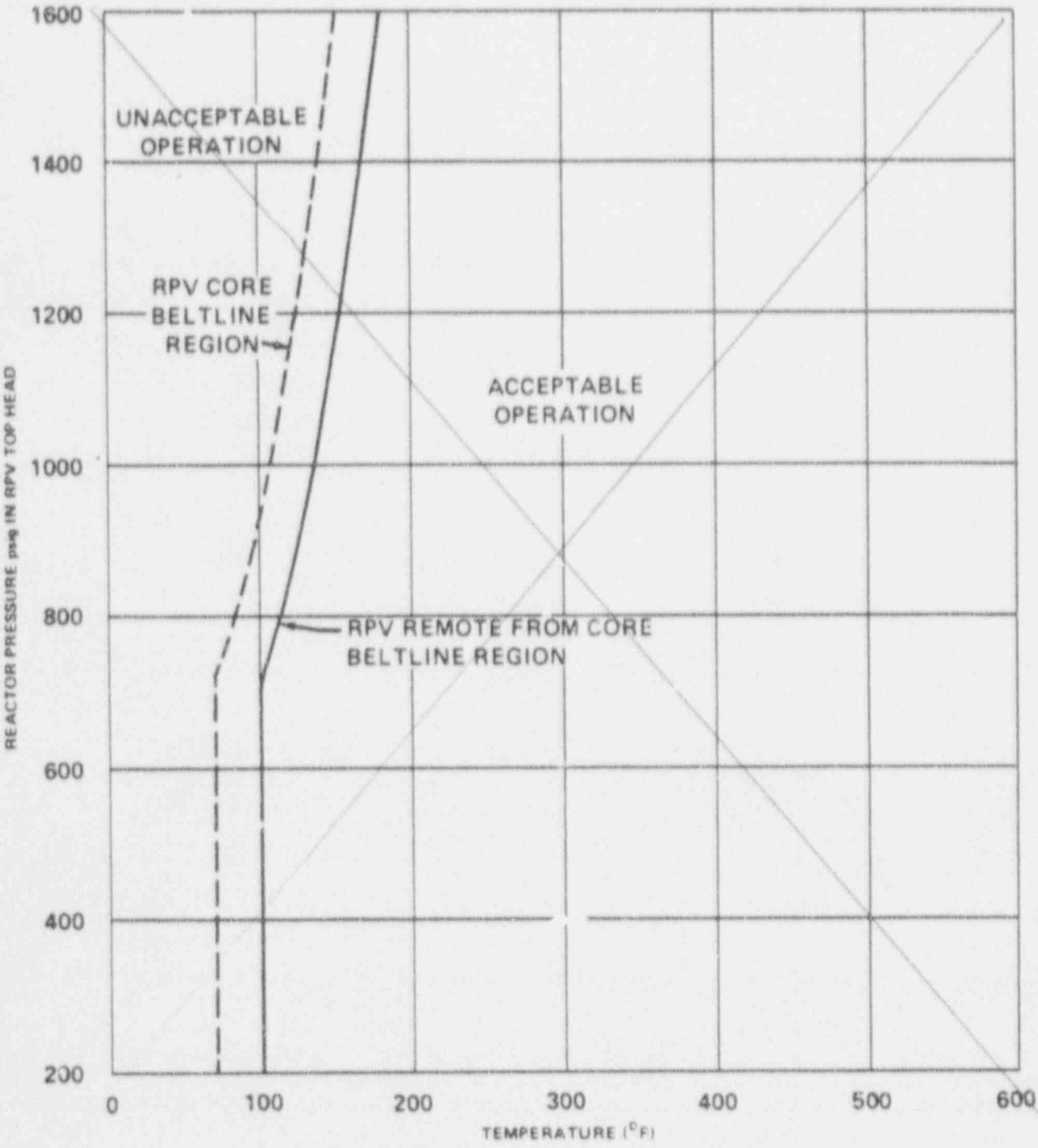

TEMPERATURE-PRESSURE LIMITS FOR
INSERVICE HYDROSTATIC TEST
FIGURE 3.4.6.1-3

TABLE 4.4.6.1.3-1

REACTOR VESSEL MATERIAL IRRADIATION SURVEILLANCE SCHEDULE

SPECIMEN	REMOVAL INTERVAL
1.	10 years
2.	30 years
3.	Reserve

Delete

3/4.4.6 PRESSURE/TEMPERATURE LIMITS

All components in the reactor coolant system are designed to withstand the effects of cyclic loads due to system temperature and pressure changes. These cyclic loads are introduced by normal load transients, reactor trips, and startup and shutdown operations. The various categories of load cycles used for design purposes are provided in Section 5.2 of the FSAR. During startup and shutdown, the rates of temperature and pressure changes are limited so that the maximum specified heatup and cooldown rates are consistent with the design assumptions and satisfy the stress limits for cyclic operation.

INSERT A

During heatup, the thermal gradients in the reactor vessel wall produce thermal stresses which vary from compressive at the inner wall to tensile at the outer wall. These thermal induced compressive stresses tend to alleviate the tensile stresses induced by the internal pressure. Therefore, a pressure-temperature curve based on steady state conditions, i.e., no thermal stresses, represents a lower bound of all similar curves for finite heatup rates when the inner wall of the vessel is treated as the governing locations.

The heatup analysis also covers the determination of pressure-temperature limitations for the case in which the outer wall of the vessel becomes the controlling location. The thermal gradients established during heatup produce tensile stresses which are already present. The thermal induced stresses at the outer wall of the vessel are tensile and are dependent on both the rate of heatup and the time along the heatup ramp; therefore, a lower bound curve similar to that described for the heatup of the inner wall cannot be defined. Subsequently, for the cases in which the outer wall of the vessel becomes the stress controlling location, each heatup rate of interest must be analyzed on an individual basis.

The reactor vessel materials have been tested to determine their initial RT_{NDT}. Reactor operation and resultant fast neutron, E>1 Mev, irradiation will cause an increase in the RT_{NDT}. Therefore, an adjusted reference temperature, based upon the fluence, can be predicted using the results of the reactor vessel materials tests and Bases Figure B 3/4 4.6.1. The pressure/temperature limit curve, Figure 3.4.6.1-1, includes predicted adjustments for this shift in RT_{NDT} at the end of 10 EFPY, as well as adjustments for possible errors in the pressure and temperature sensing instruments.

INSERT A

(TS PG B 3/4 4-4)

one quarter of the material thickness (1/4 T)

During heatup or cooldown, the thermal gradients in the reactor vessel wall produce thermal stresses. During heatup, the stresses are compressive in the inner wall and tensile in the outer wall. During cooldown, the opposite is the case. Thus, the ~~1/4 T~~ location is critical during cooldown and the 3/4 T location is critical during heatup. However, a conservative simplification is made by applying the absolute value of the thermal stress at the 1/4 T location, where the RT_{NDT} is the highest. In this manner, a single curve is generated for both the heatup and cooldown conditions.

reference temperature for ductility temperature

The reactor vessel materials have been tested, and analyses performed to determine their initial RT_{NDT} values. Reactor operation and resultant fast neutron (E>1 MeV) irradiation will cause an increase in the RT_{NDT} values of the beltline materials. Adjusted reference temperatures, based upon the fluence, have been predicted using Regulatory Guide 1.99, Revision 2, and the beltline material test results. The adjusted reference temperature for the most limiting beltline material is plotted versus EFPY of operation in Bases Figure B 3/4.4.6-1. The pressure/temperature limit curves, shown in Figures 3.4.6.1-1 through 3.4.6.1-3, include predicted adjustments in RT_{NDT} for 32 EFPY of operation. Comparison with the nonbeltline curves shows the nonbeltline curves are limiting for 32 EFPY of operation.

During inservice hydrostatic or leak testing, Figure 3.4.6.1-1 is used for nonnuclear heatup until the test temperature is achieved. After the test temperature is reached, performance of the inservice hydrostatic or leak test is governed by Figure 3.4.6.1-3. After test completion, vessel cooldown is in accordance with Figure 3.4.6.1-1.

REPLACE WITH NEW FIGURE B 3/4.4.6-1

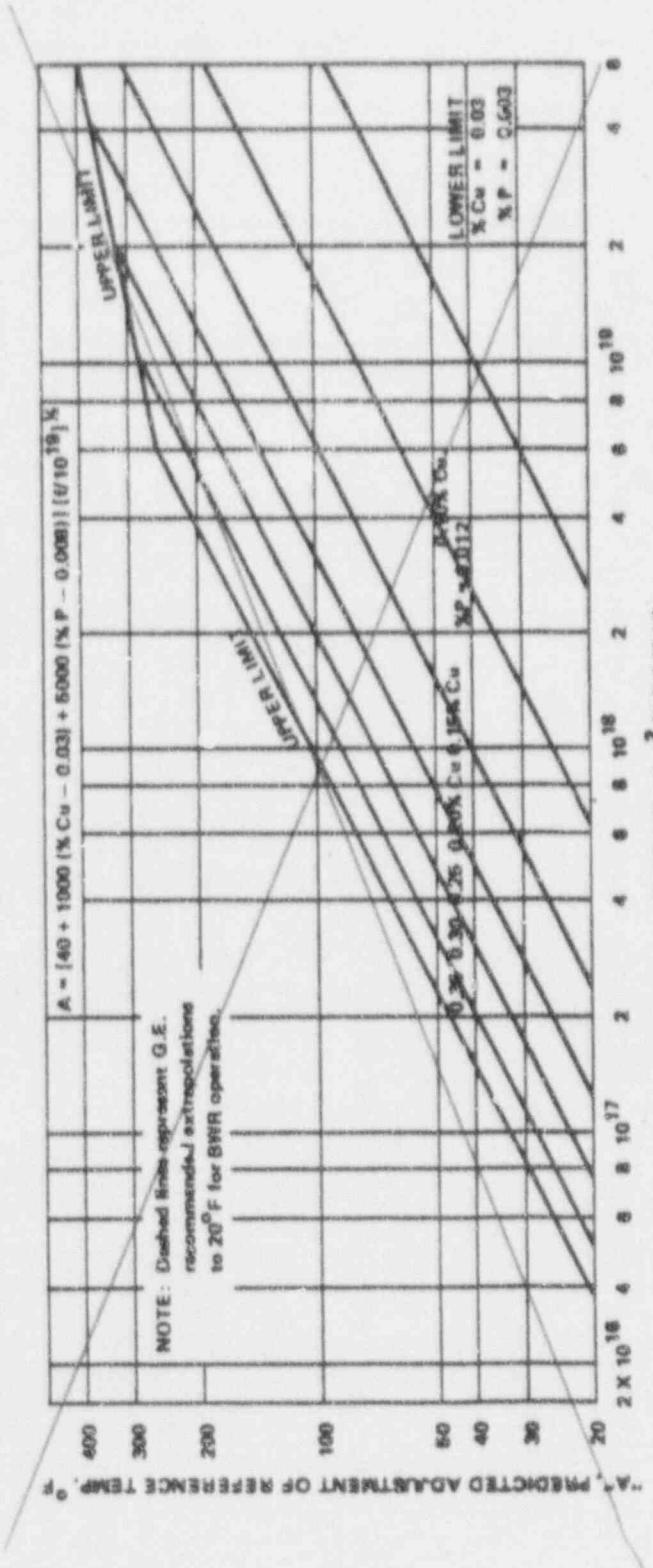

Predicted Adjustment of Reference Temperature, "A", as a Function of Fluence and Copper Content.
For Copper and Phosphorus Contents Other Than Those Plotted, Use the Expression for "A" Given on the Figure.

Bases Figure B 3/4.4.6-1

PRESSURE/TEMPERATURE LIMITS (Continued)

The actual shift in RT_{NDT} of the vessel material will be established periodically during operation by removing and evaluating reactor vessel material irradiation surveillance specimens installed near the inside wall of the reactor vessel in the core area. Since the neutron spectra at the irradiation samples and vessel inside radius are essentially identical, the measured transition shift for a sample can be applied with confidence to the adjacent section of the reactor vessel. The heatup and cooldown curves must be recalculated when the ΔRT_{NDT} determined from the surveillance capsule is different from the calculated ΔRT_{NDT} for the equivalent capsule radiation exposure.

The pressure-temperature limit lines shown in Figures 3.4.6.1-2 and 3.4.6.1-3 for reactor criticality and for inservice leak and hydrostatic testing have been provided to assure compliance with the minimum temperature requirements of Appendix G to 10 CFR Part 50 for reactor criticality and for inservice leak and hydrostatic testing.

The number of reactor vessel irradiation surveillance specimens and the frequencies for removing and testing these specimens are provided in Unit 2 UFSAR Section 5.2. The removal of the specimens meets ~~Table 4.4.6.1.3-1 to assure compliance with~~ the requirements of Appendix H to 10 CFR Part 50.

3/4.4.7 MAIN STEAM LINE ISOLATION VALVES

Double isolation valves are provided on each of the main steam lines to minimize the potential leakage paths from the containment in case of a line break. Only one valve in each line is required to maintain the integrity of the containment. The surveillance requirements are based on the operating history of this type valve. The maximum closure time has been selected to contain fission products and to ensure the core is not uncovered following line breaks.

3/4.4.8 STRUCTURAL INTEGRITY

The inspection programs for ASME Code Class 1, 2 and 3 components ensure that the structural integrity of these components will be maintained at an acceptable level throughout the life of the plant. To the extent applicable, the inspection program for these components is in compliance with Section XI of the ASME Boiler and Pressure Vessel Code.

Test pressures for inservice hydrostatic and leak testing required by the ASME B&PV Code, Section XI, are a function of testing temperature and component material. For the Hatch 1 reactor pressure vessel, the ISI hydrostatic test pressure would be approximately 1.1 times operating pressure, or about 1106 psig, depending on the reactor water temperature. The temperatures for pressures above 440 psig are determined by the RPV core beltline with a shift in RT_{NDT} of 123°F, appropriate for operation up to 16 effective full power years (EFPY).

Figure 3.6-2 provides appropriate limitations for plant heatup and cooldown when the reactor is not critical. Figure 3.6-2 is also applicable to low power physics tests. These curves assume heatup and cooldown rates up to 100°F per hour. Temperatures for pressures above 300 psig represent the limits of the RPV core beltline with a shift in RT_{NDT} of 123°F, appropriate for 16 EFPY of operation.

Figure 3.6-3 establishes operating limits when the core is critical. Figure 3.6-3 is not applicable to low power physics tests. These limits include a margin of 40°F as required by 10CFR50 Appendix G. In accordance with the May 1983 revision of 10CFR50 Appendix G, core critical operation may be initiated at temperatures at or above (RT_{NDT} + 60°F) of the closure flange region, or 76°F. Temperatures for pressures above 300 psig represent the limits of the RPV core beltline with a RT_{NDT} shift of 123°F, appropriate for 16 EFPY of operation.

The fracture toughness of all ferritic steels gradually and uniformly decreases with exposure to fast neutrons above a threshold value, and it is prudent and conservative to account for this in the operation of the RPV. Two types of information are needed in this analysis: (a) a relationship between the change in fracture toughness of the RPV steel and the neutron fluence (integrated neutron flux); and (b) a measure of the neutron fluence at the point of interest in the RPV wall. A method of relating shift in RT_{NDT} to accumulated fast nuetron (>1 MeV) fluence is contained in Regulatory Guide 1.99, Revision 1. Experimental results of irradiated surveillance specimens taken from the RPV show a shift in RT_{NDT} greater than predicted by Regulatory Guide 1.99, so the surveillance results were used with the methods of 1.99 to establish the RT_{NDT} shift. The shift for 16 EFPY was added to the unirradiated RPV core beltline curves, resulting in the beltline being the limiting region in the vessel for higher pressure-temperature conditions.

During inservice hydrostatic or leak testing, Figure 3.6-2 is used for nonnuclear heatup until the test temperature is achieved. After the test temperature is reached, performance of the inservice hydrostatic or leak test is governed by Figure 3.6-1. After test completion, vessel cooldown is in accordance with Figure 3.6-2.

ENCLOSURE 4

SASR 90-104
DRF B11-00495
May 1991

E. I. HATCH NUCLEAR POWER STATION, UNIT 2 VESSEL SURVEILLANCE MATERIALS TESTING AND FRACTURE TOUGHNESS ANALYSIS

Prepared by: T. A. Caine

T. A. Caine, Senior Engineer
Materials Monitoring &
Structural Analysis Services

Verified by: B. J. Branlund

B. J. Branlund, Engineer
Materials Monitoring &
Structural Analysis Services

Approved by: S. Ranganath

S. Ranganath, Manager
Materials Monitoring &
Structural Analysis Services

IMPORTANT NOTICE REGARDING
CONTENTS OF THIS REPORT
PLEASE READ CAREFULLY

This report was prepared by General Electric solely for the use of Georgia Power Company. The information contained in this report is believed by General Electric to be an accurate and true representation of the facts known, obtained or provided to General Electric at the time this report was prepared.

The only undertakings of the General Electric Company respecting information in this document are contained in the contract between the customer and General Electric Company, as identified in the purchase order for this report and nothing contained in this document shall be construed as changing the contract. The use of this information by anyone other than the customer or for any purpose other than that for which it is intended, is not authorized; and with respect to any unauthorized use, General Electric Company makes no representation or warranty, and assumes no liability as to the completeness, accuracy, or usefulness of the information contained in this document.

CONTENTS

CONTENTS (continued)

APPENDICES

TABLES

ILLUSTRATIONS

ILLUSTRATIONS (continued)

ABSTRACT

Surveillance capsules were removed from the Hatch Unit 2 reactor at the end of Fuel Cycle 8. The capsule contained flux wires for neutron fluence measurement and Charpy and tensile test specimens for material property evaluation. A combination of flux wire testing and computer analysis was used to establish the vessel peak flux location and magnitude. Charpy V-Notch impact testing and uniaxial tensile testing were performed to establish the properties of the irradiated surveillance materials. The irradiation effects were projected, based on Regulatory Guide 1.99, Revision 2, to conditions for 32 effective full power years (EFPY) of operation. The 32 EFPY conditions are predicted to be less severe than the limits in 10CFR50 Appendix G requiring provisions for vessel thermal annealing. Pressure-temperature operating limits curves valid to 32 EFPY were developed to 10CFR50 Appendix G requirements, accounting for irradiation shift per Regulatory Guide 1.99, Revision 2.

The irradiated Charpy data for the Unit 2 plate and weld specimens were compared to unirradiated data to determine the shift in Charpy curves due to irradiation. The results are within the predictions of the Regulatory Guide.

ACKNOWLEDGMENTS

The author gratefully acknowledges the efforts of the people mentioned below.

Flux wire testing was performed by G. C. Martin. Charpy testing was completed by G. P. Wozadlo and G. E. Dunning. Tensile specimen testing was done by S. B. Wisner and G. H. Henderson, and chemical composition analysis was performed by C. R. Judd. The Charpy and tensile test result evaluations, as well as the overall verification of this report, were completed by B. J. Branlund.

1. INTRODUCTION

Part of the effort to assure reactor vessel integrity involves evaluation of the fracture toughness of the vessel ferritic materials. The key values which characterize a material's fracture toughness are the reference temperature of nil-ductility transition (RT_{NDT}) and the upper shelf energy (USE). These are defined in 10CFR50 Appendix G (Reference 1) and in Appendix G of the ASME Boiler and Pressure Vessel Code, Section XI (Reference 2). These documents contain requirements used to establish the pressure-temperature operating limits which must be met to avoid brittle fracture.

Appendix H of 10CFR50 (Reference 3) and ASTM E185 (Reference 4) establish the methods to be used for surveillance of the reactor vessel materials. The first vessel surveillance specimen capsule required by Reference 3 were removed from Unit 2 in late 1989. The capsule was sent to the GE Vallecitos Nuclear Center (VNC) for testing after exposure to eight fuel cycles of irradiation. The surveillance capsule contained flux wires for neutron flux monitoring and Charpy V-Notch impact test specimens and uniaxial tensile test specimens fabricated from materials from, or representative of, the vessel materials nearest the core (beltline). The impact and tensile specimens were tested to establish properties for the irradiated materials.

The results of the surveillance specimen testing are presented in this report. The irradiated material properties are compared to available unirradiated properties from fabrication records. Predictions of the RT_{NDT} and USE at 32 EFPY are made for comparison with allowable values in Reference 1. Predictions of 32 EFPY properties were made based on Regulatory Guide 1.99, Revision 2 (Reference 5).

Operating limits curves for the Unit 2 reactor vessel are presented in this report. The curves account for current requirements of References 1 and 2. Geometric discontinuities and highly stressed regions, such as the feedwater nozzles and the closure flanges, are evaluated separately from the core beltline region. The operating limits developed consider the most limiting conditions of the discontinuity regions and the beltline region, so as to bound all operating conditions. The operating limits developed for the beltline region include irradiation shift, based on Reference 5 methods.

2. SUMMARY AND CONCLUSIONS

2.1 SUMMARY OF RESULTS

Surveillance capsule 3 was removed from Hatch Unit 2 at the end of Fuel Cycle 8 and shipped to VNC. The flux wires, Charpy V-Notch and tensile test specimens removed from the capsule were tested according to ASTM E185-82 (Reference 4). Revised operating limits curves were developed using the flux wire test results and the requirements and methods of 10CFR50 Appendix G (Reference 1) and Appendix G of ASME Code Section XI (Reference 2). The methods and results of the fracture toughness evaluation are presented in this report as follows:

a. Section 3: Surveillance Program Background

b. Section 4: Peak RPV Fluence Evaluation

c. Section 5: Charpy V-Notch Impact Testing

d. Section 6: Tensile Testing

e. Section 7: Development of Operating Limits Curves

Photographs of fractured Charpy specimens are in Appendix A. The significant results of the evaluation are below:

a. Capsule 3 was removed from the 30° azimuth position of the reactor. The capsule contained 9 flux wires: 3 copper (Cu), 3 iron (Fe), and 3 nickel (Ni). There were 36 Charpy V-Notch specimens in the capsule: 12 each of plate material, weld material and heat affected zone (HAZ) material. The 10 tensile specimens removed consisted of 3 plate, 4 weld and 3 HAZ metal specimens.

b. The chemical compositions of the beltline materials were determined from data obtained from GE QA records or from Combustion Engineering. The copper (Cu) and nickel (Ni) contents were determined for all heats of plate material. The values for the limiting beltline plate are 0.08% Cu and 0.58% Ni. The Ni content of the beltline longitudinal welds was not recorded, so the maximum possible Ni content from the weld type specification was assumed. The limiting beltline weld values are 0.23% Cu and 0.50% Ni.

c. Charpy and dropweight test results from the fabrication program materials certification testing were adjusted to be equivalent to test results done to current standards. The initial RT_{NDT} values for locations of interest in the vessel were determined. They are -4°F for the limiting beltline plate, -50°F for the limiting beltline weld, 30°F for the closure flange region, 26°F for the limiting nozzle and 50°F for the bottom head region.

d. The flux wires were tested to determine the neutron flux at the surveillance capsule location. The fast flux (>1.0 MeV) measured was 1.12×10^{9} n/cm^2-sec. Based on the flux wire data, the surveillance specimens received a best estimate fluence of 2.3×10^{17} n/cm^2 at removal.

e. The vessel inside surface lead factors were established using an analysis performed for Hatch Unit 1 that combined two-dimensional and one-dimensional finite difference transport analysis. The flux peak occurs at an azimuthal location 45° past the vessel quadrant references, and about 106 inches above the bottom of active fuel elevation. The lead factor for the surveillance capsules is 0.79 to the peak vessel inside surface location.

f. The maximum accumulated neutron fluence at 32 EFPY was determined at the peak 1/4 T location, using the flux wire test results, the lead factor and the methods of Reference 5. The maximum 1/4 T vessel 32 EFPY fluence is 1.0×10^{18} n/cm^2 for the lower intermediate shell (5.38 inches thick) and 9.5×10^{17} n/cm^2 for the lower shell (6.38 inches thick).

g. The surveillance Charpy V-Notch specimens were impact tested at temperatures selected to define the transition of the fracture toughness curves of the plate, weld, and HAZ materials. Measurements were taken of absorbed energy, lateral expansion and percentage shear. Fracture surface photographs of each specimen are presented in Appendix A. From absorbed energy and lateral expansion results for the plate and weld materials the following values were calculated: index temperatures for 30 ft-lb, 50 ft-lb, and 35-mil lateral expansion (MLE) values and USE.

h. The curves of irradiated specimen Charpy impact energy and lateral expansion were compared to data for unirradiated specimens retrieved from the site to establish the 30 ft-lb index temperature irradiation shift and decrease in USE. The surveillance plate material showed an estimated 3°F shift and a 0% decrease in USE. The weld material showed a 0°F shift and a -1% decrease in USE.

i. The irradiated tensile specimens were tested at room temperature (70°F), reactor operating temperature (550°F), and estimated onset to upper shelf temperature (120°F). The results tabulated for each specimen include yield and ultimate tensile strength, uniform and total elongation, and reduction of area.

j. The irradiated plate and weld tensile test results for Unit 2 were compared to unirradiated data from the vessel fabrication test program records. The results generally showed increasing strength and decreasing ductility, consistent with expectations for irradiation embrittlement.

k. As a part of the development of the pressure-temperature (P-T) operating limits curves, the irradiation shifts in RT_{NDT} were predicted, based on the methods of Regulatory Guide 1.99, Revision 2 (Reference 5). For information purposes, the measured surveillance shifts were compared to the shifts predicted by Reference 5. The measured shifts of 3°F for plate and 0°F for weld, for a fluence of 2.3×10^{17} n/cm^2, are less than the respective predicted shift values of 9.6°F and 12.9°F.

l. The beltline material USE values at 32 EFPY were predicted using the methods in Reference 5, with initial beltline plate and weld USE values taken from fabrication records. The lowest beltline transverse plate and weld USE values were predicted to be 61 ft-lb and 72 ft-lb, respectively, at 32 EFPY.

m. P-T curves were developed for three reactor conditions: hydrostatic pressure test (Curve A), non-nuclear heatup and cooldown (Curve B), and core critical operation (Curve C). The curves are valid up to 32 EFPY of operation. The limiting regions of the vessel affecting the curves' shapes are the nozzle, bottom head and closure flange regions. The bolt preload and minimum permissible operating temperatures were determined to be 90°F. The predicted irradiation shifts for the Unit 2 beltline materials are low enough that the beltline is not predicted to be limiting through 32 EFPY of operation. The P-T curves for Unit 2 are shown in Figures 2-1 through 2-3.

2.2 CONCLUSIONS

The requirements of Reference 1 deal basically with vessel design life conditions and with limits of operation designed to prevent brittle fracture. Based on the evaluation of surveillance testing results, and the associated analyses, the following conclusions are made:

a. The adjusted reference temperatures at 32 EFPY for the limiting beltline material of 69°F is below the Reference 1 allowable limit of 200°F, above which special analyses or provisions for annealing are required.

b. The 32 EFPY values of USE, calculated to be 61 ft-lb and 72 ft-lb for plate and weld, respectively, are well above the Reference 1 allowable minimum of 50 ft-lb. Thus, there is no need, based on USE values, for special analyses or provisions for annealing the Unit 2 vessel beltline.

c. Examination of the normal and upset operating conditions expected for the reactor shows that the worst pressure-temperature conditions expected from unplanned temperature transients are acceptable relative to the limits in Figures 2-1 through 2-3. Therefore, the only operating conditions for which the operating limits are a concern are those involving operator interaction, such as pressure testing and initiation of core criticality.

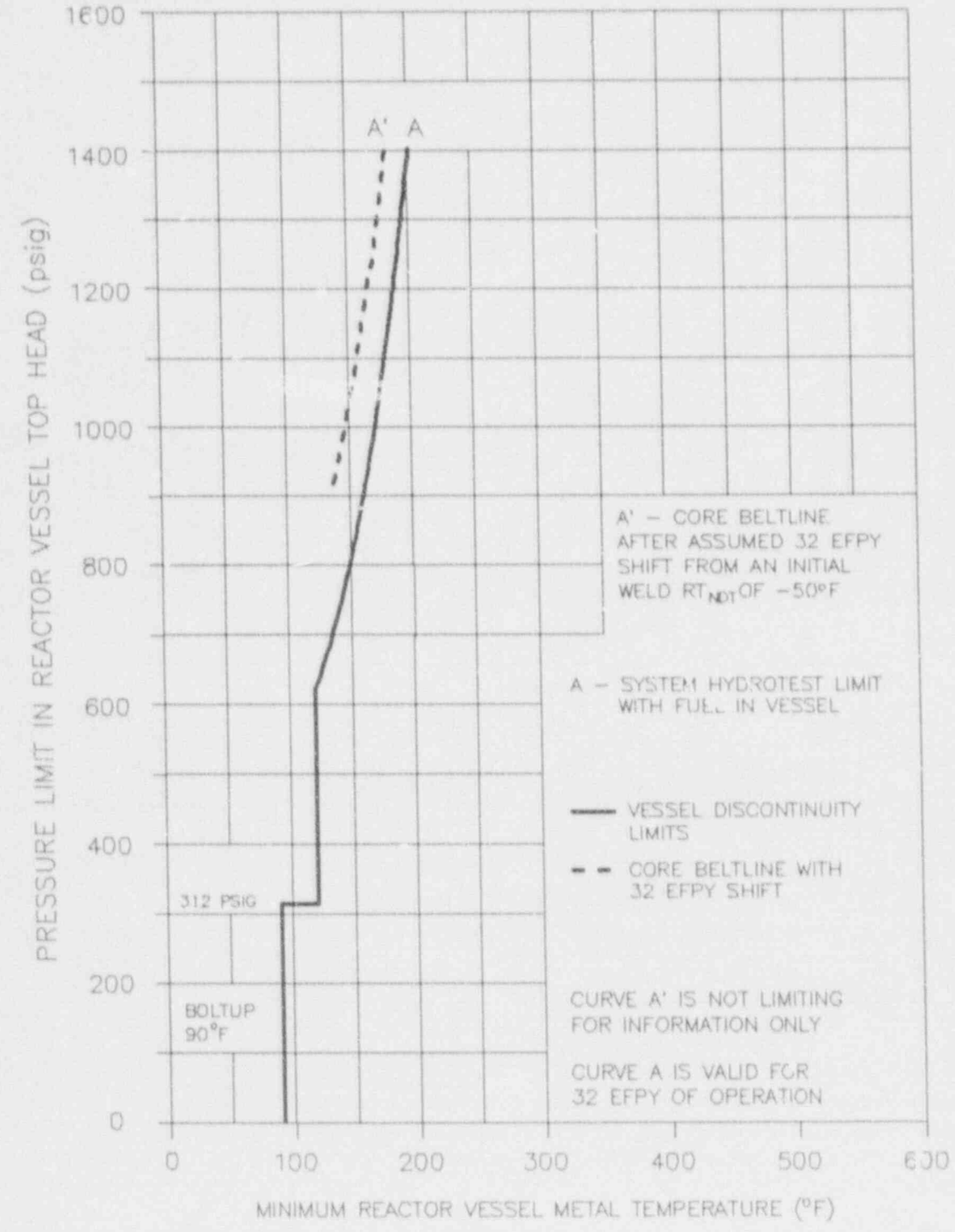

Figure 2–1. P–T Curves for Pressure Tests

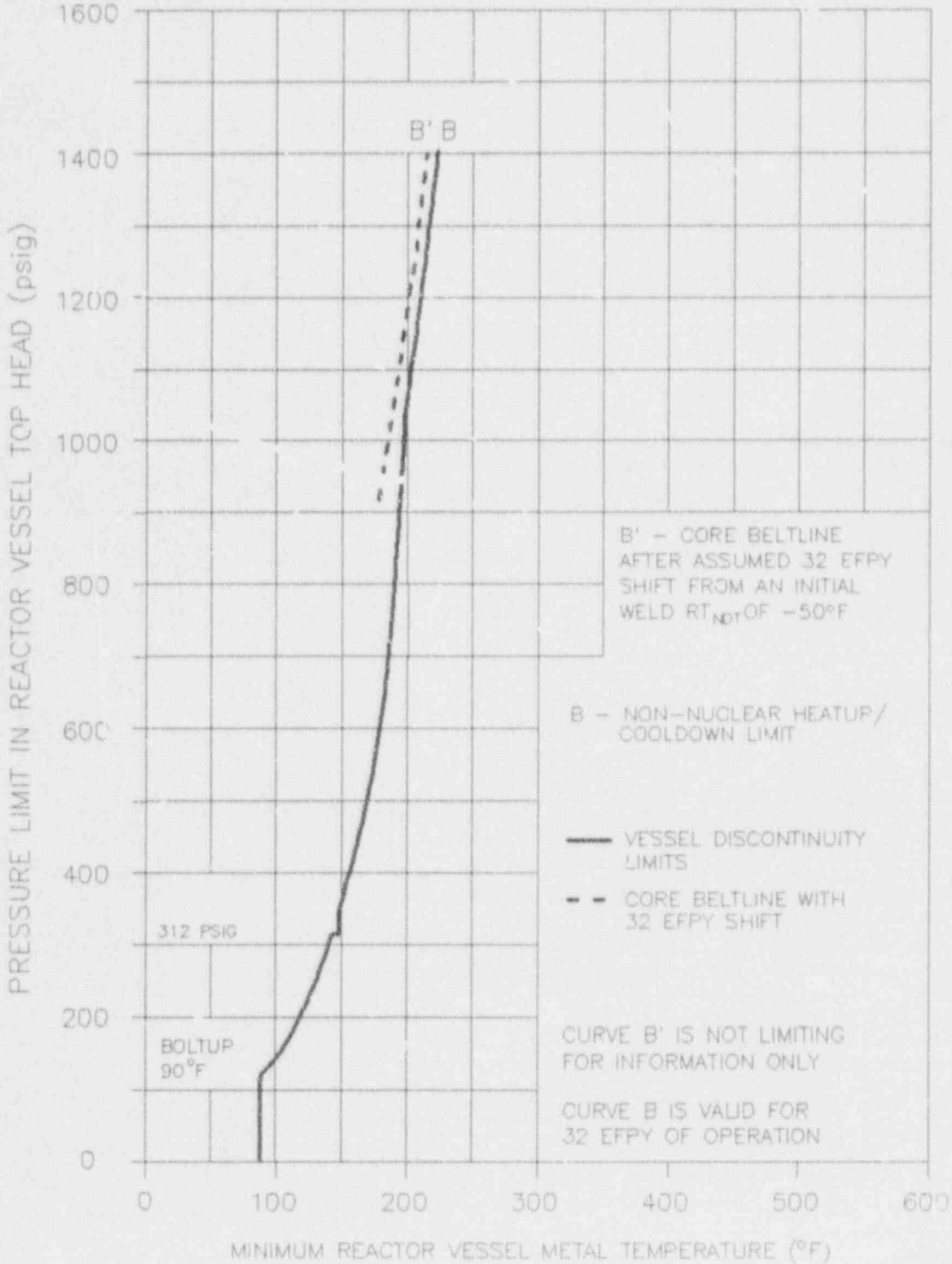

Figure 2–2. P–T Curves for Non–Nuclear Heatup/Cooldown

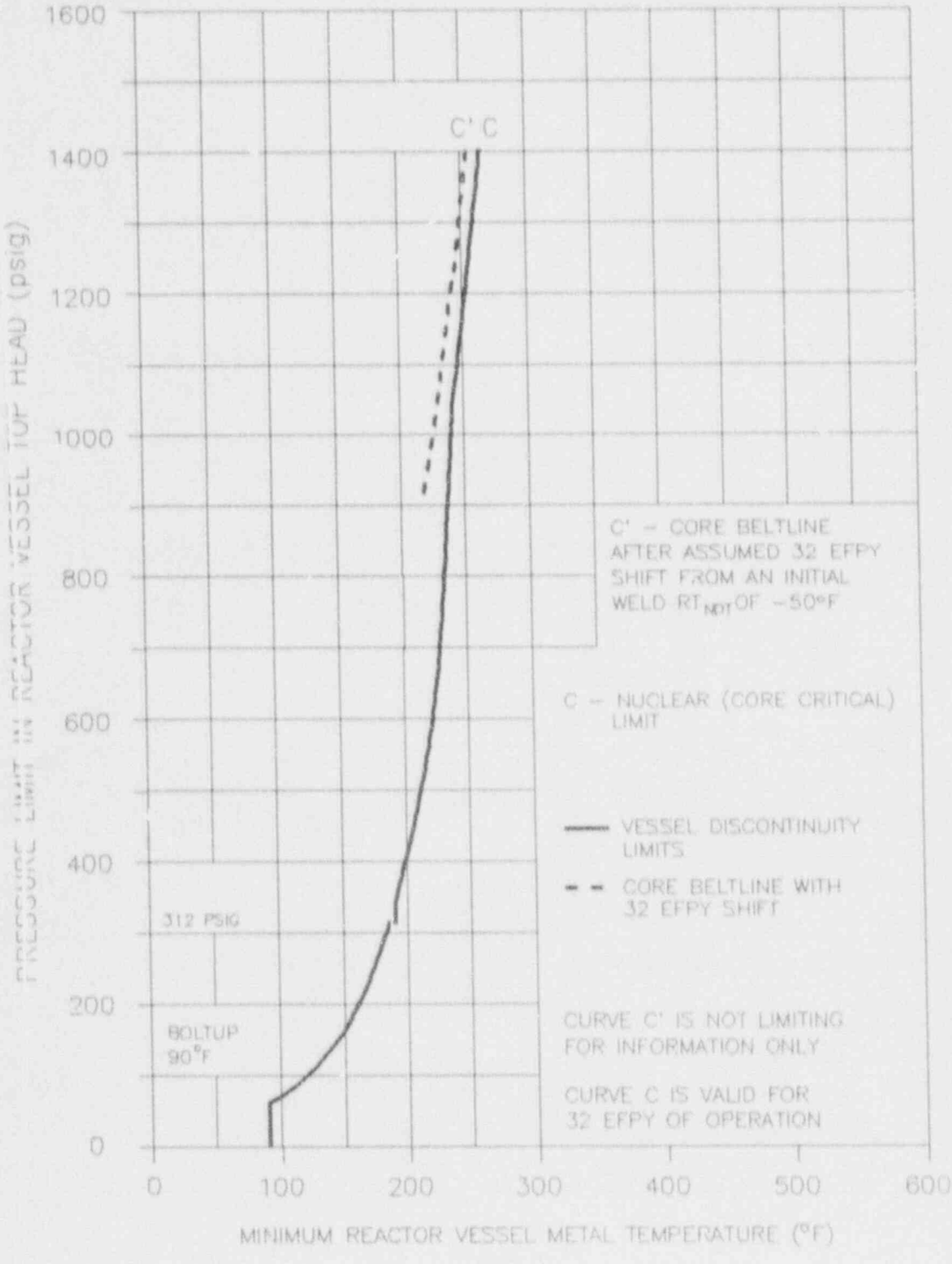

Figure 2-3. P-T Curves for Core Critical Operation

3. SURVEILLANCE PROGRAM BACKGROUND

3.1 CAPSULE RECOVERY

The Hatch Unit 2 reactor was shut down in September, 1989 for refueling and maintenance. The accumulated thermal power output was 5.86×10^6 MWd or 6.58 EFPY. The reactor pressure vessel (RPV) originally contained three surveillance capsules, at 30°, 120° and 300° azimuths at the core midplane. The specimen capsules are held against the RPV inside surface by a spring loaded specimen holder. Each capsule receives equal irradiation because of core symmetry. During the 1989 outage, Capsule 3 at 30° was removed. The capsule was cut from its holder assembly and shipped by cask to the GE Vallecitos Nuclear Center (VNC), where testing was performed.

Upon arrival at VNC, the capsules were examined for identification. The drilled hole code normally on the basket was not present, but the reactor code of 46 for Unit 2 was stamped on the specimens, providing the essential positive identification of the surveillance materials. The general condition of the basket as received is shown in Figure 3-1. As shown, the capsule contained three Charpy specimen packets and five tensile specimen tubes. Each tensile specimen tube contained two tensile specimens. Each Charpy specimen packet contained 12 plate, weld or HAZ Charpy specimens and 3 flux wires (one iron, one copper and one nickel) in a sealed helium environment.

3.2 RPV MATERIALS AND FABRICATION BACKGROUND

3.2.1 Fabrication History

The Hatch 2 RPV is a 218 inch diameter BWR/4 design. Construction was performed by Combustion Engineering (CE) to the Summer 1970 Addenda of the 1968 edition of the ASME Code. The shell and head plate materials are ASME SA533, Grade B, Class 1 low alloy steel (LAS). The nozzles and closure flanges are ASME SA508 Class 2 LAS, and the closure flange bolting materials are ASME SA540 Grade B23 or B24 LAS. The vessel plates were heat treated prior to welding in two steps: 1600°F for 3/4 hour per inch

thickness followed by water quenching, and 1225°F for 3/4 hour per inch thickness. Submerged arc welding of plates was followed by post-weld heat treatment. The post-weld heat treatment was typically one hour per inch of thickness at temperatures at 1150°F. The fabrication impact test specimens were given a simulated post weld heat treatment of 40 hours. The identification of plates and welds in the beltline region is shown in Figure 3-2.

3.2.2 Material Properties of RPV at Fabrication

Material certification records were retrieved from GE Quality Assurance (QA) records to determine chemical and mechanical properties of the vessel materials. In addition, CE was contacted directly to retrieve information on the weld wire heat used to fabricate the surveillance weld. Table 3-1 shows the chemistry data for the Unit 2 beltline materials. The Ni content of the longitudinal submerged arc welds was not reported, because the weld wire used was type B-4, for which Ni is not required at any specified level. ASME Section II, Part C (Reference 6) requires that non-specified elements constitute less than 0.50% of the weld wire composition. Review of several dozen B-4 weld chemistries show Ni content typically around 0.10%. As shown in Table 3-1, Ni content levels of 0.50% were conservatively assumed for the longitudinal beltline welds.

Results of certification mechanical property tests performed during RPV fabrication were examined, specifically Charpy V-Notch and dropweight impact test results. Properties of the beltline materials and other locations of interest are presented in Table 3-2. The Charpy data collected were used to establish the RT_{NDT} values for each vessel component, as described in Subsection 3.2.4.

3.2.3 Specimen Chemical Composition

Samples were taken from the surveillance plate and weld tensile specimens after they were tested. Chemical analyses were performed using a Spectraspan III plasma emission spectrometer. Each sample was dissolved in an acid solution to a concentration of 40 mg steel per ml solution. The spectrometer was calibrated for determination of Mn, Ni, Mo and Cu by

diluting National Institute of Standards and Technology (NIST) Spectrometric Standard Solutions. The phosphorus calibration involved analysis of four reference materials from NIST with known phosphorus levels. Analysis accuracies are ±0.003% (absolute) for phosphorus and ±5% (relative) for other elements. The chemical composition results are given in Table 3-3 for the Unit 2 surveillance plate and weld materials. The results show good agreement with corresponding data from fabrication records in Table 3-1. Of particular interest is the Ni content of the B-4 type surveillance weld (0.12% or less).

3.2.4 Initial Reference Temperatures

The requirements for establishing the vessel component RT_{NDT} values per the ASME Code prior to 1972 are summarized as follows:

a. Test specimens shall be longitudinally oriented Charpy V-Notch specimens.

b. At the RT_{NDT}, no impact test result shall be less than 25 ft-lb, and the average of three test results shall be at least 30 ft-lb.

c. Pressure tests shall be conducted at a temperature at least 60°F above the acceptable RT_{NDT} for the vessel.

The current requirements for establishing RT_{NDT} are significantly different. For plants constructed to the ASME Code after Summer 1972, the requirements are as follows:

a. Charpy V-Notch specimens shall be oriented normal to the rolling direction (transverse).

b. RT_{NDT} is defined as the higher of the dropweight NDT or 60°F below the temperature at which Charpy V-Notch 50 ft-lb energy and 35 mils lateral expansion are met.

c Bolt-up in preparation for a pressure test or normal operation shall be performed at or above the RT_{NDT} or lowest service temperature (LST), whichever is greater.

Reference 1 states that for vessels constructed to a version of the ASME Code prior to the Summer 1972 Addendum, fracture toughness data and data analyses must be supplemented in an approved manner. GE has developed methods for analytically converting fracture toughness data for vessels constructed before 1972 to comply with current requirements. GE developed these methods from data in WRC Bulletin 217 (Reference 7) and from data collected to respond to NRC questions on FSAR submittals in the late 1970s. These methods and example RT_{NDT} calculations for vessel plate, weld, weld HAZ, forging, and bolting material are summarized in the remainder of this subsection. Calculated RT_{NDT} values for selected RPV locations are given in Table 3-2.

For vessel plate material, the first step in calculating RT_{NDT} is to establish the 50 ft-lb transverse test temperature from longitudinal test specimen data. There are typically three energy values at a given test temperature. The lowest energy Charpy value is adjusted by adding 2°F per ft-lb energy to 50 ft-lb. For example, for the limiting Unit 2 beltline plate the test temperature and lowest Charpy energy from Table 3-2 is 28 ft-lb at +10°F for Heat C8553-1. The equivalent 50 ft-lb longitudinal test temperature is:

$$T_{50L} = 10°F + [(50 - 28)\ \text{ft-lb} * 2°F/\text{ft-lb}] = 54°F$$

The transition from longitudinal data to transverse data is made by adding 30°F to the test temperature. In this case, the 50 ft-lb transverse Charpy test temperature is $T_{50T} = 84°F$. The RT_{NDT} is the greater of NDT or (T_{50T} - 60°F). From Table 3-2, the NDT for Heat C8553-1 is 0°F, and (T_{50T} - 60°F) is 24°F. Thus, the RT_{NDT} for that beltline plate is 24°F.

For vessel weld material, the Charpy V-Notch results are usually limiting in establishing RT_{NDT}. The 50 ft-lb test temperature is established as for the plate material, but the 30°F adjustment to convert longitudinal data to transverse data is not applicable to weld metal. All beltline weld Charpy V-Notch energies are well above 50 ft-lb, as shown in Table 3-2, so

T_{50T} = 10°F.

There are no NDT data available for the longitudinal welds, but the circumferential weld, which has very similar Charpy results, has a NDT of -50°F. Furthermore, the GE procedure requires that, when no NDT is available, the resulting RT_{NDT} be -50°F or higher. In this example, (T_{50T} - 60°F) is -50°F, so the RT_{NDT} is -50°F.

For the vessel weld HAZ material, the RT_{NDT} is assumed to be the same as for the base material since ASME Code weld procedure qualification test requirements and post-weld heat treatment data indicate this assumption is valid.

For vessel forging material, such as nozzles and closure flanges the method for establishing RT_{NDT} is the same as for vessel plate material. For the steam outlet nozzles N3, the lowest Charpy data at 10°F is 27 ft-lb, and the NDT is 10°F. In this case, (T_{50T} - 60°F) is greater than NDT, so the RT_{NDT} is [10 + (50-27)*2 + 30 - 60], or 26°F.

For bolting material, the current ASME Code requirements define the lowest service temperature (LST) as the temperature at which transverse Charpy V-Notch energy of 45 ft-lb and 25 mils lateral expansion (MLE) are achieved. If the required Charpy results are not met, or are not reported, but the Charpy V-Notch energy reported is above 30 ft-lb, the requirements of the ASME Code at construction are applied, namely that the 30 ft-lb test temperature plus 60°F is the LST for the bolting materials. Charpy data for the studs did not meet the 45 ft-lb, 25 MLE requirement, but 30 ft-lb energies were met at 10°F. Therefore, the bolting material LST is 70°F.

3.3 SPECIMEN DESCRIPTION

The surveillance capsule contained 36 Charpy specimens: base metal (12), weld metal (12), and HAZ (12). There were 10 tensile specimens: base metal (3), weld metal (4), and HAZ (3). The capsule contained 9 flux wires: 3 iron, 3 nickel and 3 copper. The chemistry and fabrication history for the Charpy and tensile specimens are described in this section.

3.3.1 Charpy Specimens

The fabrication of the Charpy specimens is described in the CE document on the surveillance test program for Hatch 2 (Reference 8). All materials used for specimens were specified to be beltline materials, but the records show that the weld wire heat used is not in the Unit 2 beltline. It is, however, representative of the beltline welds, as discussed below.

The base metal specimens were cut from Heat C8554, but the documentation does not distinguish whether they are from slab 1 or 2. Fortunately, the properties of the two slabs are very similar, as shown in Tables 3-1 and 3-2. The test plates received the same heat treatment as the fabrication specimens for Heat C8554, including the post-weld heat treatment for 40 hours at 1150°F ± 25°F. The method used to machine the specimens from the test plate is shown in Figure 3-3. Specimens were machined from the 1/4 T and 3/4 T positions in the plate, in the longitudinal orientation (long axis parallel to the rolling direction). The base metal Charpy specimens recovered from the surveillance capsule were stamped on one end with the reactor number, 46, and on the other end with "P1", which designates base metal.

The weld metal and HAZ Charpy specimens were fabricated by welding together two pieces of the surveillance test plate with a weld which was specified to be identical to the beltline longitudinal seam welds. The same weld procedure was used, and the same types of weld wire and flux were used, but the actual weld wire heat and flux lot were not used in the vessel beltline welds. Actual welding records obtained from CE show the

surveillance weld to be a submerged arc weld with wire heat 51912 and Linde 0091 flux lot 3490. The weld qualification test chemistry results, shown in Table 3-1, agree fairly well with the specimen test results in Table 3-3. The welded test plate for the weld and HAZ Charpy specimens each received stress relief heat treatment at 1150°F ± 25°F for 40 hours to simulate the fabrication specimen conditions. The weld specimens and HAZ specimens were fabricated as shown in Figures 3-4 and 3-5, respectively. The base metal orientation in the weld and HAZ specimens was longitudinal. The specimens were stamped on one end with the reactor number and on the other with "P2" for weld metal or "P3" for HAZ.

3.3.2 Tensile Specimens

Fabrication of the surveillance tensile specimens is described in Reference 8. The materials, and thus the chemical compositions and heat treatments for the base, weld and HAZ tensiles are the same as those for the corresponding Charpy specimens. The identifications of the base, weld, and HAZ tensile specimens are identical as well: reactor number on one end and P1, P2 or P3 on the other end. A summary of the fabrication methods follows.

The base metal specimens were machined from material at the 1/4 T and 3/4 T depth. The specimens, oriented along the plate rolling direction, were machined to the dimensions shown in Figure 3-6. The gage section was tapered to a minimum diameter of 0.250 inch at the center. The weld metal tensile specimen materials were cut from the welded test plates, as shown in Figure 3-7. The specimens were machined entirely from weld metal, scrapping material that might include base metal. The fabrication method for the HAZ tensile specimens is illustrated in Figure 3-8. The specimen blanks were cut from the welded test plates such that the gage section minimum diameters were machined at the weld fusion line. The finished HAZ specimens are approximately half weld metal and half base metal oriented along the plate rolling direction.

Table 3-1
CHEMICAL COMPOSITION OF RPV BELTLINE MATERIALS

Identification	Heat/Lot No.	Composition by Weight Percent							
		C	Mn	P	S	Si	Ni	Mo	Cu
Lower Shell Plates:									
G6603-1	C8553-2	0.23	1.26	0.010	0.016	0.26	0.58	0.55	0.08
G6603-2	C8553-1	0.19	1.26	0.010	0.017	0.24	0.58	0.55	0.08
G6603-3	C8571-1	0.20	1.28	0.012	0.019	0.22	0.53	0.56	0.08
Lower-Intermediate Shell Plates:									
G6602-2	C8554-1	0.22	1.32	0.010	0.018	0.22	0.57	0.52	0.08
G6602-1	C8554-2	0.23	1.31	0.010	0.016	0.24	0.58	0.52	0.08
G6601-4	C8579-2	0.20	1.29	0.013	0.018	0.29	0.48	0.48	0.11
Surveillance Plate:									
G6602	C8554	see above for slabs 1 and 2							
Lower Longitudinal Welds:									
101-842	10137, Linde 0091 Flux Lot 3999	0.20	1.13	0.016	0.010	0.14	<.50	0.49	0.23
Lower-Intermediate Longitudinal Welds:									
101-834	51874, Linde 0091 Flux Lot 3458	0.15	1.08	0.009	0.006	0.13	<.50	0.51	0.16
Lower to Lower-Intermediate Girth Weld:									
301-871	4P6052, Linde 0091 Flux Lot 0145	0.14	1.25	0.011	0.009	0.12	0.03	0.48	0.07
Surveillance Weld:									
	51912, Linde 0091 Flux Lot 3490	0.15	1.13	0.014	0.007	0.20	<.50	0.53	0.16

Table .

MECHANICAL PROPERTIES OF BELTLINE AND OTHER SELECTED ...V MATERIALS

Location	Ident. Number	Heat Number	Test Temp. (°F)	Charpy Energy (ft-lb)	NDT (°F)	T_{50T}-60 (°F)	RT_{NDT} (°F)
Beltline:							
Lower Shell Plates	G6603-1	C8553-2	10	60,57,65	-20	-20	-20
	G6603-2	C8553-1	10	28,37,65	0	24	24
	G6603-3	C8571-1	10	44,40,51	-20	0	0
Lower Intermediate Shell Plates	G6602-2	C8554-1	10	51,66,71	-20	-20	-20
	G6602-1	C8554-2	10	45,65,68	-20	-10	-10
	G6601-4	C8579-2	10	48,42,53	-10	-4	-4
Longitudinal Welds	101-842	10137	10	101,108,107	N/A	-50	-50
	101-834	51874	10	89,64,87	N/A	-50	-50
Girth Weld	301-871	4P6052	10	75,65,126	-50	-50	-50
Surveillance Weld		51912	10	93,84,92	-50		
(2 Qualification reports)			10	98,100,109	N/A		
Non-Beltline:							
Upper Shell Plate	G6601-1	C8579-1	10	25,30,31,35	0	30	30
Vessel Flange	G6611-1	BJT406	10	96,99,102	10	-20	10
Head Flange	G6612-1	BUD382	10	93,102,107	10	-20	10
Top Head Torus	G6627-1	C1232-1	10	31,35,42	-30	18	18
Bottom Head Dome	G6606-2	C8658-2	40	30,32,34	20	50	50
Steam Outlet N3	G6618-1	Q2Q30W	10	27,34,33	10	26	26

NOTE: N/A = not available

Table 3-3

CHEMICAL COMPOSITION OF IRRADIATED SURVEILLANCE SPECIMENS

Identification	Composition by Weight Percent							
	C	Mn	P	S	Si	Ni	Mo	Cu
Plate:								
P1-46-A	-[a]	1.40	0.011	-	-	0.63	0.59	0.08
P1-46-B	-	1.38	0.009	-	-	0.63	0.60	0.08
Weld:								
P2-46-A	-	1.18	0.013	-	-	0.12	0.57	0.13
P2-46-B	-	1.19	0.014	-	-	0.07	0.56	0.12

[a] A - mark denotes an element that was not evaluated.

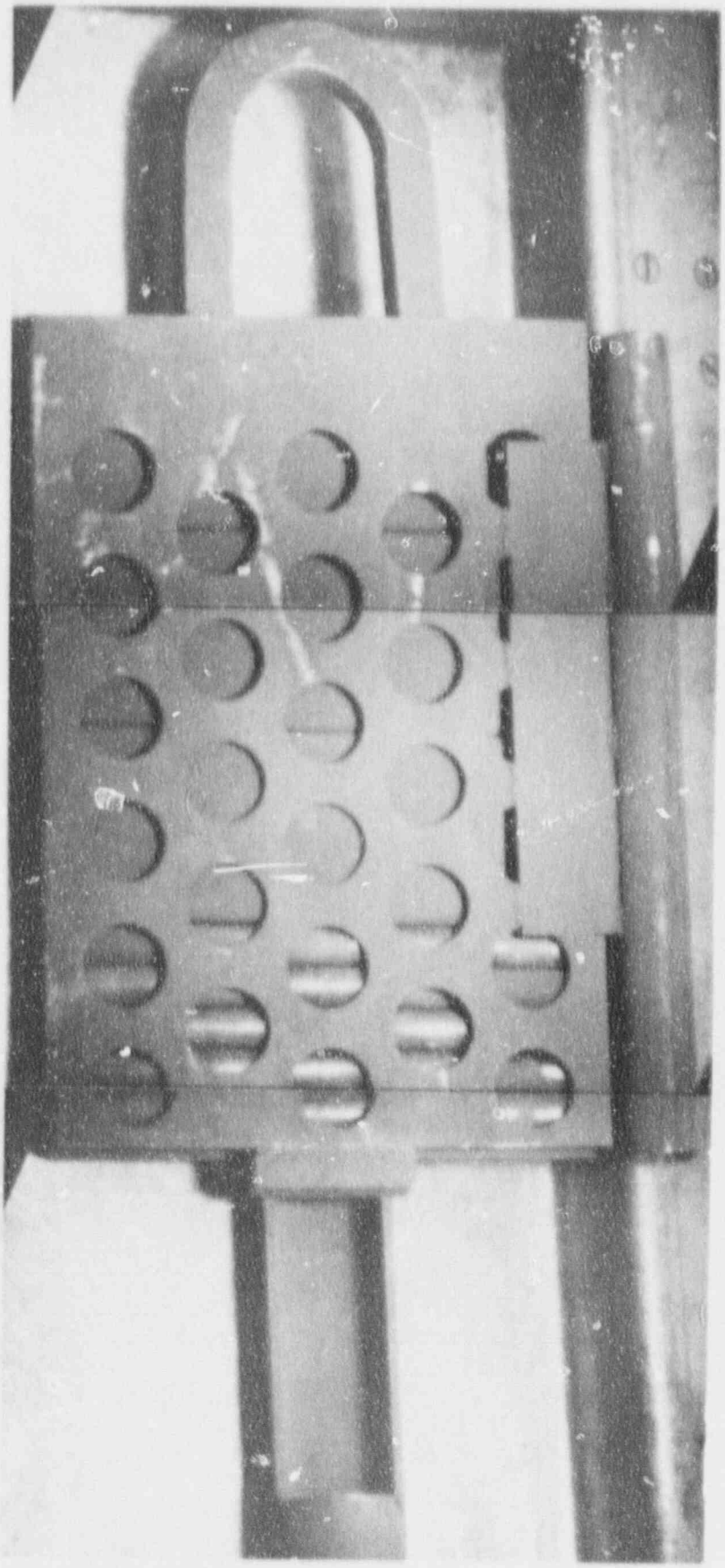

Figure 3-1. Surveillance Capsule Recovered From Hatch Unit 2 Reactor

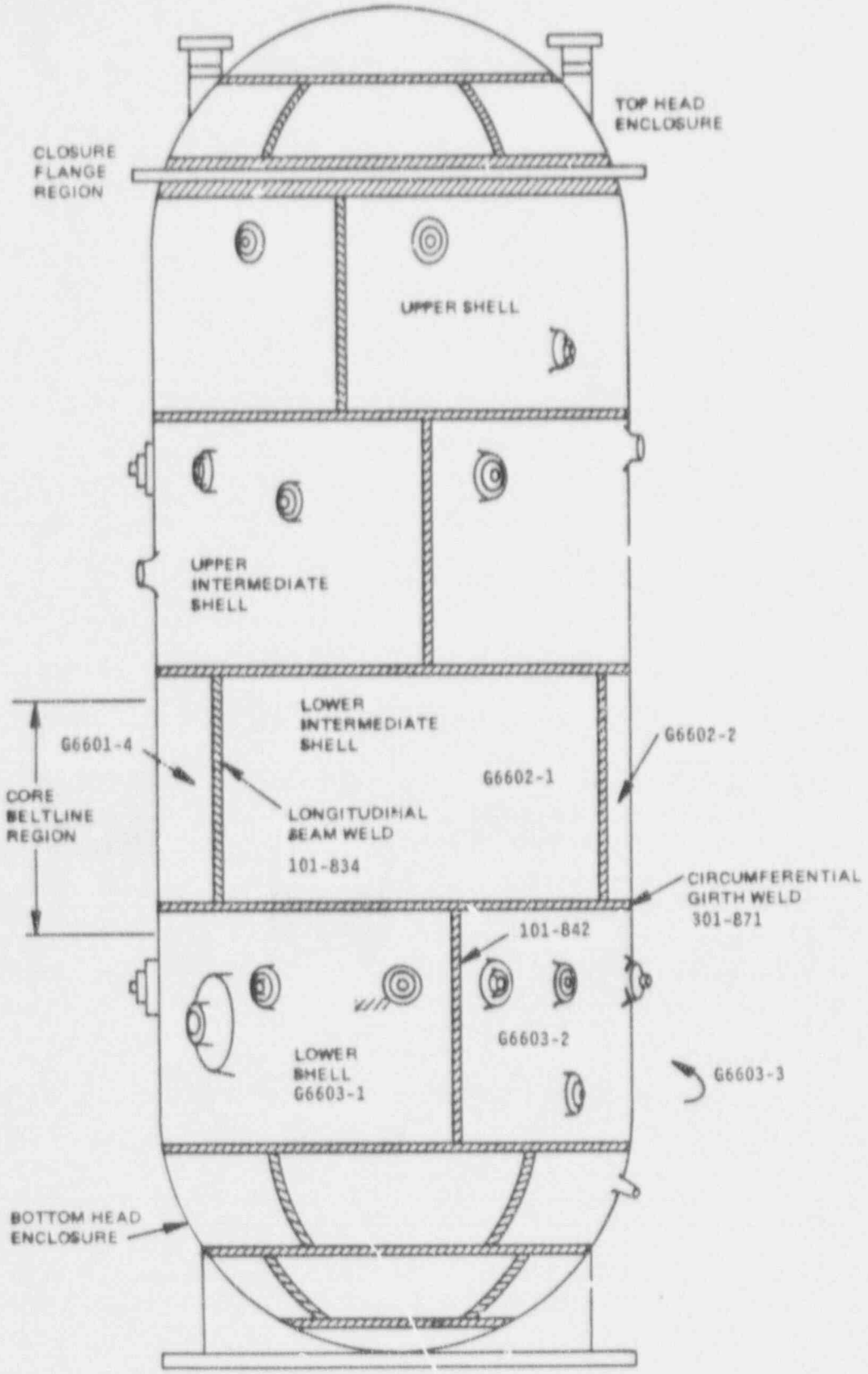

Figure 3-2. Schematic of the RPV Showing Arrangement of Vessel Plates and Welds

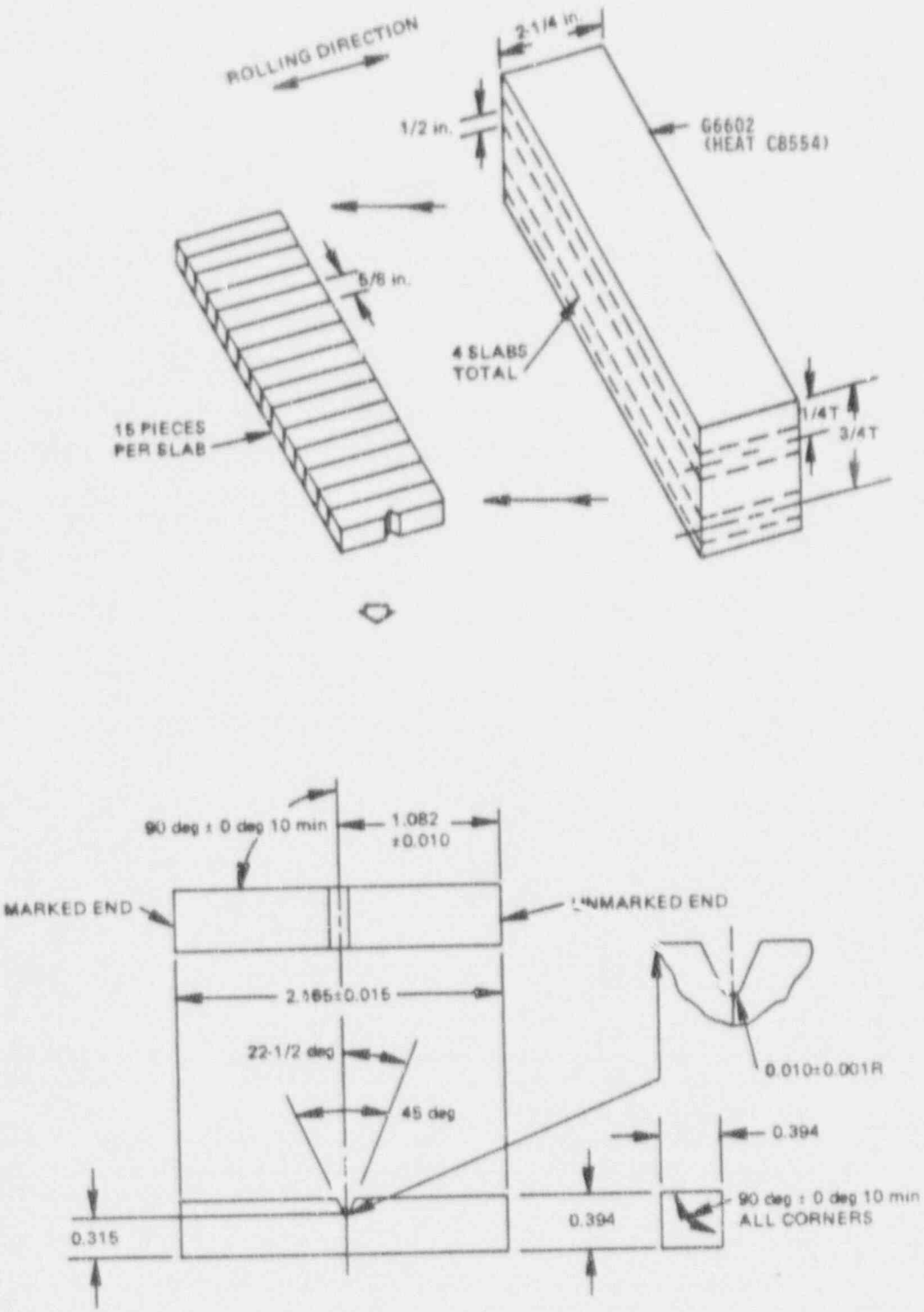

Figure 3-3. Fabrication Method for Base Metal Charpy Specimens

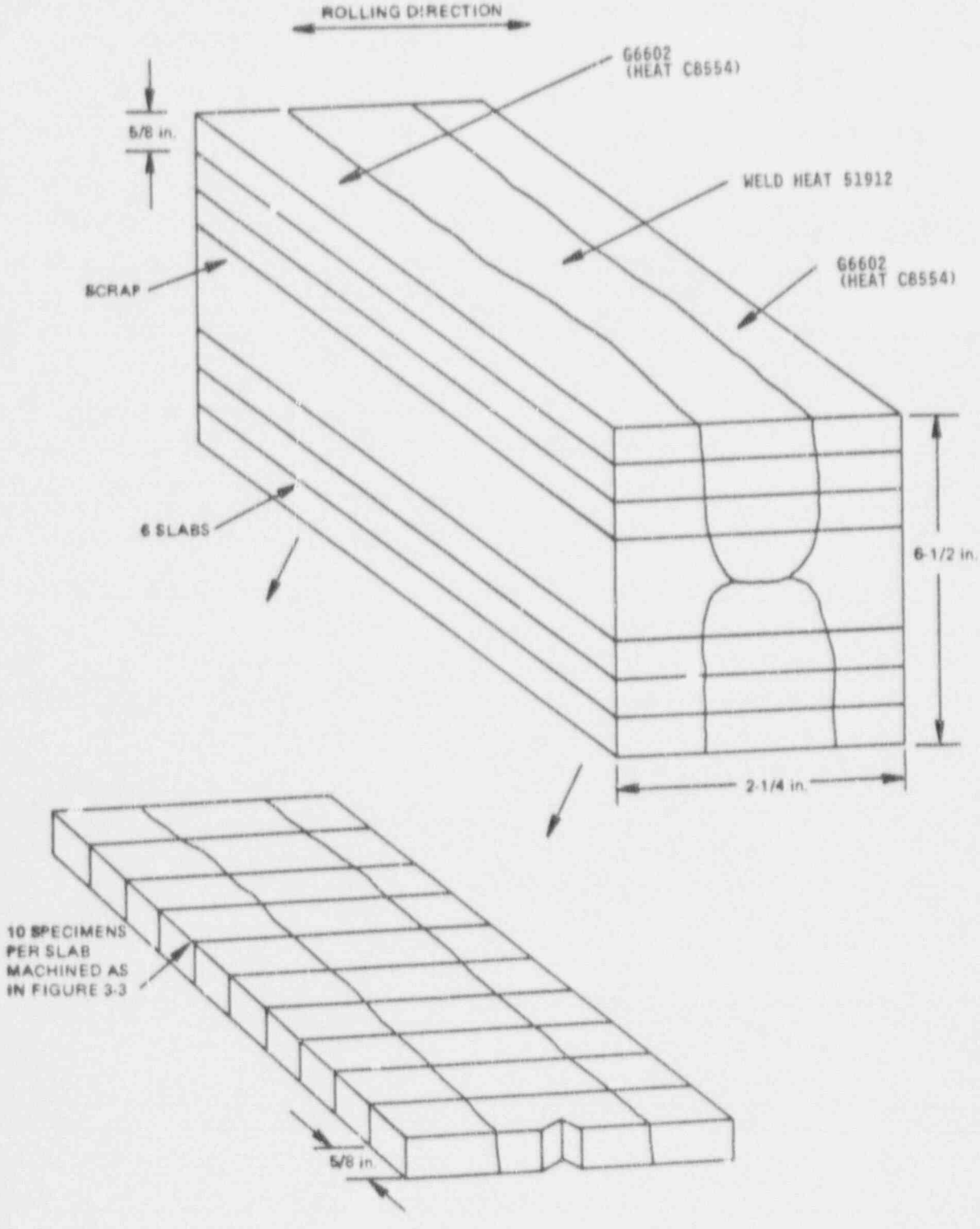

Figure 3-4. Fabrication Method for Weld Metal Charpy Specimens

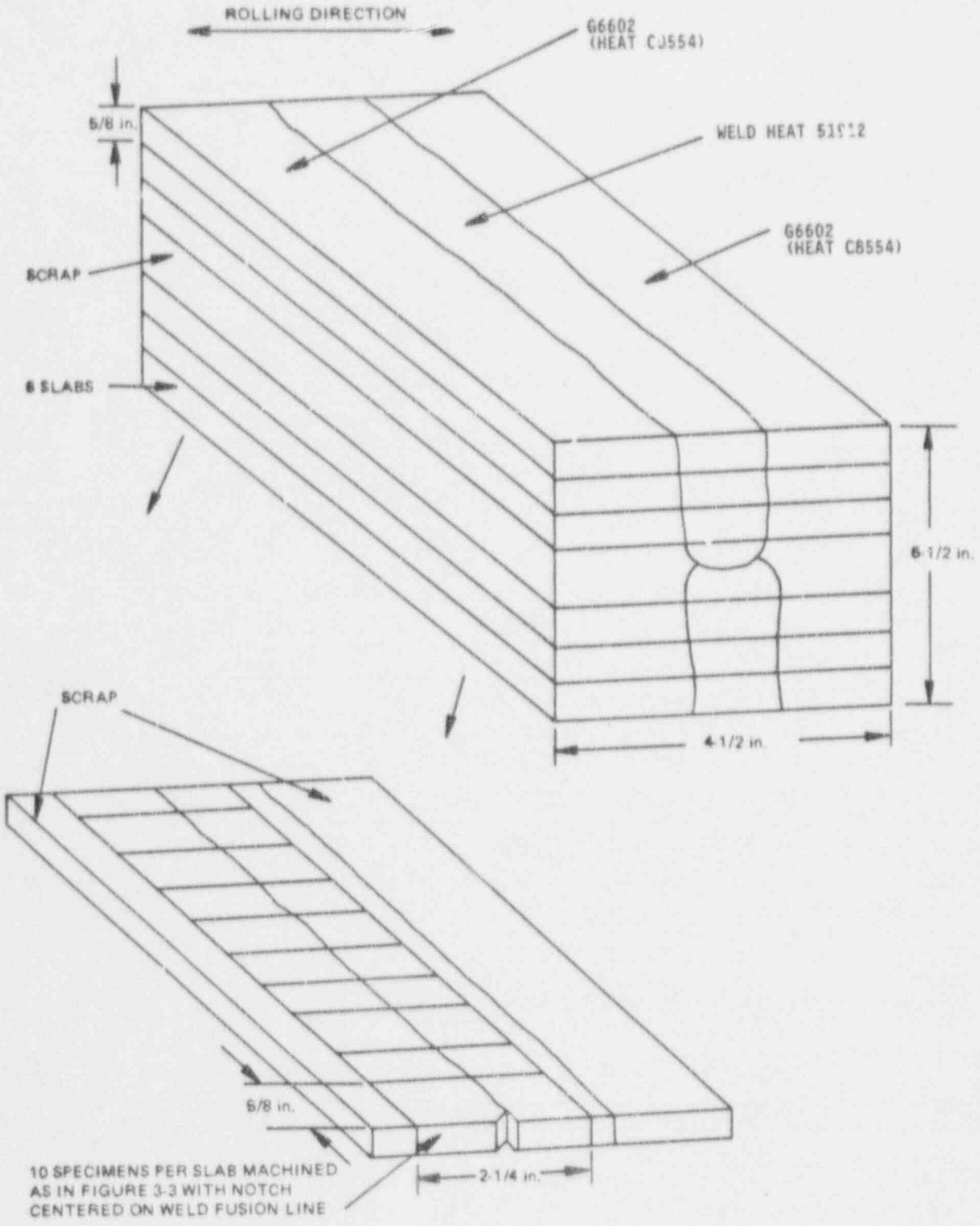

Figure 3-5. Fabrication Method for HAZ Charpy Specimens

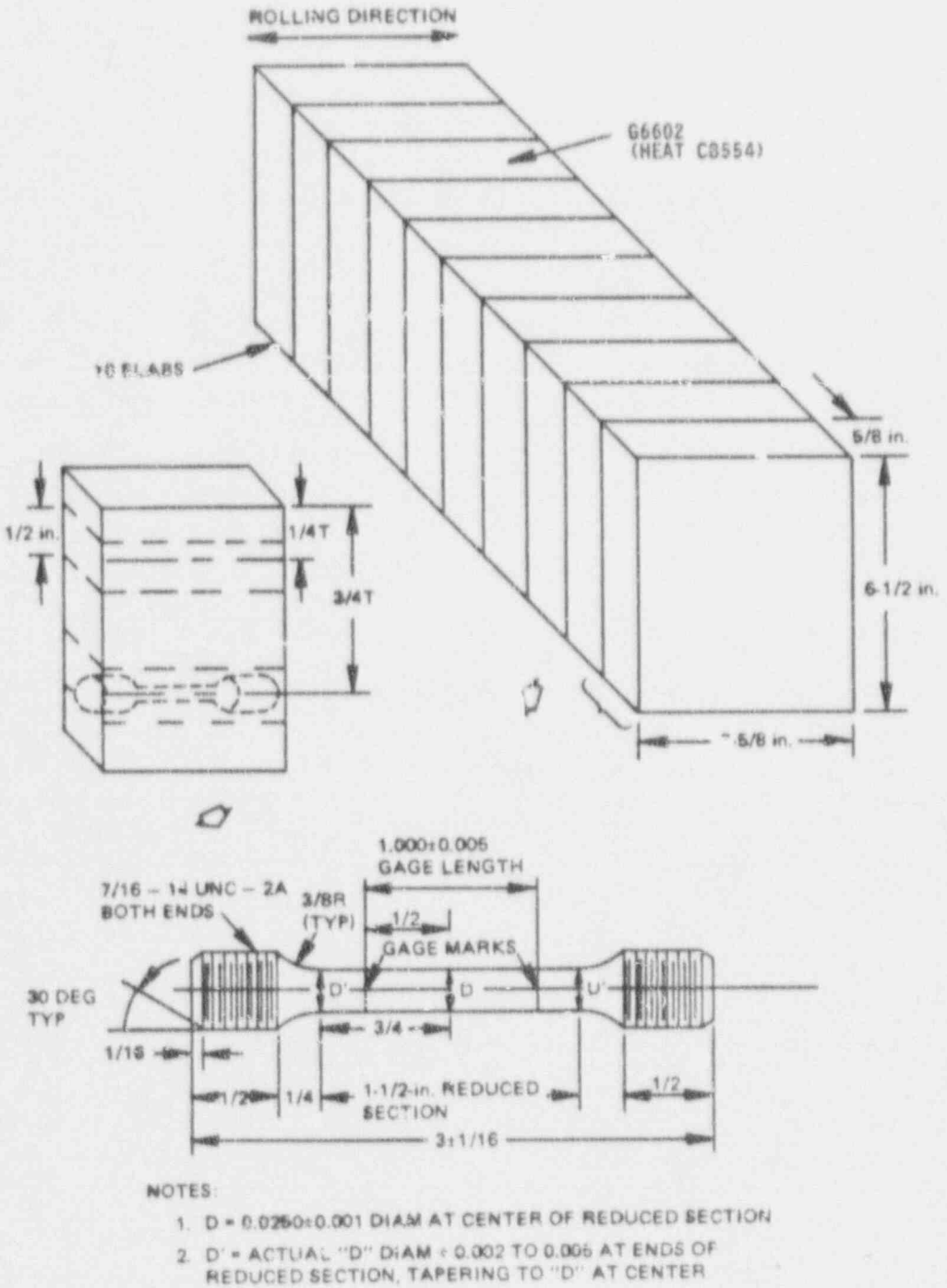

NOTES:

1. D = 0.0250±0.001 DIAM AT CENTER OF REDUCED SECTION
2. D' = ACTUAL "D" DIAM + 0.002 TO 0.006 AT ENDS OF REDUCED SECTION, TAPERING TO "D" AT CENTER

Figure 3-6. Fabrication Method for Base Metal Tensile Specimens

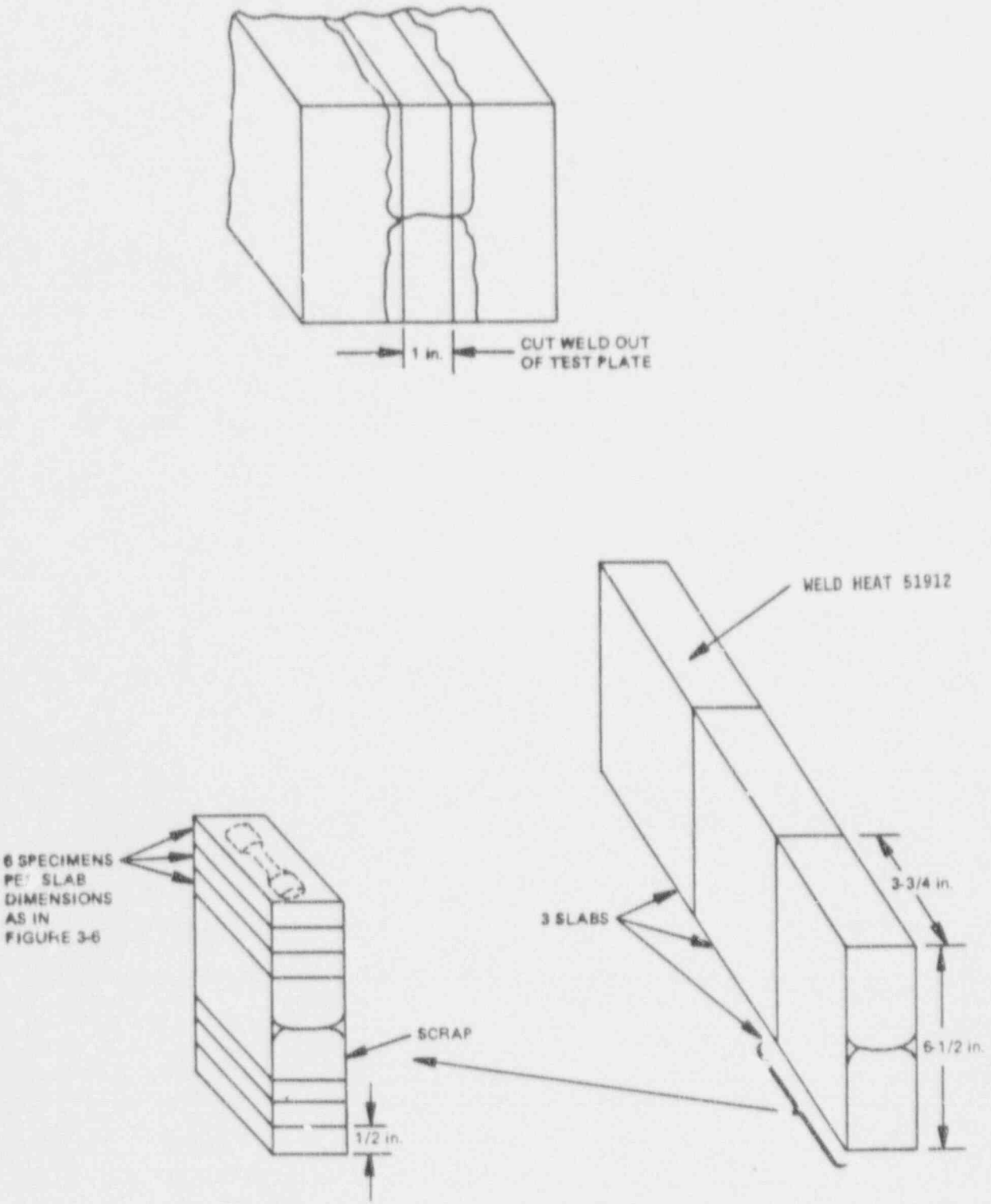

Figure 3-7. Fabrication Method for Weld Metal Tensile Specimens

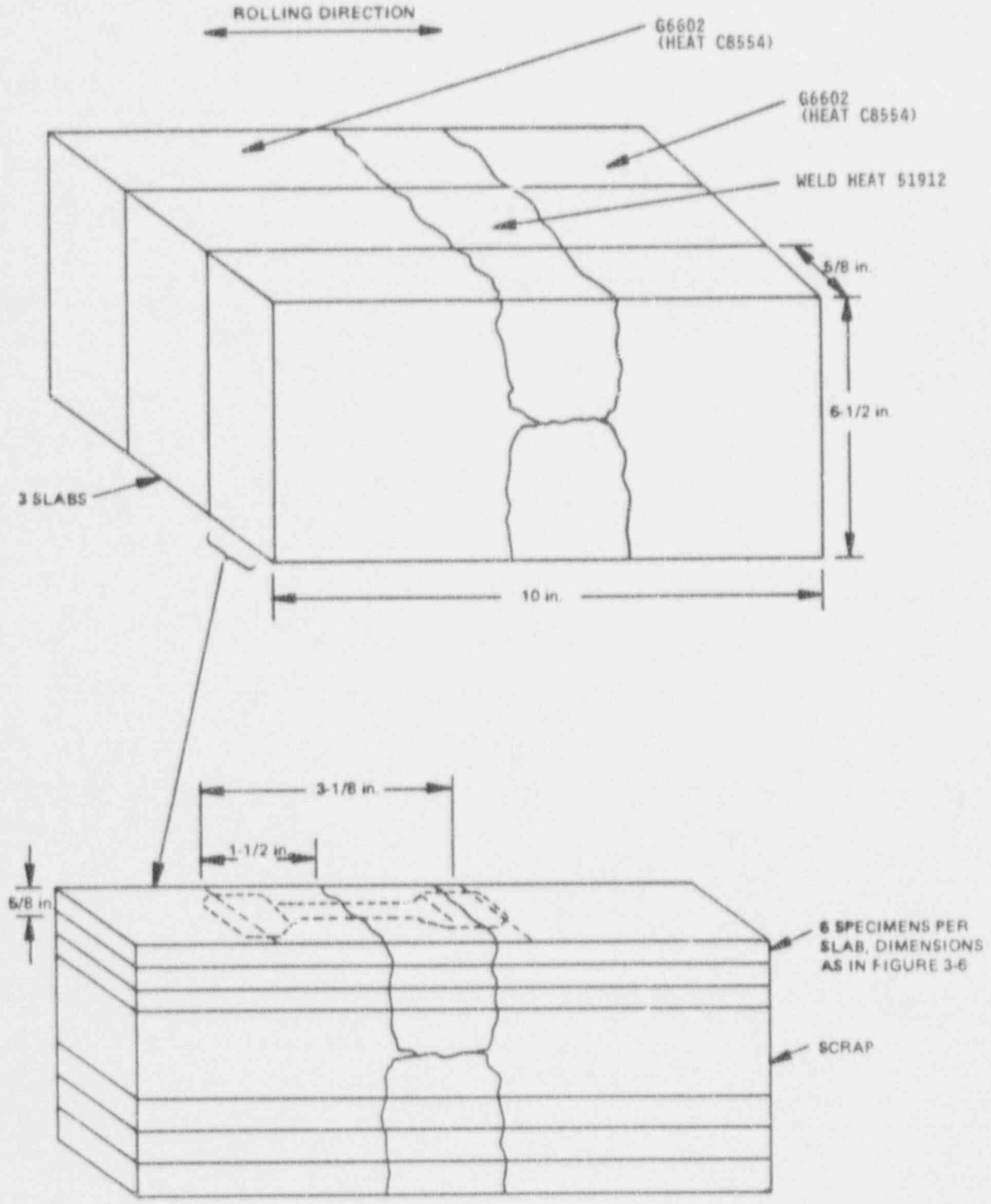

Figure 3-8. Fabrication Method for HAZ Tensile Specimens

4. PEAK RPV FLUENCE EVALUATION

Flux wires were analyzed to determine flux and fluence received by the surveillance capsule. An analysis combining two-dimensional and one-dimensional flux distribution computer calculations done for Hatch Unit 1 (Reference 9) was evaluated to establish the location of peak vessel fluence and the lead factors of the Unit 2 surveillance capsule relative to the peak vessel location.

4.1 FLUX WIRE ANALYSIS

4.1.1 Procedure

The Unit 2 surveillance capsule contained 9 flux wires: three iron, three copper and three nickel. Each wire was removed from the capsule, cleaned with dilute acid, weighed, mounted on a counting card, and analyzed for its radioactivity content by gamma spectrometry. Each iron wire was analyzed for Mn-54 content, each copper wire for Co-60 and each nickel wire for Co-58 at a calibrated 4-cm or 10-cm source-to-detector distance with 100-cc and 80-cc Ge(Li) detector systems.

To properly predict the flux and fluence at the surveillance capsule from the activity of the flux wires, the periods of full and partial power irradiation and the zero power decay periods were considered. Operating days for each fuel cycle and the reactor average power fraction are shown in Table 4-1. Zero power days between fuel cycles are listed as well.

From the flux wire activity measurements and power history, reaction rates for Fe-54 (n,p) Mn-54, Cu-63 (n,α) Co-60 and Ni-58 (n,p) Co-58 were calculated. The >1 MeV fast flux reaction cross sections for the iron, copper and nickel wires were estimated to be 0.177 barn, 0.00309 barn and 0.230 barn, respectively. These values were obtained from measured cross section functions determined at GE's Vallecitos Nuclear Center from more than 65 spectral determinations for BWRs and for the General Electric Test Reactor using activation monitors and spectral unfolding techniques. These data functions are applied to BWR pressure vessel locations based on water gap

(fuel to vessel wall) distances. The cross sections for >0.1 MeV flux were determined from the measured 1-to-0.1 MeV cross section ratio of 1.6.

4.1.2 Results

The measured activity, reaction rate and determined full-power flux results for the surveillance capsule are given in Table 4-2. The >1 MeV flux value of 1.12×10^9 n/cm^2-s from the flux wires was calculated by dividing the reaction rate measurement data by the appropriate cross sections. The corresponding fluence results, 2.3×10^{17} n/cm^2 (>1 MeV) was obtained by multiplying the full-power flux density values by the product of the total time of irradiation and the full power fraction, shown in Table 4-1.

Generally, for long-term irradiations, dosimetry results from copper flux wires are considered the most accurate because of Co-60's long half-life (5.27 years). The iron flux monitor reaction yielding Mn-54 gave results very consistent with the copper reaction despite the shorter half-life of 312.5 days for Mn-54. Nickel wire results are least accurate, because of the 70.8 day half life of Co-58. The nickel wire data is not factored into the evaluation of vessel flux, because of its isotope's short half life. The consistency in results between the iron and copper wire results indicates an accurate power-history evaluation and a consistent core radial power shape.

The accuracies of the values in Tables 4-2 for a 2σ deviation are estimated to be:

± 5% for dps/g (disintegrations per second per gram)
± 10% for dps/nucleus (saturated)
± 25% for flux and fluence >1 MeV
± 35% for flux and fluence >0.1 MeV

Flux wires from Unit 1 were evaluated by General Electric in 1985 (Reference 9). The >1 MeV flux value was 1.3×10^9 n/cm^2-s. The results from this study are only 14% lower, indicating that the plants, which have the same diameter and number of fuel bundles, are in fact accumulating approximately the same vessel wall fluences.

4.2 DETERMINATION OF LEAD FACTORS

The flux wires detect flux at a single location. The wires will therefore reflect the power fluctuations associated with the operation of the plant. However, the flux wires are not necessarily at the location of peak vessel flux. Lead factors are required to relate the flux at the wires' location to the peak flux. These lead factors are a function of the core and vessel geometry and of the distribution of bundles in the core. Lead factors were generated for the Unit 1 geometry in 1985, using a typical fuel cycle to determine power shape. Based on a review of core management and the similarity of the Unit 1 and 2 flux wire results, it is appropriate to use the lead factors calculated in Reference 9 to compute the peak location flux for Unit 2. The methods used to calculate the lead factors in Reference 9 are discussed below.

4.2.1 Procedure

Determination of the lead factor for the RPV inside wall was made using a combination of one-dimensional and two-dimensional finite difference computer analysis. The two-dimensional analysis established the relative fluence in the azimuthal direction at the vessel surface. A series of one-dimensional analyses were done to determine the core height of the axial flux peak and its relationship to the surveillance capsule height. The combination of azimuthal and axial distribution results provides the ratio of flux, or the lead factor, between the surveillance capsule location and the peak flux location.

The two-dimensional DOT IV computer program was used to solve the Boltzman transport equation using the discrete ordinate method on an (R,θ) geometry, assuming a fixed source. Quarter core symmetry was used with reflective boundary conditions at 0° and 90°. Neutron cross sections were determined for 26 energy groups, with angular scattering approximated by a third-order Legendre expansion. A schematic of the two-dimensional vessel model is shown in Figure 4-1. A total of 99 radial intervals and 90 azimuthal intervals was used. The model consists of an inner and outer core region, the shroud, water regions inside and outside the shroud, the vessel wall and the drywell. Flux as a function of azimuth was calculated, establishing the

azimuth of the peak flux and its magnitude relative to the flux at the surveillance capsule azimuth of 30°.

The one-dimensional computer code (SN1D) was used to calculate radial flux distribution at several core elevations at the azimuth angle of 45°, where the edge of the core is closest to the vessel wall. The elevation of the peak flux was determined, as well as its magnitude relative to the flux at the surveillance capsule elevation.

4.2.2 Results

The two-dimensional calculation in Reference 9 indicated the flux to be a maximum 45° past the RPV quadrant references (0°, 90°, etc.), at an elevation about 106 inches above the bottom of active fuel. The peak closest to the 30° location of the surveillance capsules removed is at 45°. The distribution calculations establish the lead factor between the surveillance capsule location and the peak location at the inner vessel wall. This lead factor is 0.79. The fracture toughness analysis is based on a 1/4 T depth flaw in the beltline region, so the attenuation of the flux to that depth is considered. This attenuation is calculated according to the requirements in Regulatory Guide 1.99, Revision 2 (Reference 5), as shown in the next subsection.

4.3 ESTIMATE OF 32 EFPY FLUENCE

The inside surface fluence (f_{surf}) at 32 EFPY is determined from the best estimate of the measured flux from Table 4-2, using the lead factor in Section 4.2. The time period 32 EFPY, typically assumed for 40-year operation (80% capacity factor) is 1.01×10^9 seconds. The resulting 32 EFPY fluence value at the vessel inside surface is:

$$f_{surf} = (1.12 \times 10^9 \text{ n/cm}^2\text{-s})(1.01 \times 10^9 \text{ s})/0.79$$

$$f_{surf} = 1.4 \times 10^{18} \text{ n/cm}^2.$$

The 1/4 T fluence (f) is calculated according to the following equations from Reference 5:

$$f = f_{surf}(e^{-0.24x}) \qquad (4\text{-}1)$$

where x = distance, in inches, from the inside surface to the 1/4 T depth.

The vessel beltline consists of the lower-intermediate shell, with a thickness of 5.38 inches, and the lower shell, with a thickness of 6.38 inches. For the thickness of 5.38 and 6.38 inches, the corresponding depths x are 1.35 and 1.60 inches, respectively. Equation 4-1 evaluated for Unit 2 is:

$f = 0.7241\ f_{surf}$ for the lower-intermediate shell, and

$f = 0.6819\ f_{surf}$ for the lower shell.

The 1/4 T values of 32 EFPY fluence, assuming that the peak inside surface fluence applies at both shells' elevations, are as follows:

Lower-Intermediate Shell: $f = 1.0 \times 10^{18}$ n/cm^2

Lower Shell: $f = 9.5 \times 10^{17}$ n/cm^2

Table 4-1

SUMMARY OF DAILY POWER HISTORY

Cycle	Cycle Dates	Operating Days	Percent of Full Power	Days Between Cycles
1	10/01/78 - 11/1/80	763	0.499	
				110
2	2/20/81 - 2/19/82	365	0.783	
				90
3	5/21/82 - 4/4/83	319	0.746	
				100
4	7/14/83 - 1/13/84	184	0.798	
				228
5	8/29/84 - 4/5/85	220	0.804	
				46
6	5/22/85 - 9/18/86	485	0.811	
				79
7	12/7/86 - 1/13/88	403	0.833	
				63
8	3/17/88 - 9/3/89	536	0.831	
		3275	0.734 (average)	

Table 4-2
SURVEILLANCE CAPSULE FLUX AND FLUENCE
FOR IRRADIATION FROM 10/1/78 TO 9/3/89

Wire (Element)	Wire Weight (g)	dps/g Element (at end of Irradiation)	Reaction Rate [dps/nucleus (saturated)]	Full Power Flux [a] (n/cm^2-s) >1 MeV	Full Power Flux [a] (n/cm^2-s) >0.1 MeV	Fluence (n/cm^2) >1 MeV	Fluence (n/cm^2) >0.1 MeV
Copper 65146	0.3268	1.13×10^{4}	3.50×10^{-18}				
Copper 65147	0.3344	1.19×10^{4}	3.68×10^{-18}				
Copper 65148	0.3221	1.21×10^{4}	3.74×10^{-18}				
			Average = 3.64×10^{-18}	1.18×10^{9}	1.9×10^{9}	2.4×10^{17}	3.9×10^{17}
Iron 65146	0.1386	9.03×10^{4}	1.87×10^{-16}				
Iron 65147	0.1229	9.10×10^{4}	1.88×10^{-16}				
Iron 65148	0.1260	9.24×10^{4}	1.91×10^{-16}				
			Average = 1.89×10^{-16}	1.07×10^{9}	1.7×10^{9}	2.2×10^{17}	3.5×10^{17}
Nickel 65146	0.3143	1.24×10^{6}	2.14×10^{-16}				
Nickel 65147	0.3147	1.28×10^{6}	2.20×10^{-16}				
Nickel 65148	0.3086	1.27×10^{6}	2.18×10^{-16}				
			Average = 2.17×10^{-16}	9.4×10^{8}	1.5×10^{9}	2.0×10^{17}	3.1×10^{17}
			Average of Copper and Iron =	1.12×10^{9}	1.8×10^{9}	2.3×10^{17}	3.7×10^{17}

[a] Full power of 2436 MW_t.

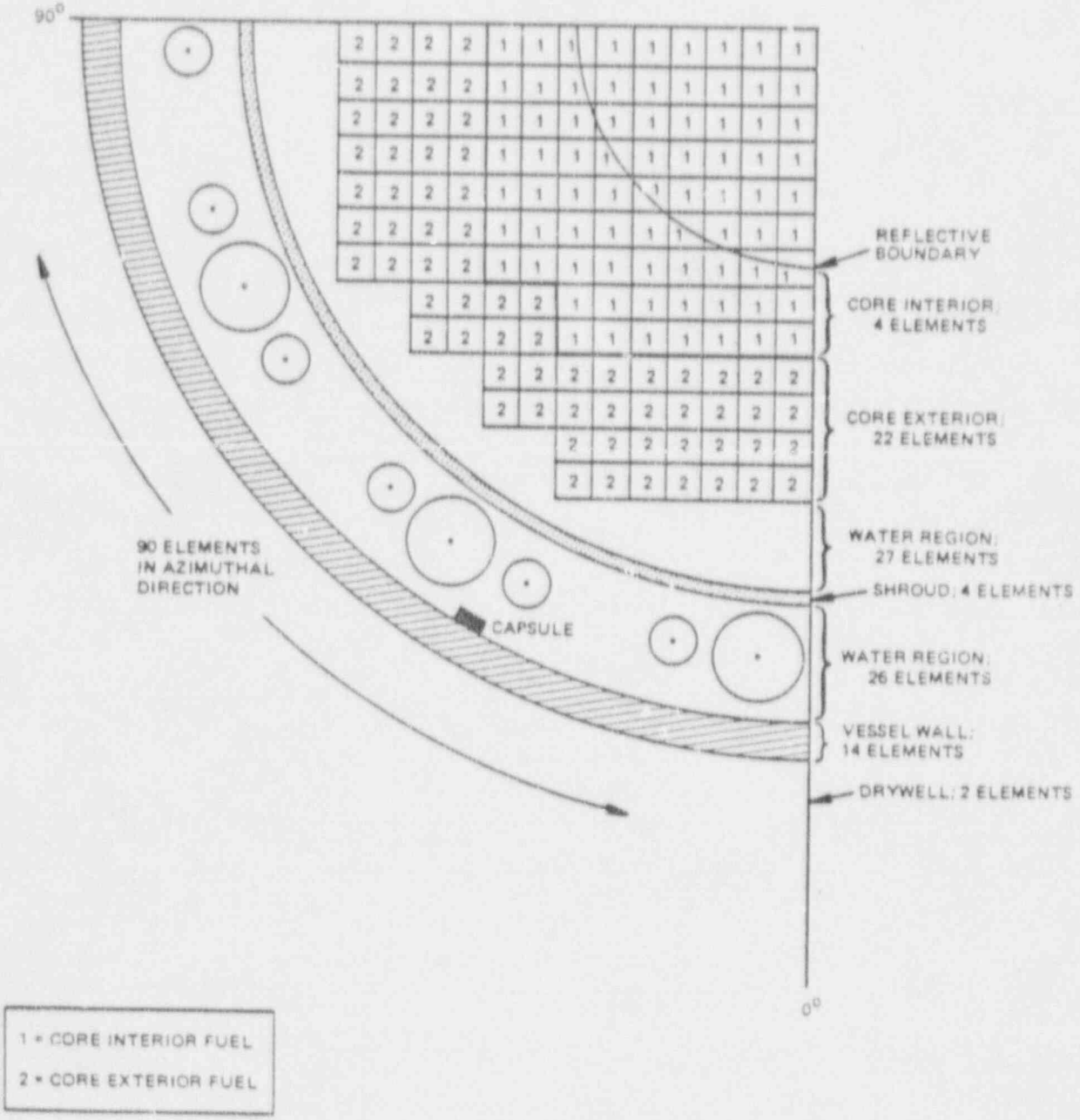

Figure 4-1. Schematic of Model for Two-Dimensional Flux Distribution Analysis

5. CHARPY V-NOTCH IMPACT TESTING

The 36 Charpy specimens recovered from the Unit 2 surveillance capsule were impact tested at temperatures selected to establish the toughness transition and upper shelf of the irradiated RPV materials. In addition, unirradiated base and weld metal specimens recovered from the Hatch site were tested for baseline data. Testing was conducted in accordance with ASTM E23-82 (Reference 10).

5.1 IMPACT TEST PROCEDURE

The Vallecitos testing machine used for irradiated specimens was a Riehle Model PL-2 impact machine, serial number P-89916. The pendulum has a maximum velocity of 15.44 ft/sec and a maximum available hammer energy of 240 ft-lb. The San Jose test machine used for unirradiated specimens was a Tinius-Olsen impact machine, serial number 119037. The pendulum has a maximum velocity of 16.8 ft/sec and a maximum available hammer energy of 264 ft-lb.

The test apparatus and operator were qualified using NIST standard reference material specimens. The standards are designed to fail both at a specified energy at the test temperature of -40°F. According to Reference 10, the test apparatus averaged results must reproduce the NIST standard values within an accuracy of ±5% or ±1.0 ft-lb, whichever is greater. The qualification of the Riehle machine and operator is summarized in Table 5-1. The calibration results for the low energy specimens are 0.4 ft-lb higher than the allowable variation in Reference 10. This is due to the occasional "kickback" of a broken specimen half contacting the hammer, which is only significant to the Charpy results at very low energies. Since the kickbacks have little effect on the results, especially compared to the typical scatter in the data, no correction to the test results was made. The calibration results of the Tinius-Olson machine, which were within specifications, are shown in Table 5-2.

Charpy V-Notch tests were conducted at temperatures between -100°F and 400°F. For tests below 70°F methanol was used as the cooling fluid. Between 70°F and 212°F water was used as the temperature conditioning fluid. The specimens were heated in oil above 212°F. Cooling of the conditioning fluids was done with liquid nitrogen, and heating by an immersion heater. The fluids were mechanically stirred to maintain uniform temperatures. The fluid temperature was measured with a calibrated thermocouple. Once at test temperature, the specimens were manually transferred with centering tongs to the Charpy test machine and impacted within 5 seconds.

For each Charpy V-Notch specimen the test temperature, energy absorbed, lateral expansion, and percent shear were evaluated. In addition, for the irradiated specimens, photographs were taken of each fracture surface pair. Lateral expansion and percent shear were measured according to Reference 10 methods. Percent shear was determined with method one of Subsection 11.2.4.3 of Reference 10, which involves measuring the length and width of the cleavage surface and locating the percent shear value from Tables 1 or 2 of Reference 10.

5.2 IMPACT TEST RESULTS

Twelve Charpy V-Notch specimens each of irradiated base, weld, and HAZ material were tested at temperatures (-60°F to 400°F) selected to define the toughness transition and upper shelf portions of the fracture toughness curves. The absorbed energy, lateral expansion, and percent shear data are listed for each material in Table 5-3. Plots of absorbed energy data for base, weld and HAZ materials are presented in Figures 5-1 through 5-3, respectively. Lateral expansion plots for base, weld and HAZ materials are presented in Figures 5-4 through 5-6, respectively. The fracture surface photographs and a summary of the test results for each specimen are contained in Appendix A.

Twelve Charpy V-Notch specimens each of unirradiated base and weld material were tested at temperatures (-150°F to 400°F) selected to define the toughness transition and upper shelf portions of the fracture toughness curves. The absorbed energy, lateral expansion, and percent shear data are listed for each material in Table 5-4. Plots of absorbed energy data for base and weld materials are presented in Figures 5-7 and 5-8, respectively, along with the corresponding irradiated specimen data. Lateral expansion plots for base and weld materials are presented in Figures 5-9 and 5-10, respectively, along with their corresponding irradiated specimen data.

The plate and weld data sets are fit with the hyperbolic tangent function developed by Oldfield for the EPRI Irradiated Steel Handbook (Reference 11):

$$Y = A + B * TANH [(T - T_0)/C],$$

where Y = impact energy or lateral expansion
T = test temperature, and
A, B, T_0 and C are determined by non-linear regression.

The TANH function is one of the few continuous functions with a shape characteristic of low alloy steel fracture toughness transition curves.

5.3 IRRADIATED VERSUS UNIRRADIATED CHARPY V-NOTCH PROPERTIES

As a part of the RPV surveillance test program, extra Charpy V-Notch specimens were fabricated and delivered to Hatch. These specimens were recovered from storage at the site and forwarded to GE for testing as described above.

The irradiated and unirradiated Charpy V-Notch data were used to estimate the values given in Table 5-5: 30 ft-lb, 50 ft-lb and 35 MLE index temperatures, and the USE for both irradiated materials and unirradiated materials. Transition temperature shift values are determined as the change in the temperature at which 30 ft-lb impact energy is achieved, as required in Reference 4. The results show very little shift due to irradiation of these materials.

5.4 COMPARISON TO PREDICTED IRRADIATION EFFECTS

5.4.1 Irradiation Shift

The measured transition temperature shift for the plate material was compared to the prediction calculated according to Regulatory Guide 1.99, Revision 2 (1.99). The 1.99 methods used to calculate shift are described in Section 7.6. The inputs for the surveillance materials are as follows:

Plate:	Copper:	0.08%
	Nickel:	0.63% (based on Table 3-3 values)
	1.99 CF:	51
	fluence:	2.3×10^{17} n/cm^2
Weld:	Copper:	0.13% (based on Table 3-3 values)
	Nickel:	0.12% (based on Table 3-3 values)
	1.99 CF:	68.8
	fluence:	2.3×10^{17} n/cm^2

CF shown above is the chemistry factors from Tables 1 or 2 of 1.99. The fluence factor is 0.1875. The predicted shifts are 9.6°F for the plate and 12.9°F for the weld. The upper bounds, including margin, are 19°F for the plate and 26°F for the weld. The measured shifts of 3°F for the plate and 0°F for the weld are less than the predicted shifts, so use of 1.99 methods to predict beltline shift appears to be conservative.

5.4.2 Decrease in USE

The measured decreases in USE are compared to prediction calculated according to 1.99. The methods for calculating predicted decrease in USE per 1.99 are described in Section 7.6. Using the copper and fluence data above with Figure 2 of 1.99, decreases of 7% for the plate and 11% for the weld are predicted. The measured values of 0% for the plate and -1% for the weld show that the 1.99 predictions are conservative.

Table 5-1

QUALIFICATION TEST RESULTS USING
NIST STANDARD REFERENCE SPECIMENS
(TESTED 3/5/90)

Specimen Identification	Bath Medium	Test Temperature (°F)	Energy Absorbed (ft-lb)	Acceptable Range (ft-lb)
MM-15 086	Methanol	-40	70.0	
MM-15 503	"	-40	69.0	
MM-15 364	"	-40	71.0	
MM-15 244	"	-40	67.5	
MM-15 326	"	-41	66.0	
	Average		68.7	70.5 ± 3.5
LL-18 105	Methanol	-40	12.5	
LL-18 246	"	-40	13.5	
LL-18 496	"	-41	13.5	
LL-18 1012	"	-40	12.5	
LL-18 040	"	-40	12.5	
	Average		12.9	11.5 ± 1.0

Table 5-2

SAN JOSE TINIUS-OLSON CHARPY MACHINE
QUALIFICATION TEST RESULTS USING
NIST STANDARD REFERENCE SPECIMENS
(TESTED 5/14/90)

Specimen Identification	Bath Medium	Test Temperature (°F)	Energy Absorbed (ft-lb)	Acceptable Range (ft-lb)
MM-16 307	Methanol	-40	71.0	
MM-16 465	"	-40	72.0	
MM-16 509	"	-40	75.0	
MM-16 552	"	-40	71.5	
MM-16 915	"	-40	73.0	
	Average		72.5	69.4 ± 3.5
LL-19 124	Methanol	-40	11.5	
LL-19 354	"	-40	11.5	
LL-19 411	"	-40	12.0	
LL-19 702	"	-40	10.5	
LL-19 925	"	-40	11.5	
	Average		11.4	11.9 ± 1.0

Table 5-3

CHARPY V-NOTCH IMPACT TEST RESULTS
FOR IRRADIATED RPV MATERIALS IN HATCH UNIT 2

	Specimen Identification	Test Temperature (°F)	Fracture Energy (ft-lb)	Lateral Expansion (mils)	Percent Shear (Method 1) (%)
Base:	P1-26833	-60	9.0	7.5	18
	P1-26829	-40	28.0	22.5	14
	P1-26832	-30	15.0	13.5	17
	P1-26835	-20	31.5	24.0	28
	P1-26834	0	36.5	28.0	20
	P1-26838	19	54.5	39.5	35
	P1-26836	40	71.5	53.0	56
	P1-26831	79	86.0	63.0	80
	P1-26837	120	115.0	76.0	100
	P1-26828	160	110.5	78.0	100
	P1-26839	201	107.0	71.0	100
	P1-26830	401	119.0	78.0	100
Weld:	P2-26850	-59	5.5	1.5	10
	P2-26848	-39	21.5	15.5	27
	P2-26842	-20	24.0	18.5	31
	P2-26844	-10	38.0	28.0	28
	P2-26840	0	61.0	43.0	40
	P2-26841	20	62.5	46.0	56
	P2-26851	40	50.5	43.0	45
	P2-26843	80	101.0	77.5	82
	P2-26845	120	122.5	95.0	96
	P2-26847	161	111.0	78.0	100
	P2-26849	199	126.0	87.0	100
	P2-26846	401	117.0	84.5	100
HAZ:	P3-26860	-60	23.5	17.0	21
	P3-26862	-60	47.0	30.5	27
	P3-26855	-41	32.0	23.0	26
	P3-26861	-20	27.0	22.0	24
	P3-26854	0	49.0	34.0	57
	P3-26853	19	75.5	53.5	62
	P3-26859	40	112.5	72.5	73
	P3-26863	80	53.0	48.0	65
	P3-26856	119	99.0	68.0	100
	P3-26852	160	107.5	74.0	100
	P3-26857	200	126.0	79.5	100
	P3-26858	401	118.0	85.0	100

Table 5-4

CHARPY V-NOTCH IMPACT TEST RESULTS

FOR UNIRRADIATED RPV MATERIALS IN HATCH UNIT 2

Specimen Identification		Test Temperature (°F)	Fracture Energy (ft-lb)	Lateral Expansion (mils)	Percent Shear (Method 1) (%)
Base:	P1-46	-100	5.5	0.5	10
	P1-46	-60	14.0	10.0	17
	P1-46	-40	26.0	20.0	30
	P1-46	-20	38.5	22.0	32
	P1-46	0	20.0	16.0	18
	P1-46	0	50.0	34.5	35
	P1-46	20	64.0	41.0	49
	P1-46	40	82.0	57.0	67
	P1-46	60	95.0	63.5	84
	P1-46	100	105.0	74.5	100
	P1-46	180	114.5	78.0	100
	P1-46	400	115.0	76.0	100
Weld:	P2-46	-100	6.0	0.0	12
	P2-46	-60	7.5	2.0	15
	P2-46	-40	12.0	9.5	25
	P2-46	-20	34.0	21.5	44
	P2-46	0	42.0	29.0	28
	P2-46	20	85.5	58.0	70
	P2-46	20	63.0	40.5	49
	P2-46	40	76.0	53.5	72
	P2-46	60	86.0	57.5	76
	P2-46	100	118.5	85.5	96
	P2-46	180	118.0	88.5	100
	P2-46	400	126.0	91.0	100

Table 5-5

SIGNIFICANT RESULTS OF IRRADIATED AND
UNIRRADIATED CHARPY V-NOTCH DATA FOR HATCH UNIT 2

Material	Index Temperature (°F) E=30 ft-lb	E=50 ft-lb	MLE=35 mil	Upper Shelf[a] Energy (ft-lb) L/T
Unirradiated Plate	-19	8	8	115/ 75
Irradiated Plate	-16	15	10	115/ 75
Difference	3	7	2	0/ 0 (0%)
Unirradiated Weld	-21	4	8	121
Irradiated Weld	-21	11	6	122
Difference	0	7	-2	-1 (-1%)

[a] Longitudinal (L) USE is from the data shown in Figure 5-7. Transverse (T) plate USE is taken as 65% of the longitudinal USE, according to Reference 12. L/T USE values are equal for weld metal, which has no orientation effect.

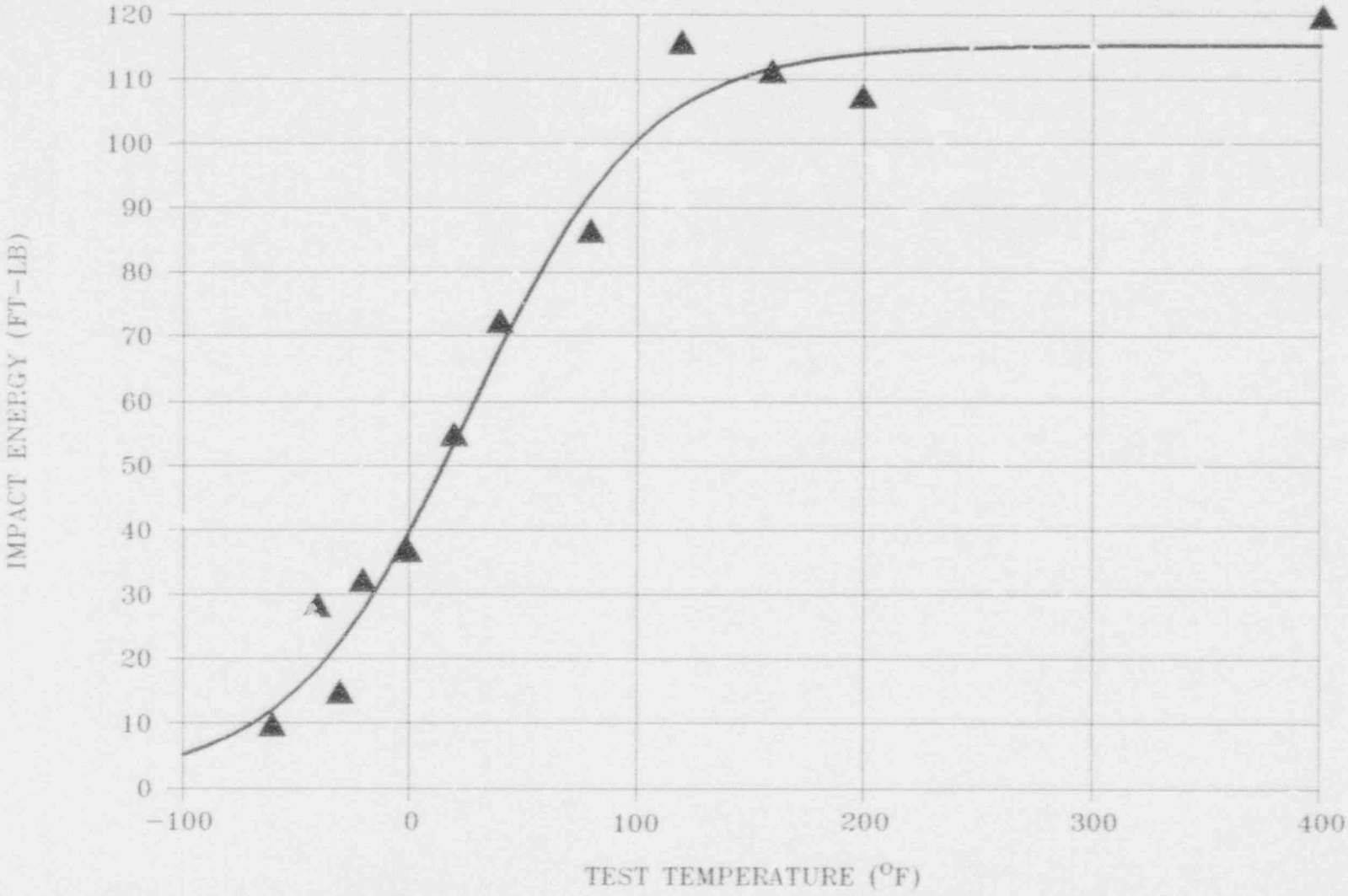

Figure 5-1. Hatch Unit 2 Irradiated Base Impact Energy

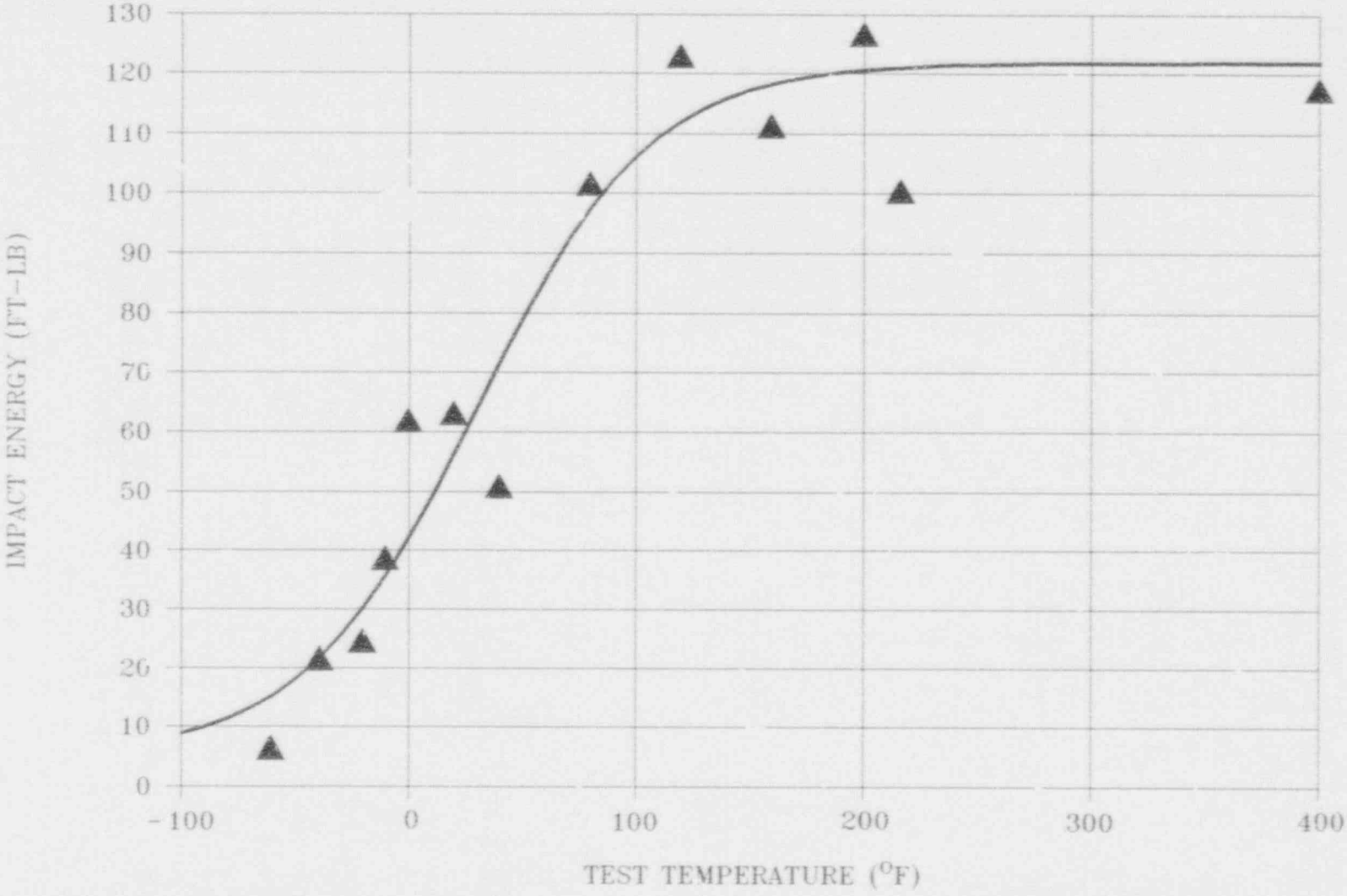

Figure 5-2. Hatch Unit 2 Irradiated Weld Impact Energy

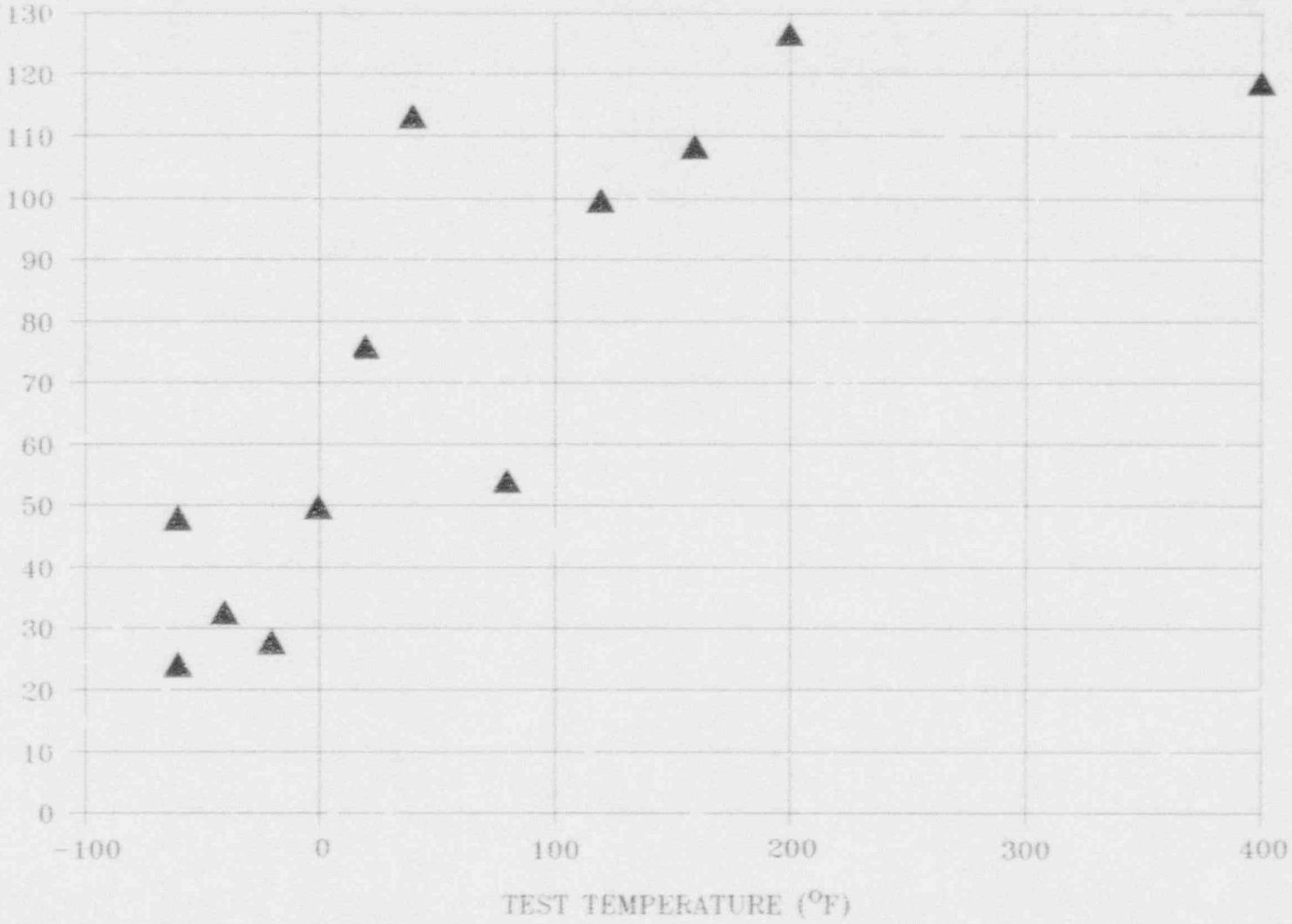

Figure 5-3. Hatch Unit 2 Irradiated HAZ Impact Energy

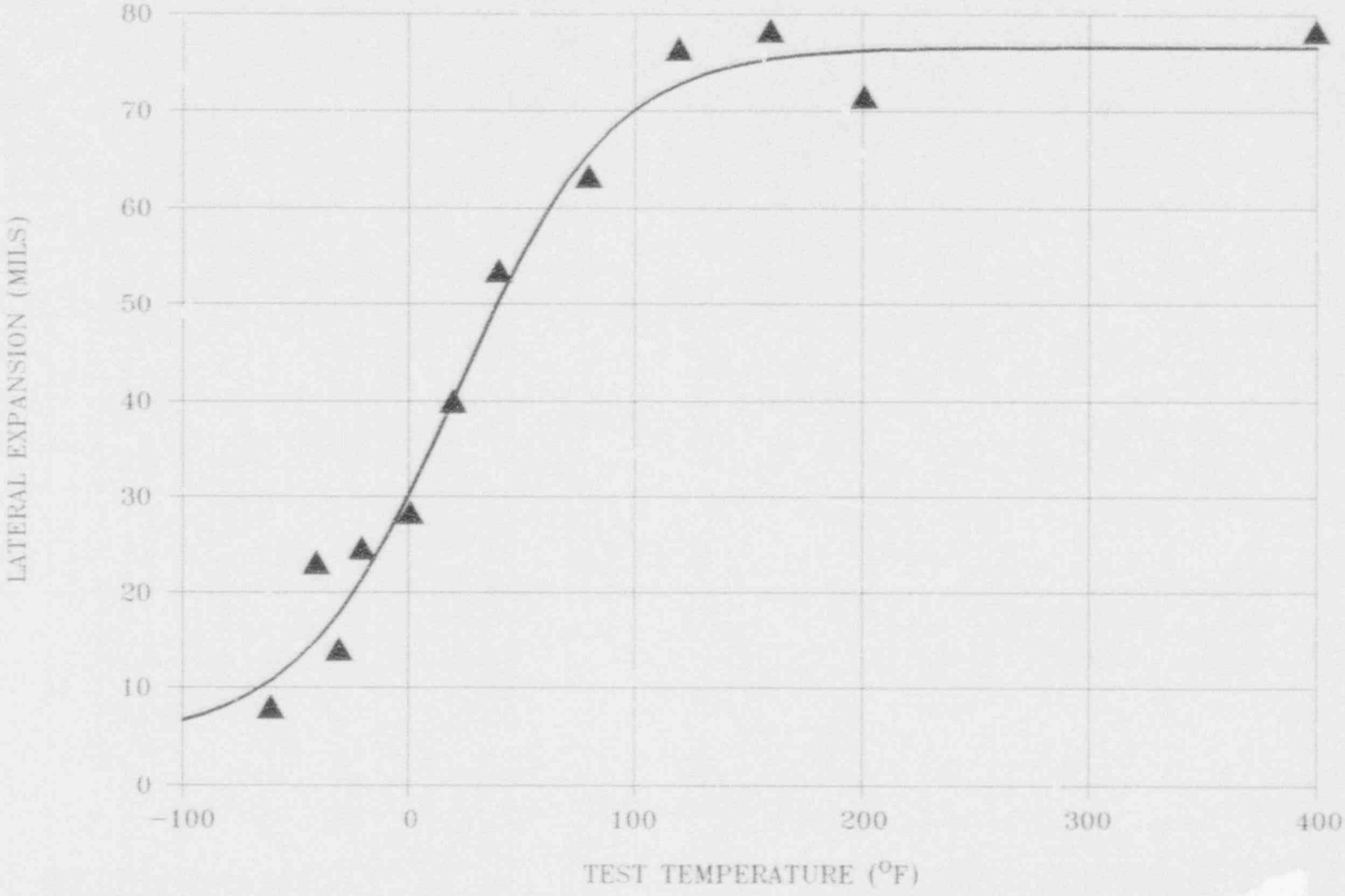

Figure 5-4. Hatch Unit 2 Irradiated Base Lateral Expansion

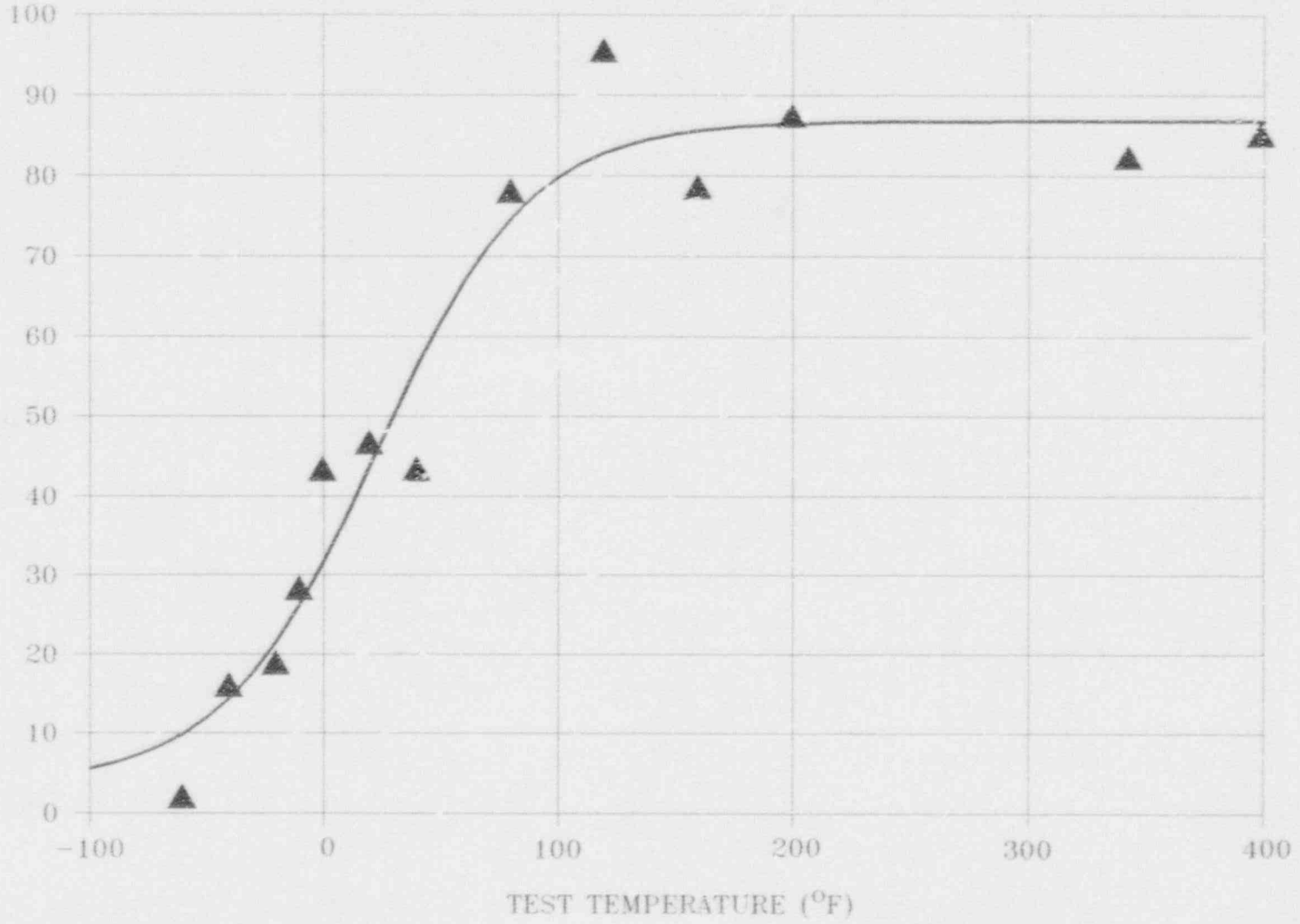

Figure 5-5. Hatch Unit 2 Irradiated Weld Lateral Expansion

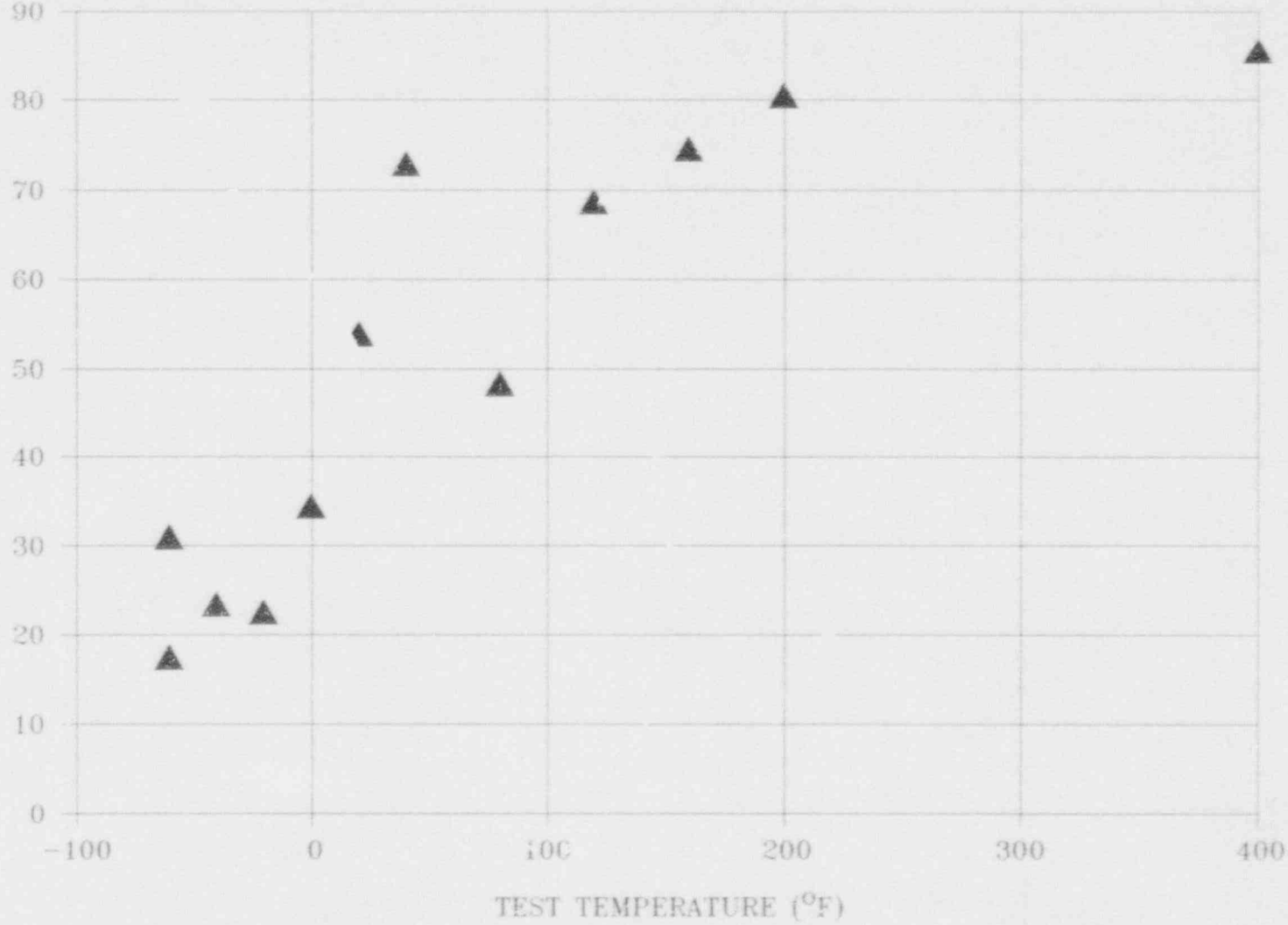

Figure 5-6. Hatch Unit 2 Irradiated HAZ Lateral Expansion

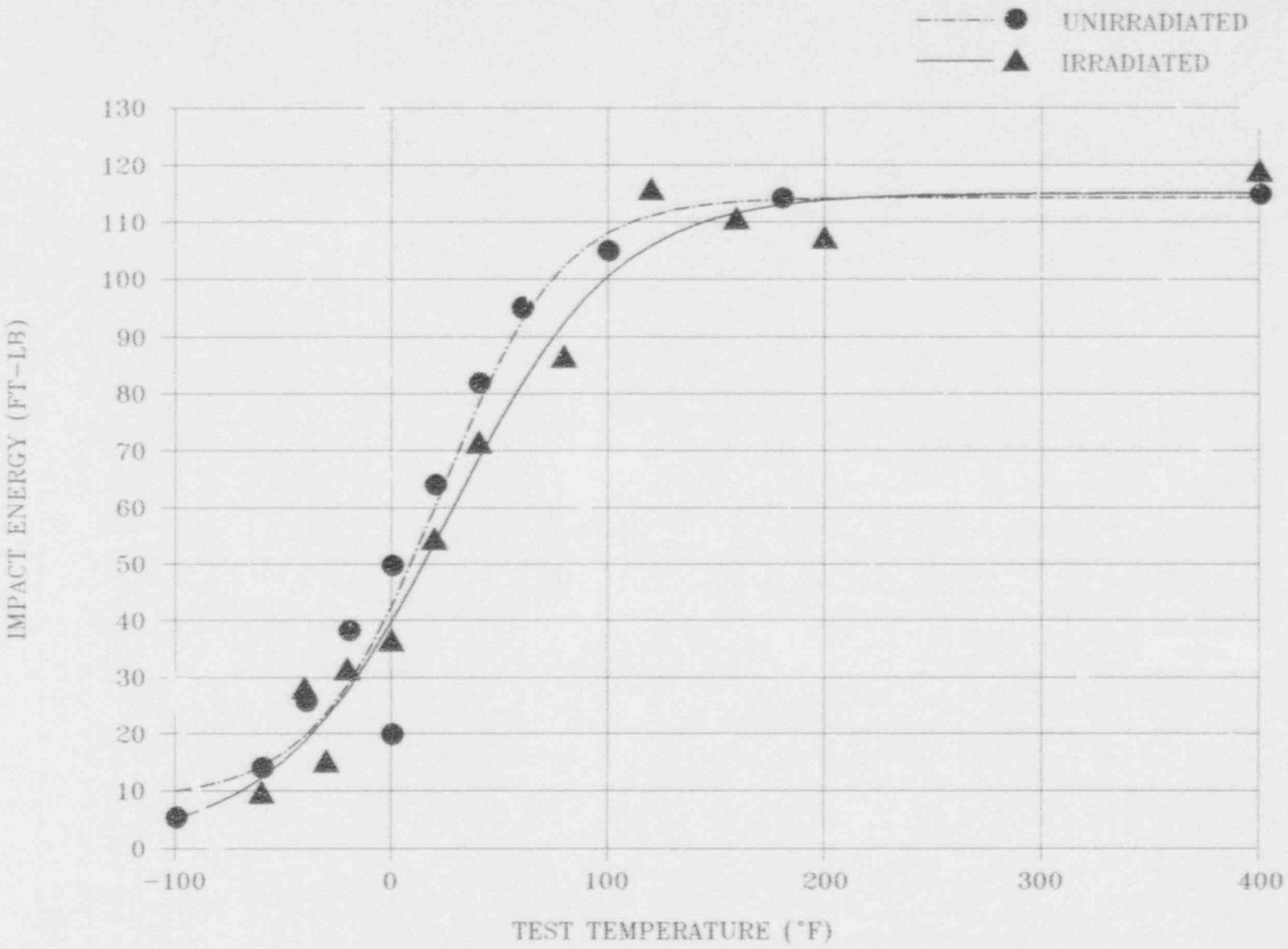

Figure 5-7. Hatch Unit 2 Irradiated & Unirradiated Base Impact Energy

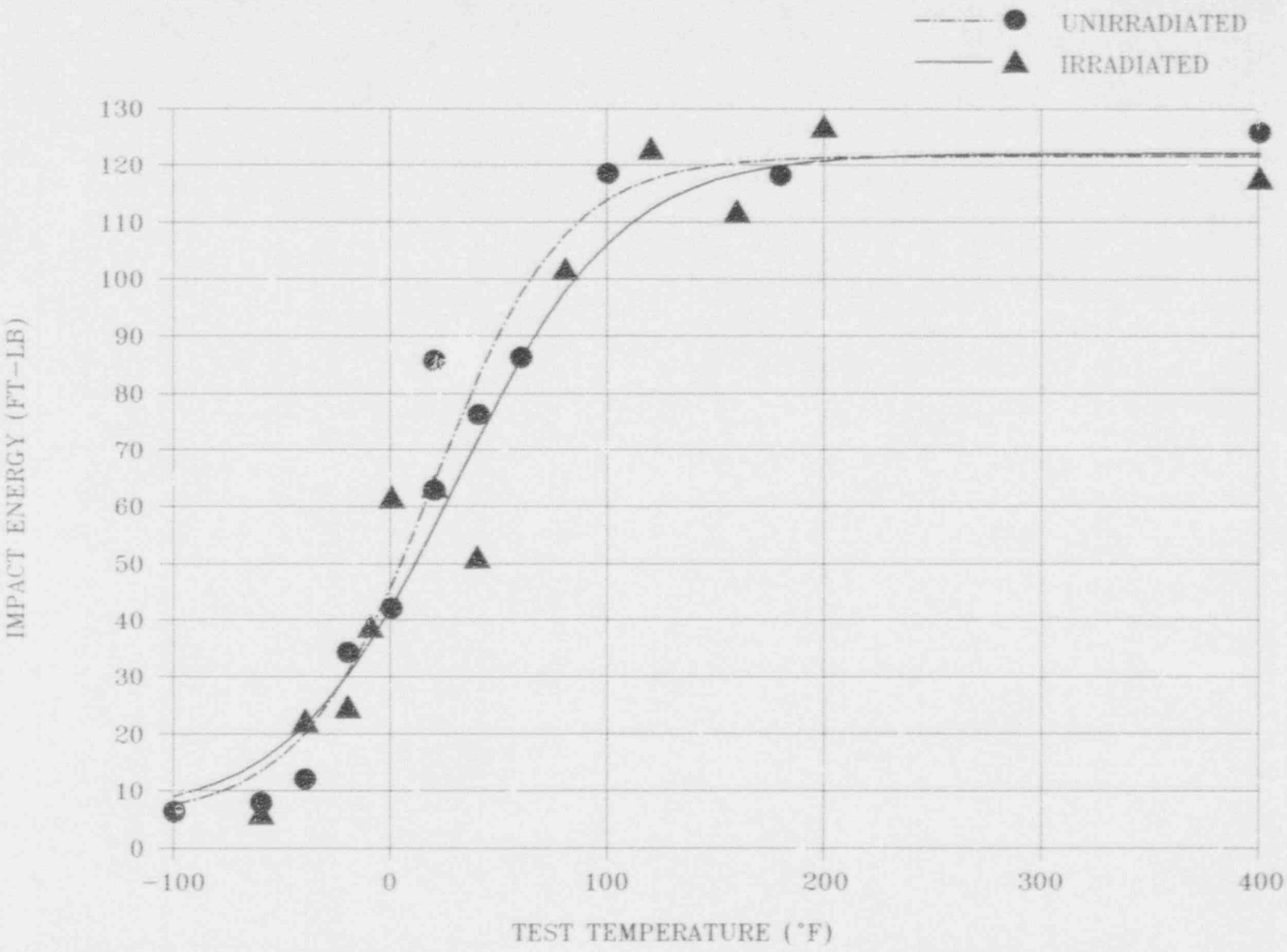

Figure 5-8. Hatch Unit 2 Irradiated & Unirradiated Weld Impact Energy

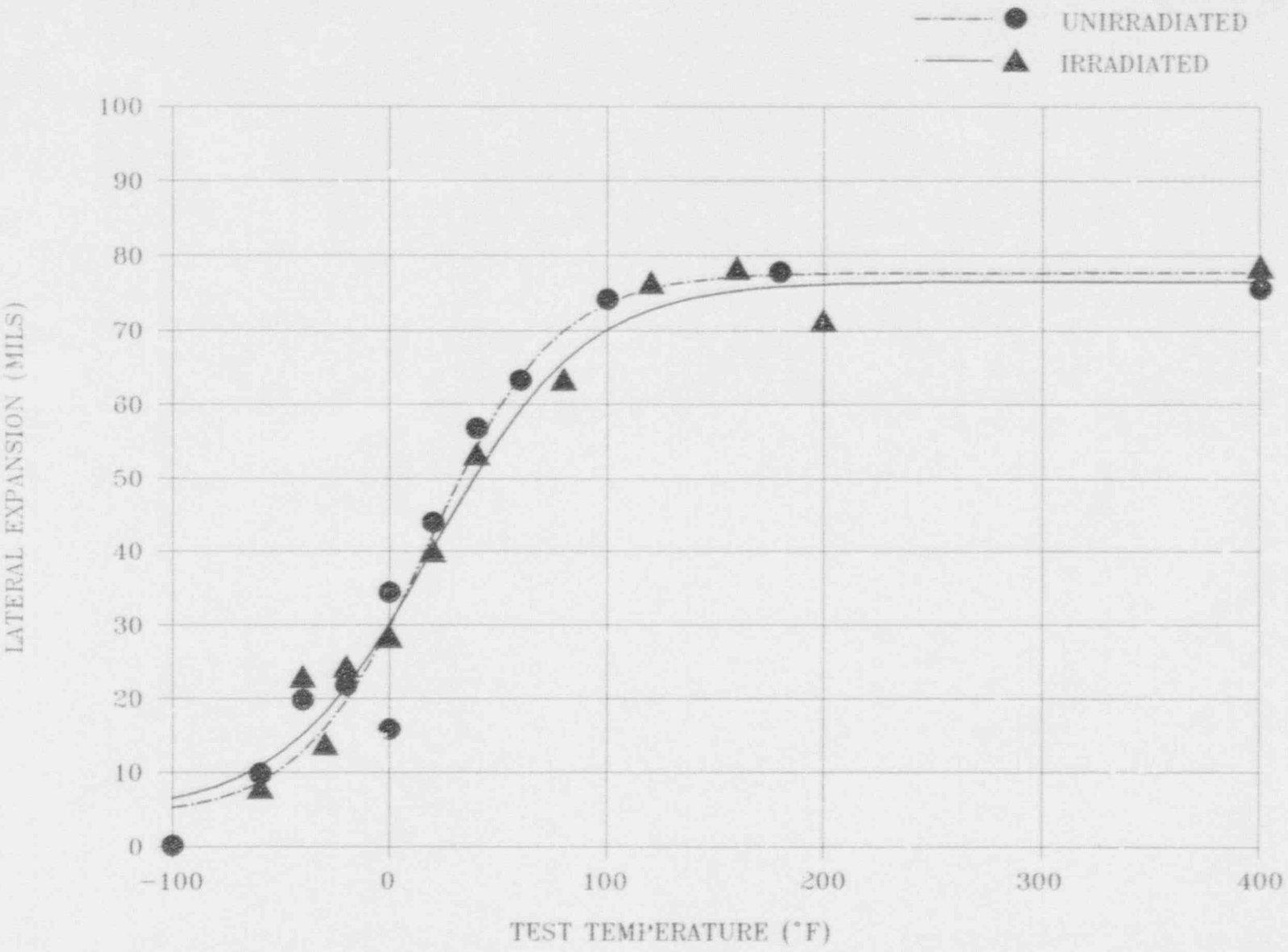

Figure 5-9. Hatch Unit 2 Irradiated & Unirradiated Base Lateral Expansion

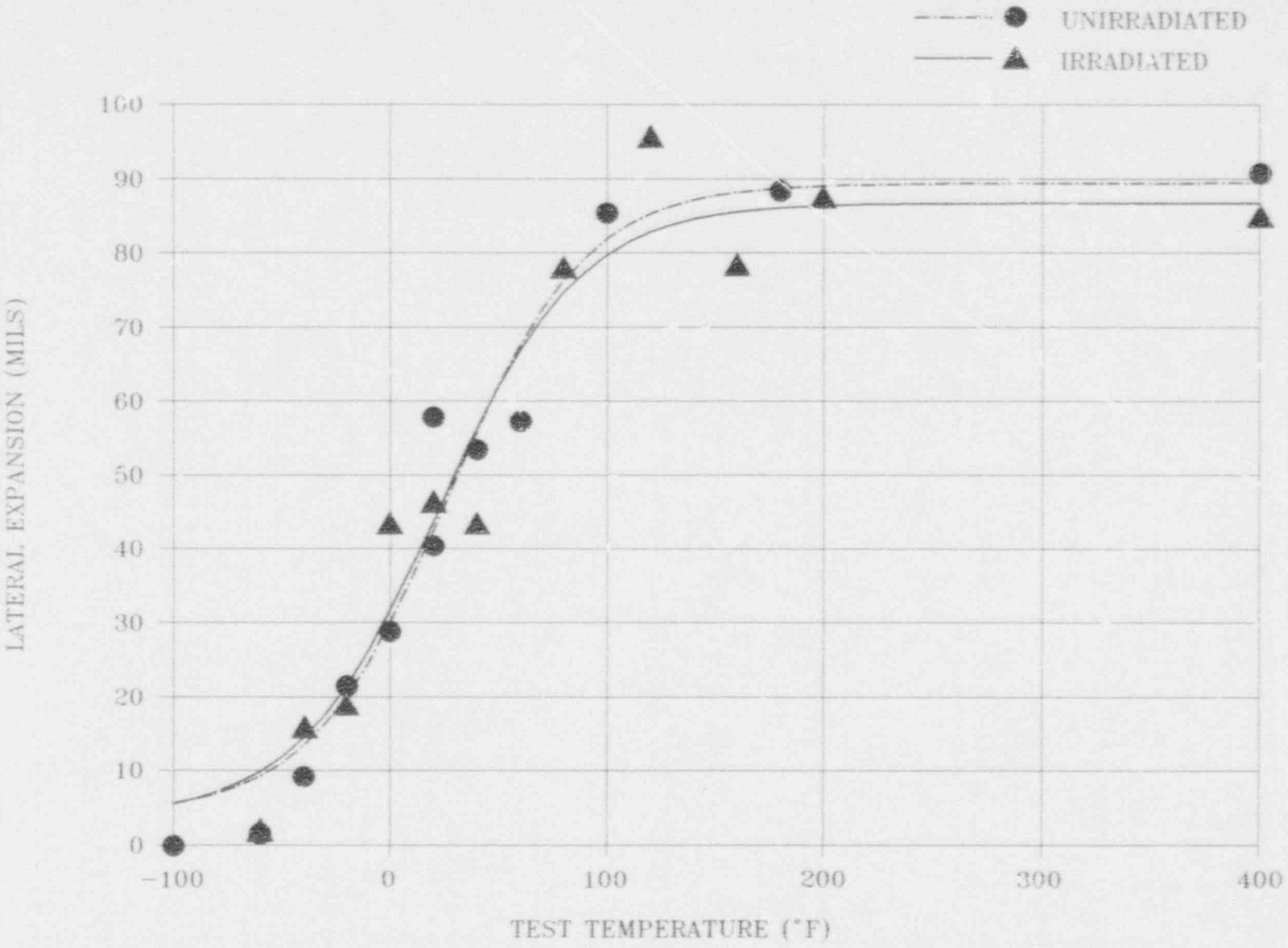

Figure 5−10. Hatch Unit 2 Irradiated & Unirradiated Weld Lateral Expansion

6. TENSILE TESTING

Ten round bar tensile specimens were recovered from the Hatch Unit 2 surveillance capsule, but only nine (three of each material) were tested. Uniaxial tensile tests were conducted in air at room temperature (70°F), RPV operating temperature (550°F), and onset of upper shelf temperature (120°F). The tests were conducted in accordance with ASTM E8-81 (Reference 13).

6.1 PROCEDURE

All tests were conducted using a screw-driven Instron test frame equipped with a 20-kip load cell and special pull bars and grips. Heating was done with a Satec resistance clamshell furnace centered around the specimen load train. The test temperature was monitored and controlled by a chromel-alumel thermocouple spot-welded to an Inconel clip that was friction-clipped to the surface of the specimen at its midline. Before the elevated temperature tests, a profile of the furnace was conducted at the test temperature of interest using an unirradiated steel specimen of the same geometry. Thermocouples were spot-welded to the top, middle, and bottom of a central 1 inch gage of this specimen. In addition, the clip-on thermocouple was attached to the midline of the specimen. When the target temperatures of the three thermocouples were within ±5°F of each other, the temperature of the clip-on thermocouple was noted and subsequently used as the target temperature for the irradiated specimens.

All tests were conducted at a calibrated crosshead speed of 0.005 inch/min until well past yield, at which time the speed was increased to 0.05 inch/min until fracture. A one inch span knife edge extensometer was attached directly to the central gage region of each specimen and was used to monitor gage extension during the test.

The test specimens were machined with a minimum diameter of 0.250 inch at the center of the gage length. The yield strength (YS) and ultimate tensile strength (UTS) were calculated by dividing the nominal area (0.0491 in^2) into the 0.2% offset load and into the maximum test load, respectively. The values listed for the uniform and total elongations were obtained from plots that recorded load versus specimen extension and are based on a 1.5 inch gage length. Reduction of area (RA) values were determined from post-test measurements of the necked specimen diameters using a calibrated blade micrometer and employing the following formula:

$$RA = 100\% * (A_o \quad A_f)/A_o$$

After testing, each broken specimen was photographed end-on, showing the fracture surface, and lengthwise, showing the fracture location and local necking behavior.

6.2 RESULTS

Irradiated tensile test properties of Yield Strength (YS), Ultimate Tensile Strength (UTS), Reduction of Area (RA), Uniform Elongation (UE), and Total Elongation (TE) are presented in Table 6-1. A stress-strain curve for a 550°F base metal irradiated specimen is shown in Figure 6-1. This curve is typical of the stress-strain characteristics of all the tested specimens. The data in Table 6-1 are shown graphically in Figures 6-2 and 6-3. As can be seen from Figures 6-2 and 6-3, the base, weld and HAZ materials generally follow the trend of decreasing properties with increasing temperature. Photographs of the fracture surfaces and necking behavior are given in Figures 6-4 through 6-6.

6.3 IRRADIATED VERSUS UNIRRADIATED TENSILE PROPERTIES

Unirradiated tensile test data, shown in Table 6-2, were recovered from QA records for surveillance plate Heat C8554 and from CE for surveillance weld heat 51912. The unirradiated data provide average values of YS, UTS, RA, and TE at room temperature. These were compared to the irradiated plate and weld metal specimen RT data to determine the irradiation effect. The trends of increasing YS and UTS and of decreasing TE and RA, characteristic of irradiation embrittlement, are seen in the plate data. The weld data show the expected decrease in ductility, but small decreases in YS and UTS with irradiation are shown. This may be due to differences in sources of surveillance and fabrication test specimens.

Table 6-1

TENSILE TEST RESULTS FOR IRRADIATED RPV MATERIALS

FOR HATCH UNIT 2

Specimen Number	Test Temp (°F)	Yield[a] Strength (ksi)	Ultimate Strength (ksi)	Uniform Elongation (%)	Total Elongation (%)	Reduction of Area (%)
Base:						
P146A	70	78.1	100.2	8.1	16.3	60.9
P146B	550	70.3	93.9	7.7	16.1	68.9
P146C	120	74.2	94.6	7.9	18.0	72.1
Weld:						
P246A	70	82.8	95.9	8.9	16.0	53.8
P246B	550	78.8	95.4	7.2	16.7	67.9
P246C	120	83.6	94.8	8.5	19.1	72.0
HAZ:						
P346A	70	68.2	92.8	6.5	16.1	72.8
P346B	550	63.2	86.8	5.4	13.6	69.1
P346C	120	68.5	89.7	6.9	15.6	74.2

[a] Yield Strength is determined by 0.2% offset.

Table 6-2

COMPARISON OF UNIRRADIATED AND IRRADIATED
TENSILE PROPERTIES AT ROOM TEMPERATURE
FOR HATCH UNIT 2

	Yield Strength (ksi)	Ultimate Strength (ksi)	Total Elongation (%)	Reduction of Area (%)
Plate:				
Unirradiated	69.4	91.1	26.4	68.2
Irradiated	78.1	100.2	16.3	60.9
Difference [a]	12.5%	10.0%	-38.3%	-10.7%
Weld:				
Unirradiated	84.7	96.1	27.0	70.8
Irradiated	82.8	95.9	16.0	53.8
Difference [a]	-2.2%	-0.2%	-40.7%	-24.0%

[a] Difference = [(Irradiated - Unirradiated)/Unirradiated] * 100%

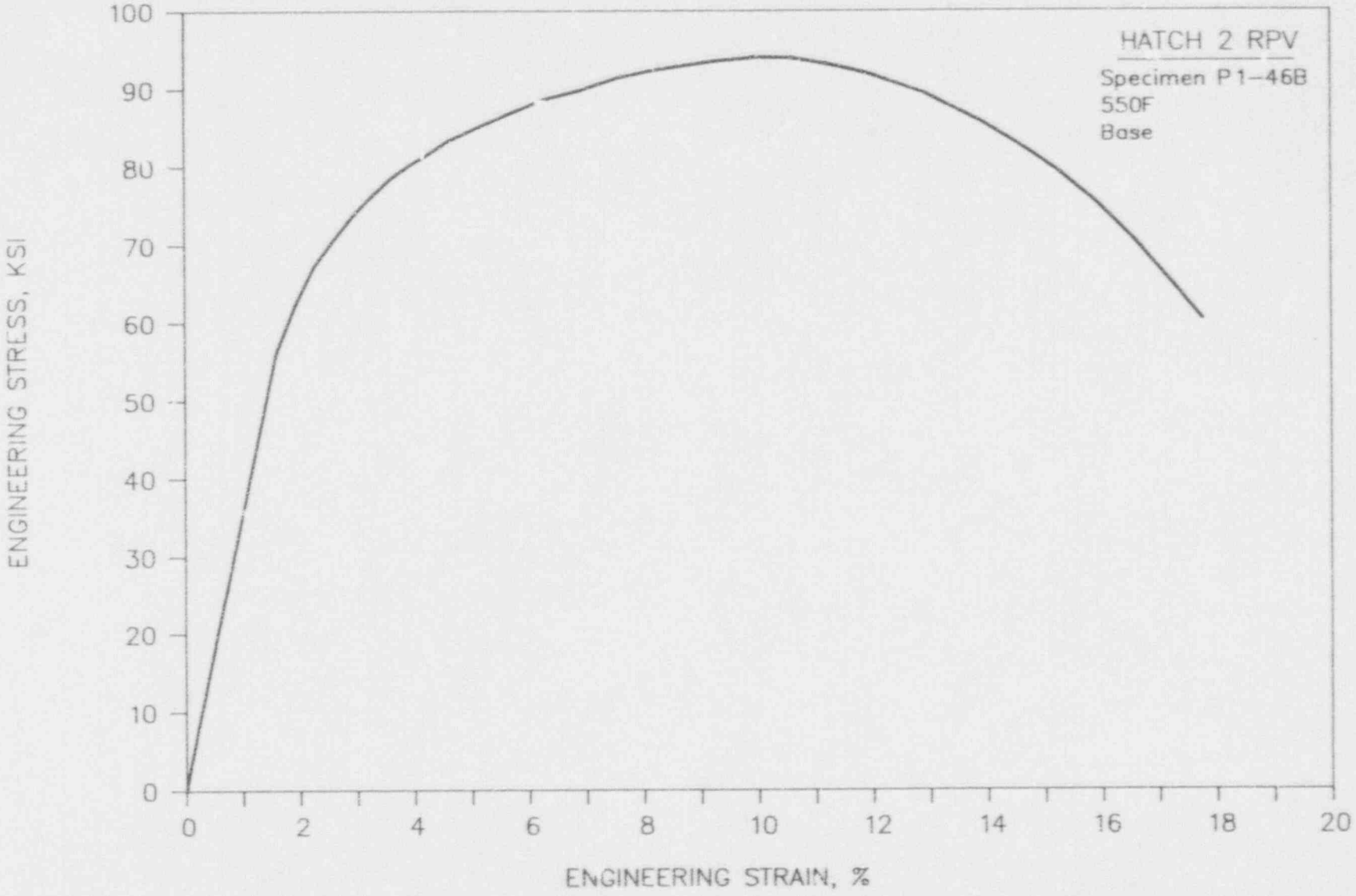

Figure 6-1. Typical Engineering Stress-Strain for Irradiated RPV Materials

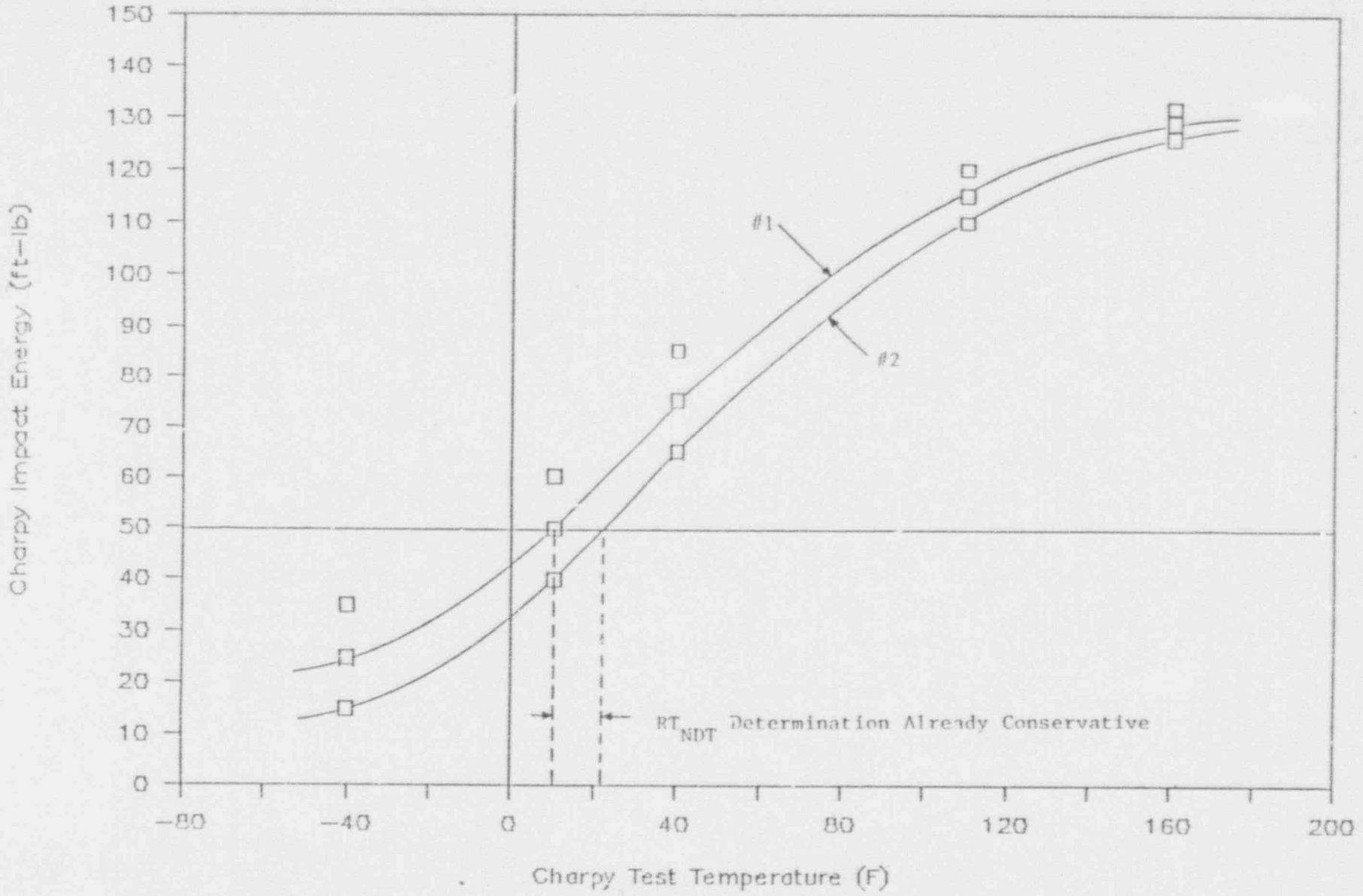

Figure B-1. Comparison of Surveillance Fit and RT_{NDT} Approach

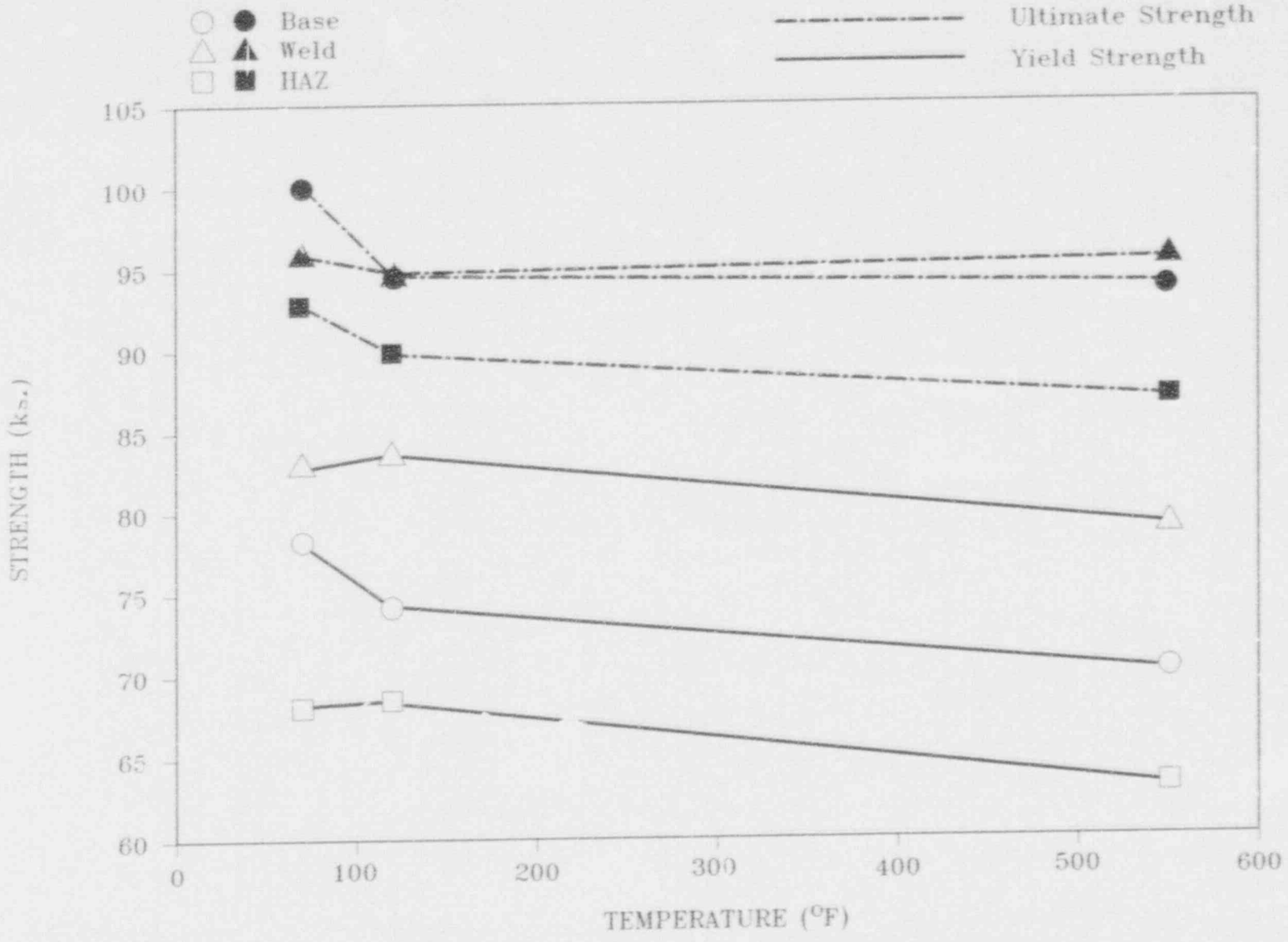

Figure 6–2. Hatch 2 irradiated Yield and Ultimate Strength

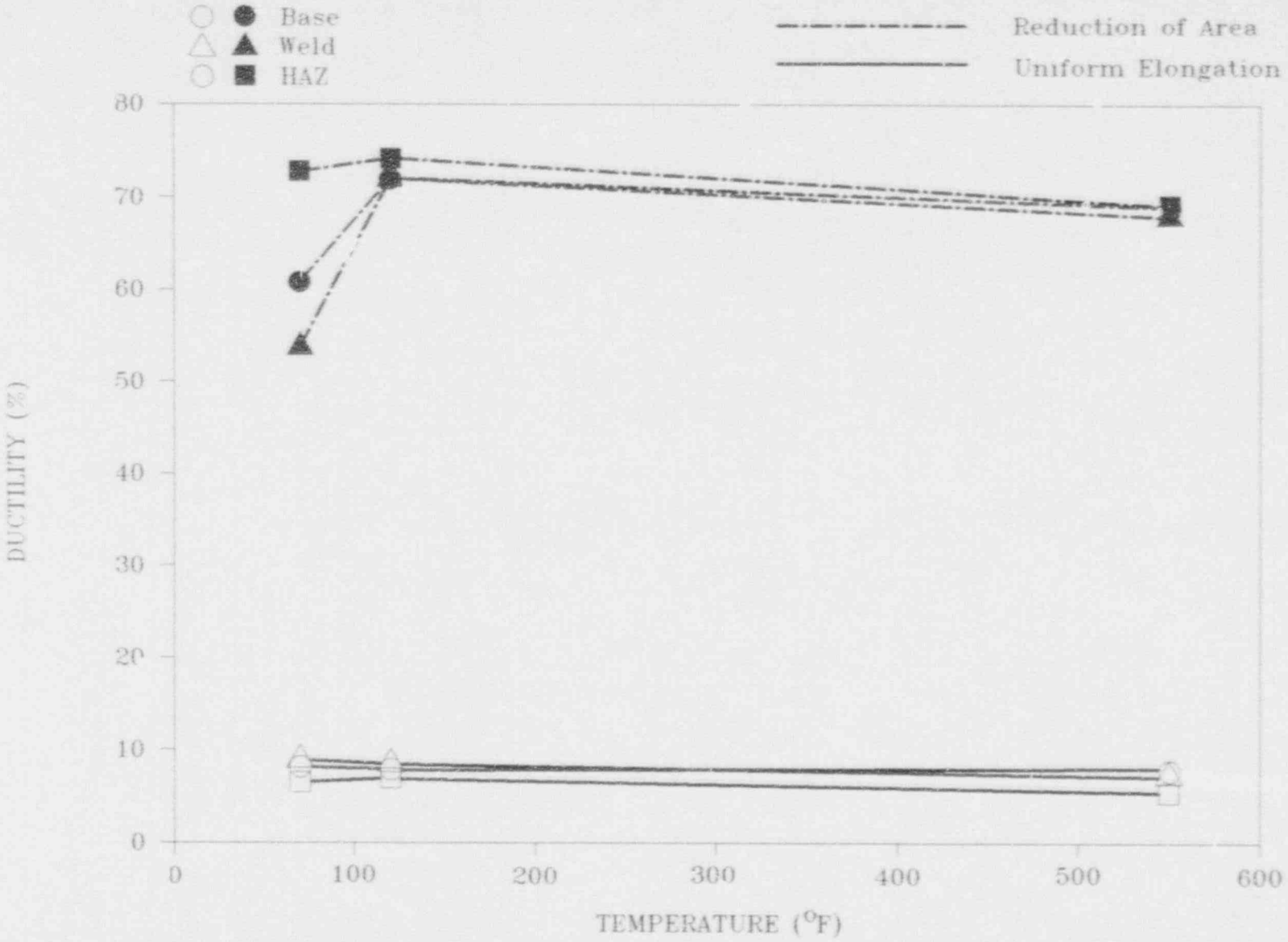

Figure 6-3. Hatch 2 Irradiated Elongation and Reduction of Area

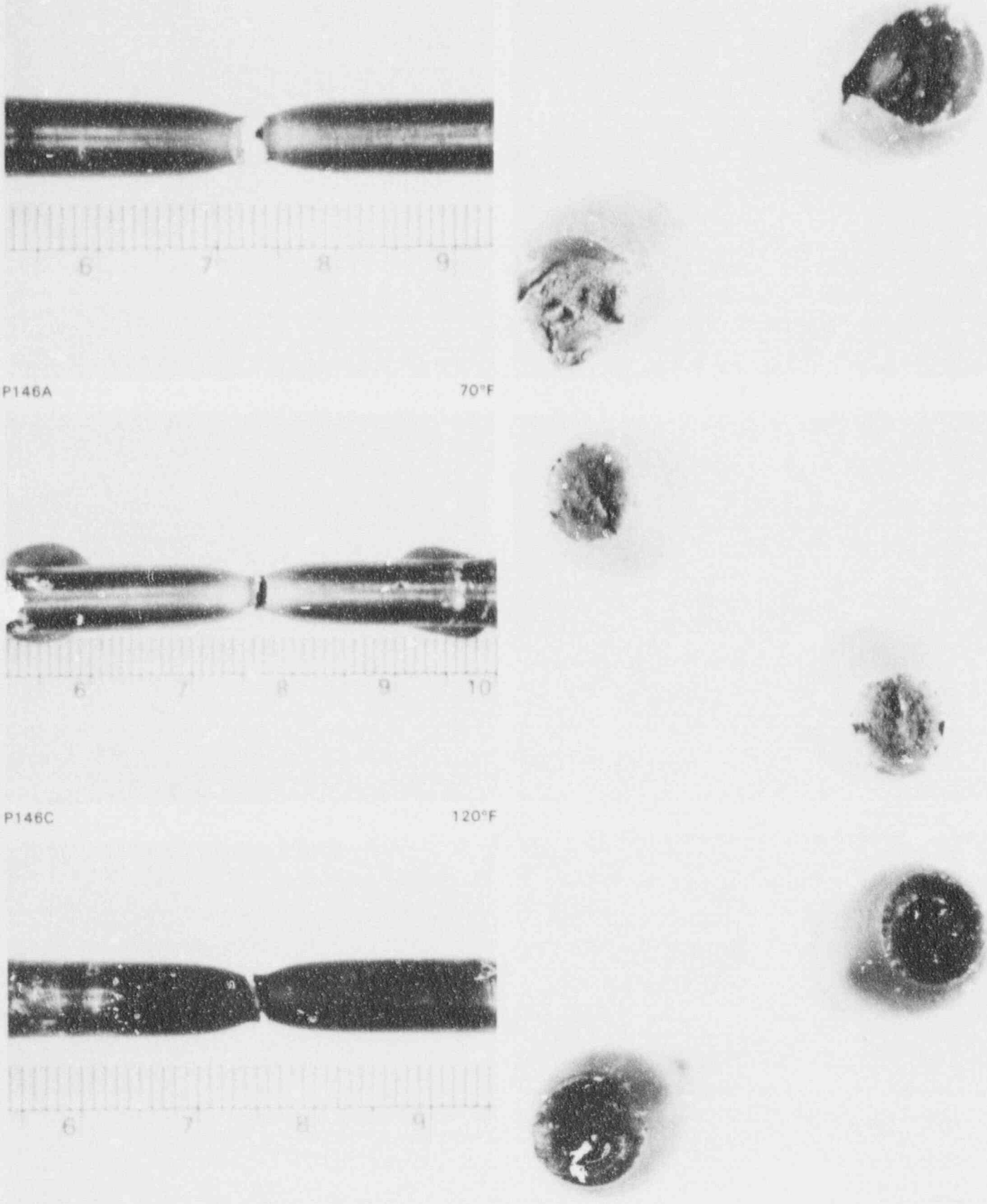

Figure 6-4. Fracture Location, Necking Behavior and Fracture Appearance for Irradiated Base Metal Tensile Specimens

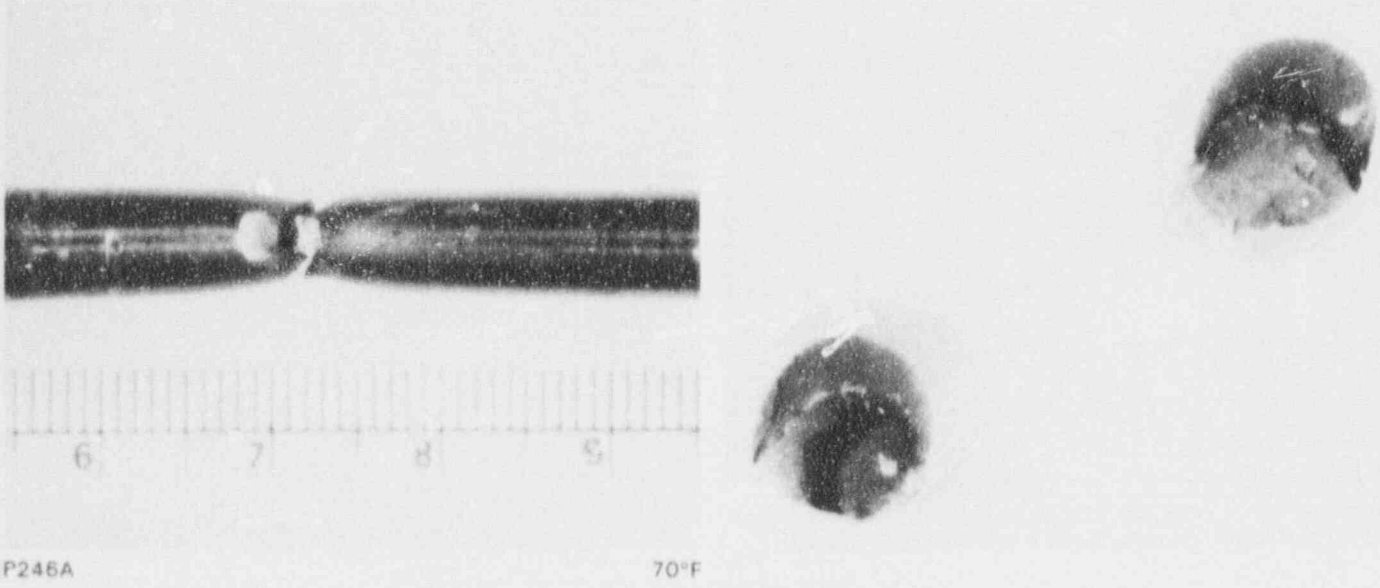

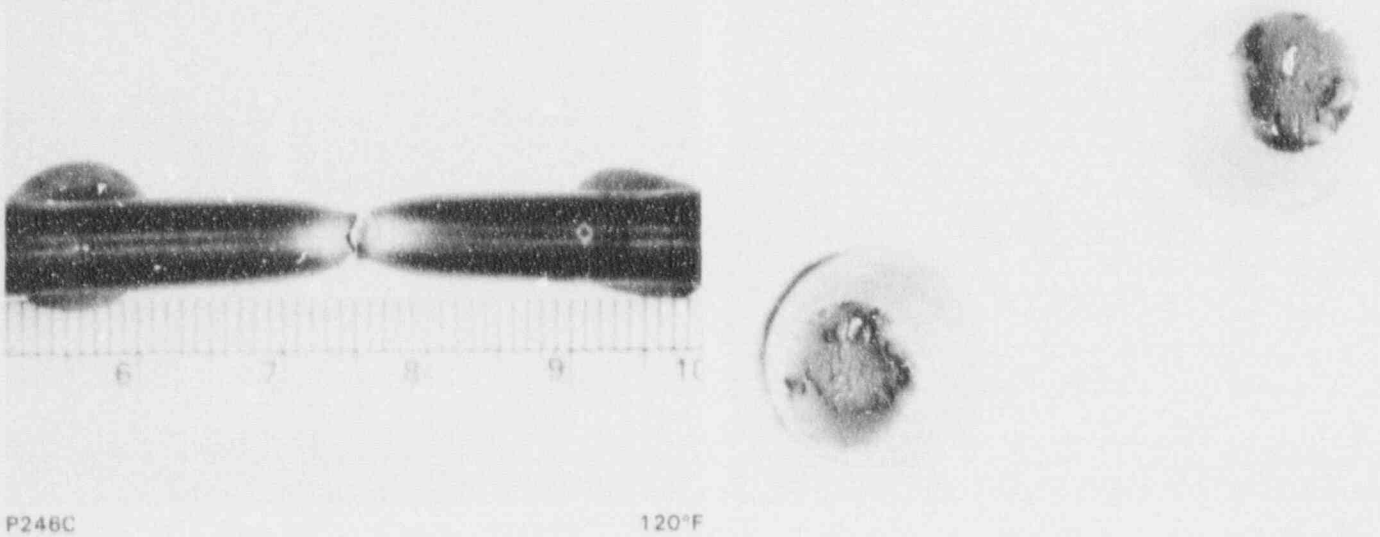

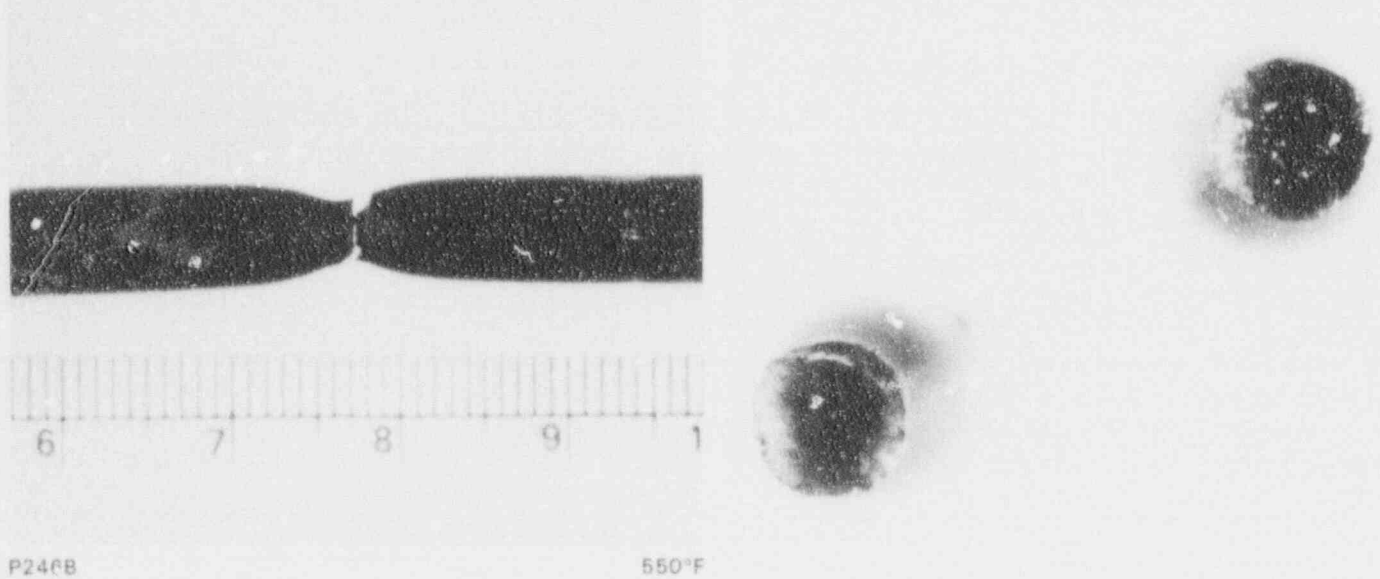

Figure 6-5. Fracture Location, Necking Behavior and Fracture Appearance for Irradiated Weld Metal Tensile Specimens

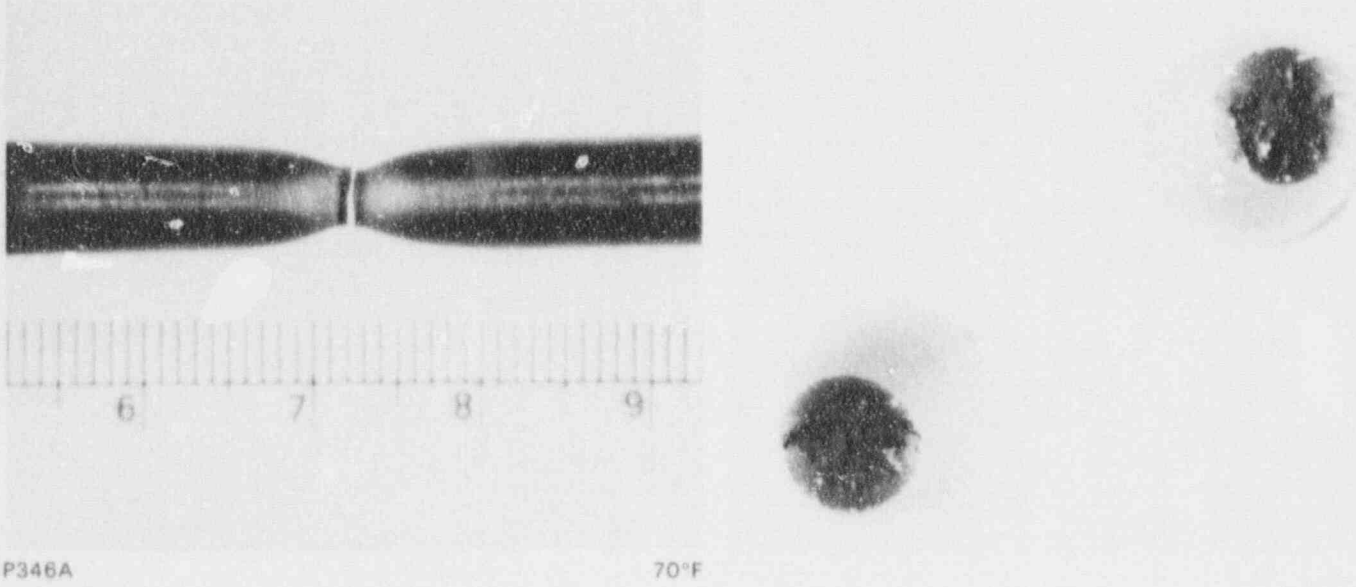

P346A 70°F

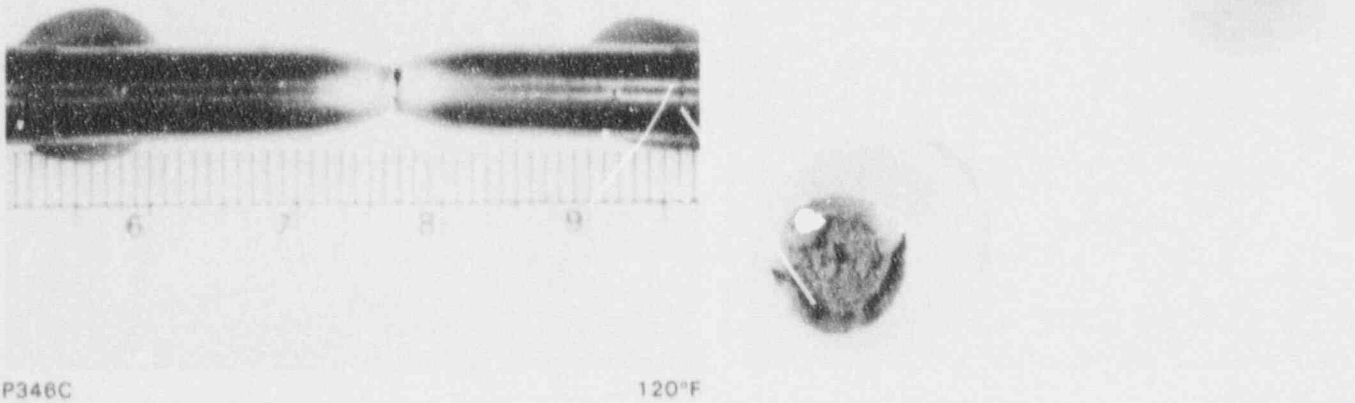

P346C 120°F

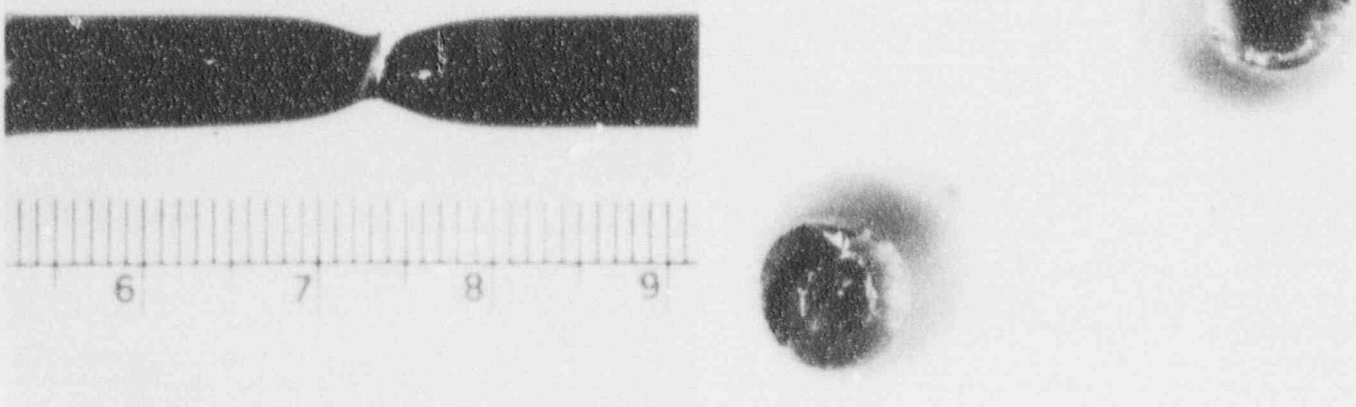

P346B 550°F

Figure 6-6. Fracture Location, Necking Behavior and Fracture Appearance for Irradiated HAZ Metal Tensile Specimens

7. DEVELOPMENT OF OPERATING LIMITS CURVES

7.1 BACKGROUND

Operating limits for pressure and temperature are required for three categories of operation: (a) hydrostatic pressure tests and leak tests, referred to as Curve A; (b) non-nuclear heatup/cooldown and low-level physics tests, referred to as Curve B; and (c) core critical operation, referred to as Curve C. There are three vessel regions that affect the operating limits: the closure flange region, the core beltline region, and the remainder of the vessel, or non-beltline regions. The closure flange region limits are controlling at lower pressures primarily because of Reference 1 requirements. The non-beltline and beltline region operating limits are evaluated according to procedures in References 1 and 2, with the beltline region minimum temperature limits increasing as the vessel is irradiated.

7.2 NON-BELTLINE RECIONS

Non-beltline regions are those locations that receive too little fluence to cause any RT_{NDT} increase. Non-beltline components include the nozzles, the closure flanges, some shell plates, top and bottom head plates and the control rod drive (CRD) penetrations. Detailed stress analyses of the non-beltline components, considering operating transients with relatively high pressures and low temperatures, were performed for the BWR/6, specifically for use in developing pressure-temperature (P-T) limits. The analyses bounded all mechanical loadings and thermal transients anticipated. Detailed stresses were used according to Reference 2 to develop plots of allowable pressure (P) versus temperature relative to the reference temperature ($T - RT_{NDT}$). These results are applicable to the Unit 2 vessel components, since the non-beltline geometries are not significantly different from BWR/6 configurations and the mechanical and thermal loadings are comparable.

The non-beltline region results were established by adding the highest RT_{NDT} for the non-beltline discontinuities to the P versus (T - RT_{NDT}) curves for the most limiting BWR/6 components, which are the CRD penetration and feedwater nozzle. Table 3-2 has the limiting RT_{NDT} values applicable to the feedwater nozzle limits and to the CRD penetration limits. They are 26°F for the feedwater nozzle limits, based on the RT_{NDT} of the steam outlet nozzles, and 50°F for the CRD penetration limits, based on the RT_{NDT} of the bottom head dome plates.

7.3 CORE BELTLINE REGION

As the beltline fluence increases during operation, the beltline P-T limit curves shift to the right by an amount discussed in Subsection 7.6. Typically, the beltline curves shift to become more limiting than the non-beltline curves at some time during plant life. The stress intensity factors calculated for the beltline region according to Reference 2 procedures are based on a combination of pressure and thermal stresses. The pressure stresses were calculated using thin-walled cylinder equations. Thermal stresses were calculated assuming the through-wall temperature distribution of a flat plate subjected to a 100°F/hr thermal gradient. The adjusted RT_{NDT} (ART) values calculated in Subsection 7.6 for the limiting beltline materials were used to adjust the P versus (T - RT_{NDT}) values from Figure G-2210-1 of Reference 2. ART is the initial RT_{NDT} plus the shift in RT_{NDT} due to irradiation.

Since the vessel thickness is a variable in the stresses as well as the ART values, P-T limits were computed for the limiting lower shell and lower-intermediate shell materials. The most limiting of the two beltline computations was compared to the non-beltline limits to establish the P-T curves.

7.4 CLOSURE FLANGE REGION

References 1 and 2 have several requirements that affect the P-T curves, based on the RT_{NDT} values in the closure flange region. As stated in Paragraph G-2222(c) of Reference 2, for application of full bolt preload and reactor pressure up to 20% of preservice hydrostatic test pressure (312 psig), the closure flange region metal temperature must be at RT_{NDT} or greater. The GE practice, however, is to recommend (RT_{NDT} + 60°F) for bolt preload, for two reasons:

a. The original ASME Code of construction required (RT_{NDT} + 60°F); and

b. The highest stressed region during boltup is the closure flange region, and the flaw size assumed in that region (0.24 inches) is less than 1/4 T. This flaw size is detectable using ultrasonic testing (UT) techniques. In fact, References 14 and 15 report that a flaw in the closure flange region of 0.09 inches can be reliably detected using UT.

For [illegible] (RT_{NDT} + 60°F) of the closure region materials is 90°F, because the RT_{NDT} of the upper shell plates is as high as 30°F. Therefore, the bolt preload temperature used in developing the P-T curves was 90°F.

Reference 1, Paragraph IV.A.2, sets requirements on minimum temperature when pressure is above 312 psig. The requirements are based on the RT_{NDT} of the closure region. Curve A temperature must be no less than (RT_{NDT} + 90°F) and Curve B temperature no less than (RT_{NDT} + 120°F). The Curve A requirement causes a 30°F shift at 312 psig on Figure 7-2. The Curve B requirement causes a small step at 312 psig on Figures 7-3 and 7-4.

7.5 CORE CRITICAL OPERATION REQUIREMENTS OF 10CFR50, APPENDIX G

Curve C, the core critical operation curve, is developed from the requirements of Reference 1, paragraph IV.A.3. Essentially paragraph IV.A.3 requires that Curve C be 40°F above any Curve A or B limits. Curve B is more limiting than Curve A, so Curve C is Curve B plus 40°F. Curve C initiates at zero pressure at (RT_{NDT} + 60°F), based on an exception for BWRs in Paragraph IV.A.3, allowing critical operation at temperatures below the hydrostatic pressure (Curve A at 1100 psig) test temperature. This exception is valid only when water level is within the normal range and pressure is below 312 psig.

7.6 EVALUATION OF RADIATION EFFECTS

The impact on adjusted reference temperature (ART) due to irradiation in the beltline materials is determined according to the methods in Reference 5, as a function of neutron fluence and the element contents of copper (Cu) and nickel (Ni). The specific relationship from Reference 5 is:

$$ART = \text{Initial } RT_{NDT} + \text{Shift} + \text{Margin} \qquad (7\text{-}1)$$

where:

$$\text{Shift} = [CF]*f^{(0.28 - 0.10 \log f)} \qquad (7\text{-}2)$$

$$\text{Margin} = 2*(\sigma_I^2 + \sigma_\Delta^2)^{1/2} \qquad (7\text{-}3)$$

CF = chemistry factor from Tables 1 or 2 of Reference 5,

f = 1/4 T fluence (n/cm^2) divided by 10^{19},

σ_I = standard deviation on initial RT_{NDT},

σ_Δ = standard deviation on RT_{NDT} shift, is 28°F for welds and 17°F for base material, except that σ_Δ need not exceed 0.50 times the Shift value.

The limiting beltline plate and weld are determined based on the Cu-Ni content and initial RT_{NDT} of the materials. Calculations to determine 32 EFPY ART values, and thus the limiting beltline materials, are summarized in Table 7-1. The results show that the longitudinal shell welds are the most limiting beltline materials.

One input to the Reference 5 calculations not shown in Table 7-1 is that σ_I = 0°F for the beltline materials, all of which have RT_{NDT} values determined from measured Charpy data. The basis for using σ_I = 0°F is discussed in more detail in Appendix B.

7.6.1 Measured Versus Predicted Surveillance Shift

Section 5 of this report compares the measured shifts for the surveillance specimens with predicted shifts based on the method shown in Equation 7-2. Reference 5 states that surveillance data may be used in place of Equations 7-2 and 7-3 when two sets of credible data are available. This is only the first set of data for Unit 2. Therefore, determinations of ART for the purposes of developing P-T curves are based on Reference 5 predictions.

7.6.2 ART Versus EFPY

Equations 7-1 through 7-3 were evaluated for the beltline plate and weld metals. Table 7-1 shows the 32 EFPY fluence at the vessel 1/4 T locations to be 1.0×10^{18} n/cm^2 for the lower-intermediate shell and 9.5×10^{17} n/cm^2 for the lower shell. Calculations of the plate and weld ART at 32 EFPY show that, for both shells, the longitudinal welds are the most limiting materials. Figure 7-1 shows the ART for the lower shell longitudinal weld, which has the highest ART at 32 EFPY.

7.6.3 Fracture Toughness Conditions at 32 EFPY

Paragraph IV.B of Reference 1 sets limits on the ART and on the upper shelf energy (USE) of the beltline materials. The ART must be less than 200°F, and the USE must be above 50 ft-lb. Based on Table 7-1, the ART values at 32 EFPY of 69°F or less are acceptable.

Calculations of 32 EFPY USE, using Reference 5 methods, are summarized in Table 7-2. The equivalent transverse USE of the plate material is taken as 65% of the longitudinal USE, according to Reference 12. The weld metal USE has no transverse/longitudinal correction because weld metal has no orientation effect. The weld metal initial USE values are based on Charpy data taken at only 10°F, so the weld results are conservative. Extrapolating to the 32 EFPY fluence according to Reference 5, the lowest predicted transverse USE values for the plate and weld materials are 61 ft-lb and 72 ft-lb, respectively.

Based on the above results, it is expected that the beltline materials will have USE values above 50 ft-lb at 32 EFPY, as required in Reference 1. Since USE and ART requirements are met, irradiation effects are not severe enough to necessitate additional analyses or preparations for RPV annealing before 32 EFPY.

7.7 OPERATING LIMITS CURVES VALID TO 32 EFPY

Figures 7-2 through 7-4 show P-T curves for Unit 2, valid to 32 EFPY. The P-T curves are developed by considering the requirements applicable to the non-beltline, beltline and closure flange regions. In reviewing the shifted beltline curves, it was determined that the non-beltline curves are still limiting at 32 EFPY. Therefore, barring any changes due to future surveillance data or revisions to regulations, the P-T curves shown in Figures 7-2 through 7-4 will apply for operation through 32 EFPY.

7.8 REACTOR OPERATION VERSUS OPERATING LIMITS

For most reactor operating conditions, pressure and temperature are at saturation conditions, which are well into the acceptable operating area (to the right of the P-T curves). The most severe unplanned transient relative to the P-T curves is an upset condition consisting of several transients which result in a SCRAM. The worst combination of pressure and temperature during this postulated event is 1180 psig with temperatures in the lower head of 250°F. In this case, the core is not critical, so the non-nuclear heatup/cooldown curve applies (Curve B). As seen for Curve B in Figure 7-3, at 1180 psi the minimum transient temperature of 250°F lies in the acceptable operating area. Therefore, violation of the P-T curves is only a concern in cases where operator interaction occurs, such as during pressure testing and initiation of criticality.

Table 7-1

BELTLINE EVALUATION FOR MATCH 2

Low-Int Shell
Thickness = 5.38 inches

Low-Int Shell:
Peak I.D. fluence = 1.4E+18
Peak 1/4 T fluence = 1.0E+18

Lower Shell
Thickness = 6.38 inches

Lower Shell:
Peak I.D. fluence = 1.4E+18
Peak 1/4 T fluence = 9.5E+1

COMPONENT	I.D.	HEAT OR HEAT/LOT	%Cu	%Ni	CF	Initial RTndt	32 Delta	EFPY RTndt	Margin	32 EFPY Shift	32 EFPY RT
PLATES:											
Lower Shell	G6603-1	C8553-2	0.08	0.58	51	-20		20.8	20.8	41.6	21.6
Lower Shell	G6603-2	C8553-1	0.08	0.58	51	24		20.8	20.8	41.6	65.6
Lower Shell	G6603-3	C8571-1	0.08	0.53	51	0		20.8	20.8	41.6	41.6
Low-Int Shell	G6602-2	C8554-1	0.08	0.57	51	-20		21.4	21.4	42.8	22.8
Low-Int Shell	G6602-1	C8554-2	0.08	0.58	51	-10		21.4	21.4	42.8	32.8
Low-Int Shell	G6601-4	C8579-2	0.11	0.48	72.8	-4		30.5	30.5	61.1	57.1
WELDS:											
Lower Long.	101-842	10137, LINDE 0091 FLUX LOT 3999	0.23	<.50	154.5	-50		63.0	56.0	119.0	69.0
Low-Int Long.	101-834	51874, LINDE 0091 FLUX LOT 3458	0.18	<.50	138	-50		57.9	56.0	113.9	63.9
Lower to Low-Int Girth	301-871	4P6052,LINDE 0091 FLUX LOT 0145	0.07	0.03	25.5	-56		10.7	10.7	21.4	-28.6

Table 7-2

ESTIMATE OF UPPER SHELF ENERGY FOR BELTLINE MATERIALS

Identification	% Cu	32 EFPY [a] Decrease in USE	Upper Shelf (ft-lb) Longitudinal/Transverse Unirradiated	32 EFPY
Lower Shell Plates:				
C8553-2	0.08	10%	147/95	132/86
C8553-1	0.08	10%	131/85	118/77
C8571-1	0.08	10%	109/71	98/64
Lower-Intermediate Shell Plates:				
C8554-1	0.08	10%	139/90	125/81
C8554-2	0.08	10%	143/93	129/84
C8579-2	0.11	12%	107/70	94/61
Lower Longitudinal Welds:				
10137	0.23	22%	108 [b]	84
Lower-Intermediate Longitudinal Welds:				
51874	0.18	19%	89 [b]	72
Lower to Lower-Intermediate Girth Weld:				
4P6052	0.07	12%	126 [b]	111

[a] USE decrease percentages based on 32 EFPY fluence of 1.0×10^{18} n/cm^2

[b] Values are highest Charpy energy from tests at 10°F.

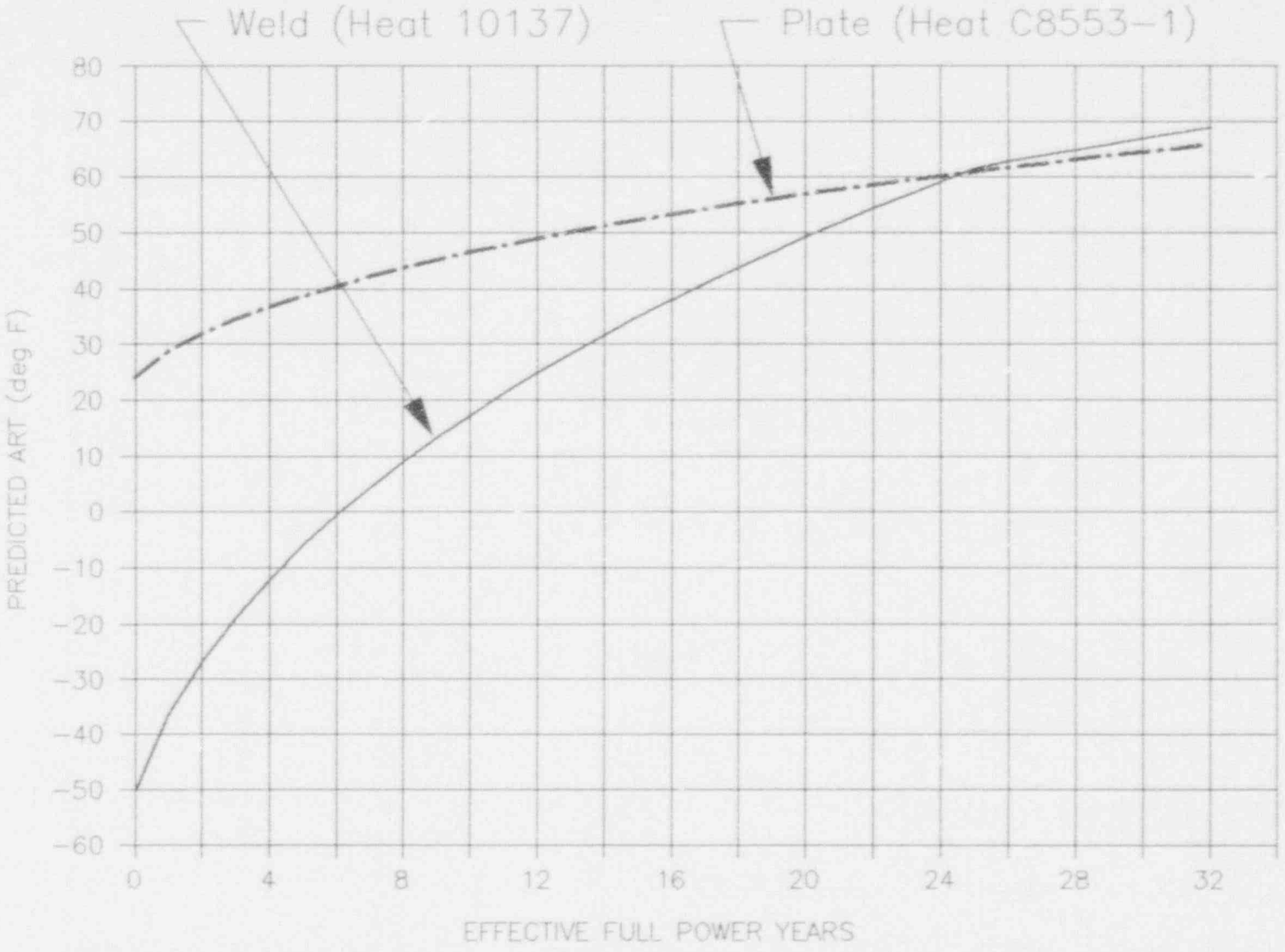

Figure 7-1. Adjusted Reference Temperature for Limiting Beltline Materials

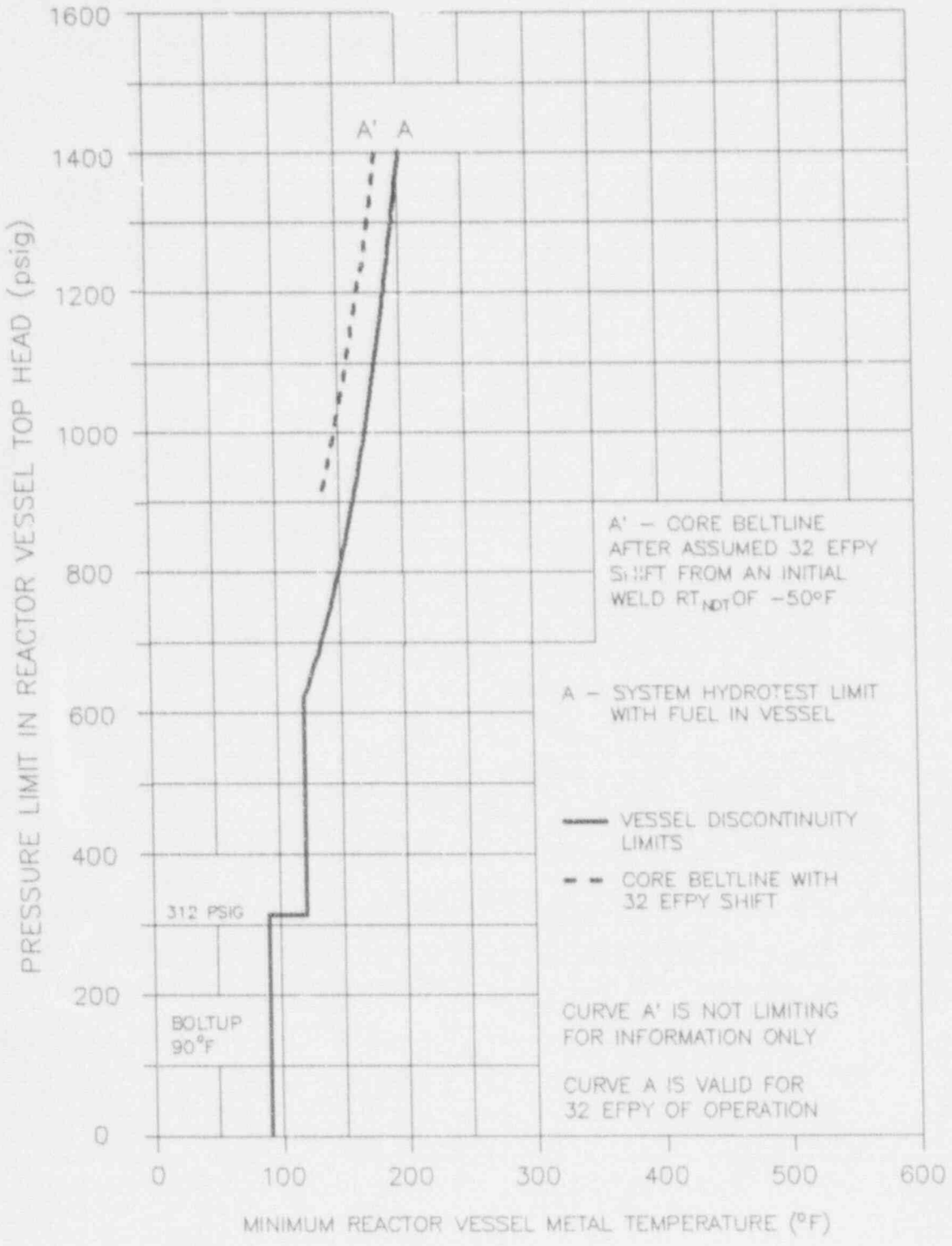

Figure 7-2. P-T Curves for Pressure Tests

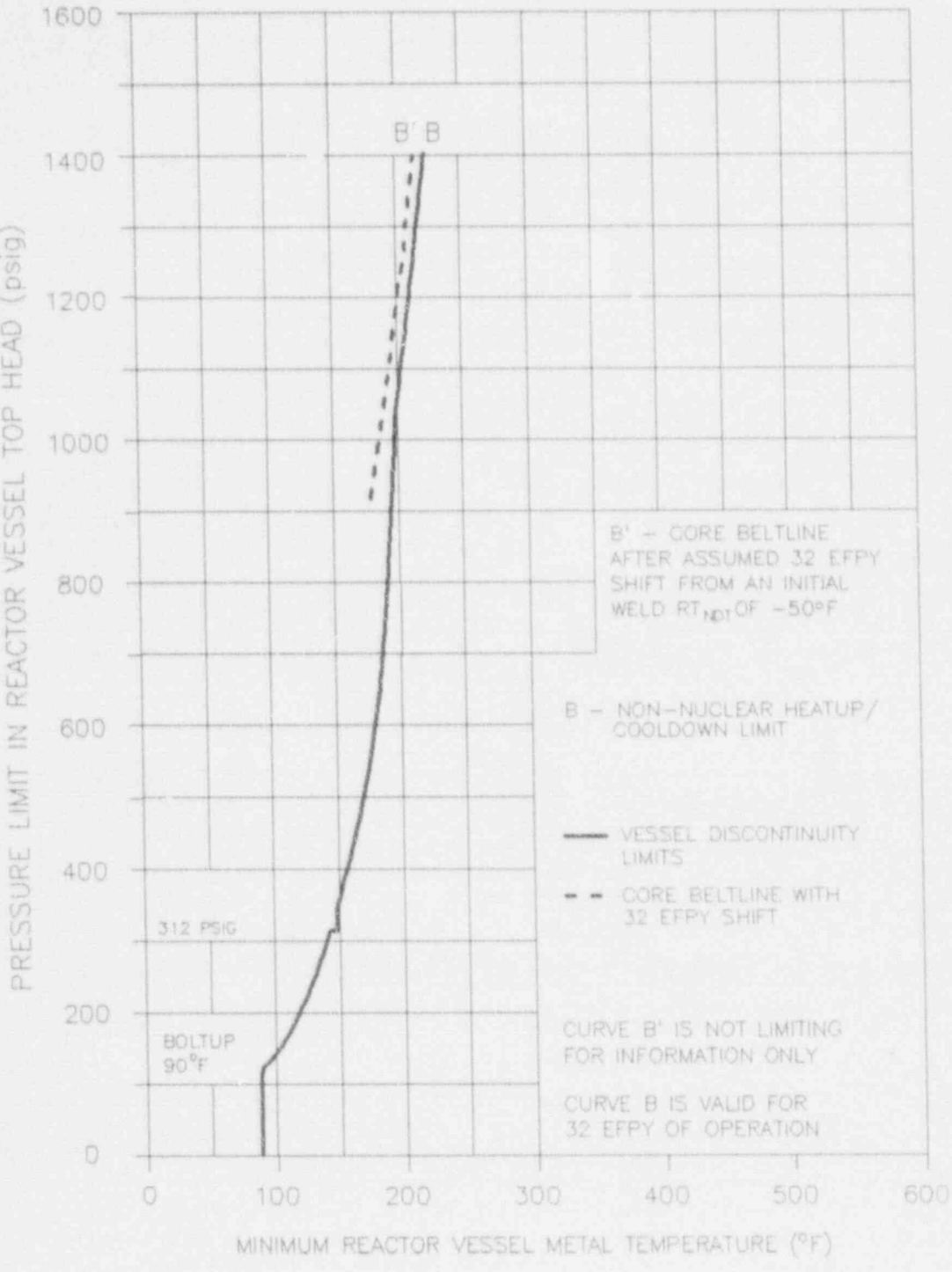

Figure 7–3. P–T Curves for Non–Nuclear Heatup/Cooldown

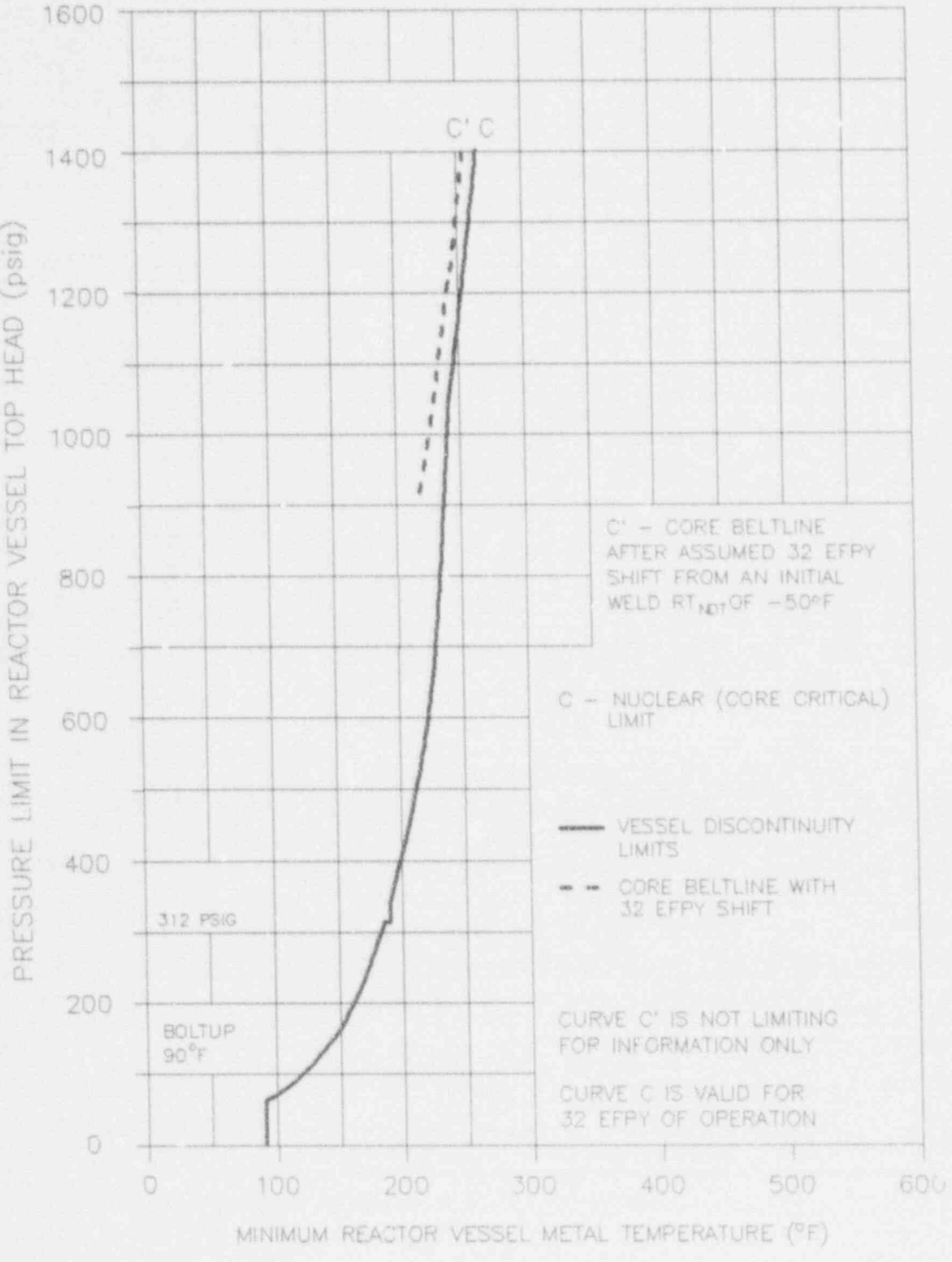

Figure 7–4. P–T Curves for Core Critical Operation

8. REFERENCES

1. "Fracture Toughness Requirements," Appendix G to Part 50 of Title 10 of the Code of Federal Regulations, July 1983.

2. "Protection Against Non-Ductile Failure," Appendix G to Section XI of the 1989 ASME Boiler & Pressure Vessel Code.

3. "Reactor Vessel Material Surveillance Program Requirements," Appendix H to Part 50 of Title 10 of the Code of Federal Regulations, July 1983.

4. "Conducting Surveillance Tests for Light Water Cooled Nuclear Power Reactor Vessels," Annual Book of ASTM Standards, E185-82, July 1982.

5. "Radiation Embrittlement of Reactor Vessel Materials," USNRC Regulatory Guide 1.99, Revision 2, May 1988.

6. "Material Specifications Part C - Welding Rods, Electrodes and Filler Metals," Section II of the 1989 ASME Boiler & Pressure Vessel Code.

7. Hodge, J. M., "Properties of Heavy Section Nuclear Reactor Steels," Welding Research Council Bulletin 217, July 1976.

8. "Surveillance Test Program for Hatch II Reactor Vessel," CE Fabrication Specification, GE VPF No. 3062-189-2, August 1971.

9. Caine, T. A., "Hatch Unit 1 RPV Surveillance Materials Testing and Fracture Toughness Analysis," GE Report NEDC-30997, October 1985.

10. "Standard Methods for Notched Bar Impact Testing of Metallic Materials," Annual Book of ASTM Standards, E23-82, March 1982.

11. "Nuclear Plant Irradiated Steel Handbook," EPRI Report NP-4797, September 1986.

12. "Fracture Toughness Requirements," USNRC Branch Technical Position MTEB 5-2, Revision 1, July 1981.

13. "Standard Methods of Tension Testing of Metallic Materials," Annual Book of ASTM Standards, E8-81.

14. "Ultrasonic Examination for Cracks in the Top Head Flange," CBI Nuclear, Development Report 74-9047, December 1975.

15. "Ultrasonic Examination for Cracks in the Shell Flange," CBI Nuclear, Development Report 74-9056, November 1975.

APPENDIX A

CHARPY SPECIMEN FRACTURE SURFACE PHOTOGRAPHS

Photographs of each Charpy specimen fracture surface were taken per the requirements of ASTM E185-82. The pages following show the fracture surface photographs along with a summary of the Charpy test results for each specimen. The pictures are arranged with the materials in the order of base, weld and HAZ.

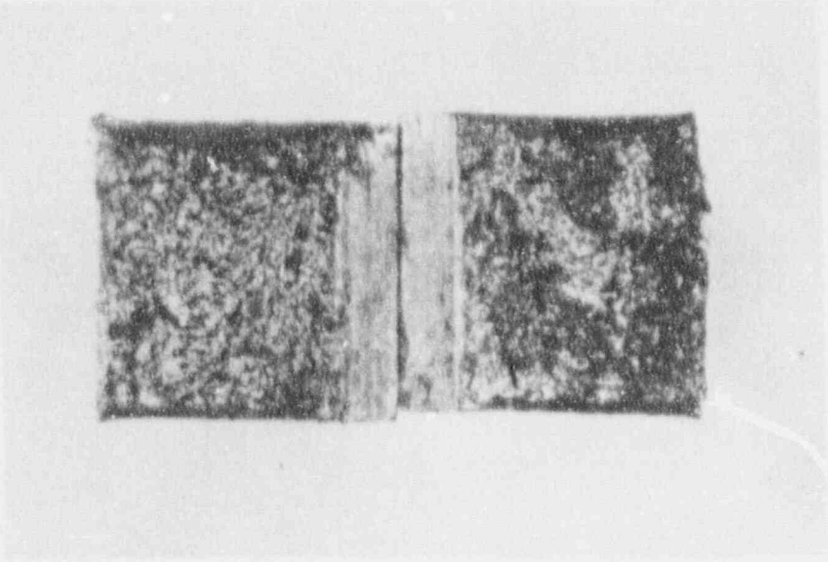

BASE: P1-26833
TEMP: −60°F
ENERGY: 9.0 ft-lb

MLE: 8
% SHEAR: 18

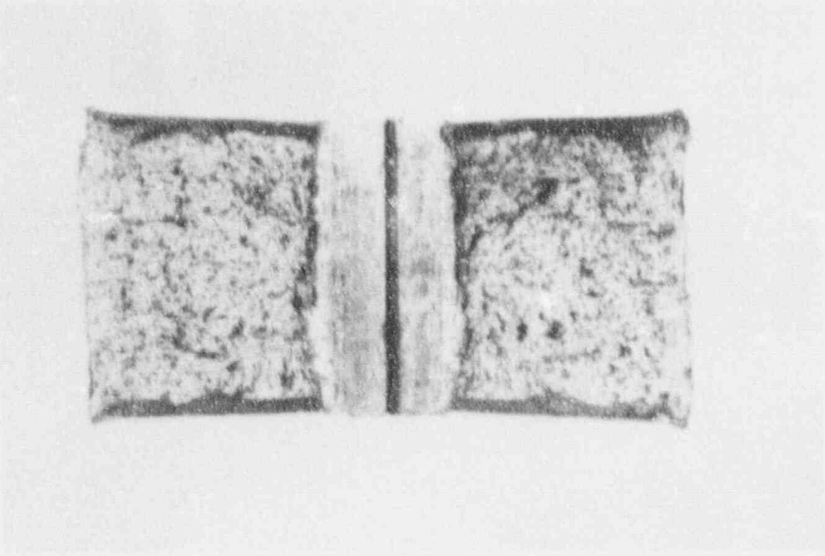

BASE: P1-26829
TEMP: −40°F
ENERGY: 28.0 ft-lb

MLE: 23
% SHEAR: 14

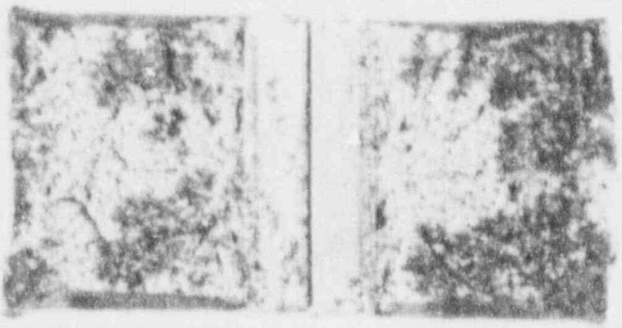

BASE: P1-26832
TEMP: -30°F
ENERGY: 15.0 ft-lb

MLE: 14
% SHEAR: 17

BASE: P1-26835
TEMP: -20°F
ENERGY: 31.5 ft-lb

MLE: 24
% SHEAR: 28

BASE: P1-26834
TEMP: 0°F
ENERGY: 36.5 ft-lb

MLE: 28
% SHEAR: 20

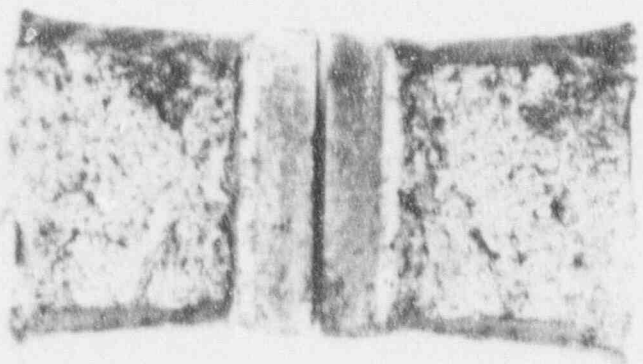

BASE: P1-26038
TEMP: 20°F
ENERGY: 54.5 ft-lb

MLE: 40
% SHEAR: 35

BASE: P1-26836
TEMP: 40°F
ENERGY: 71.5 ft-lb

MLE: 53
% SHEAR: 56

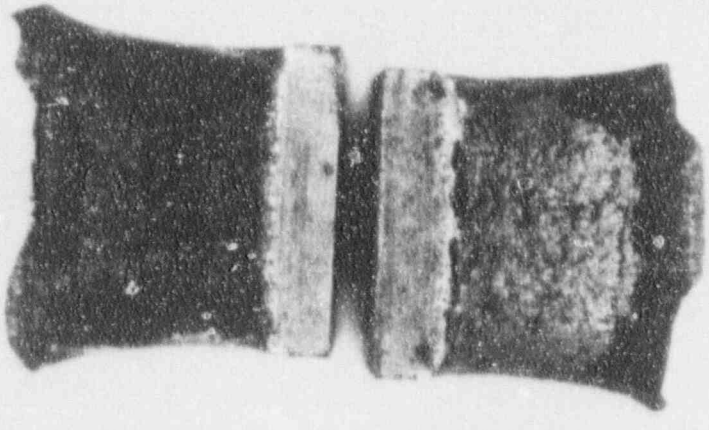

BASE: P1-26831
TEMP: 80°F
ENERGY: 86.0 ft-lb

MLE: 63
% SHEAR: 80

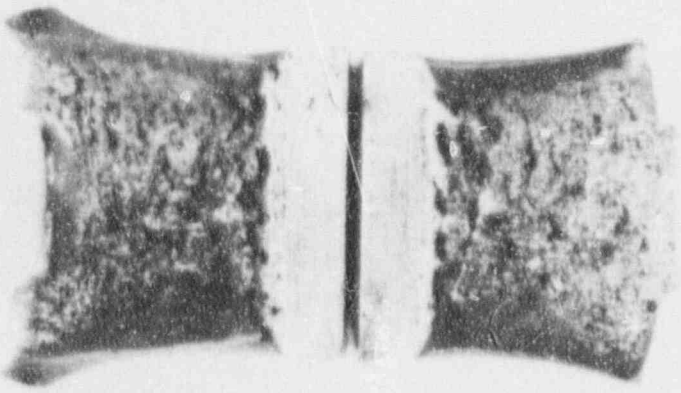

BASE: P1-26837
TEMP: 120°F
ENERGY: 115.0 ft-lb

MLE: 76
% SHEAR: 100

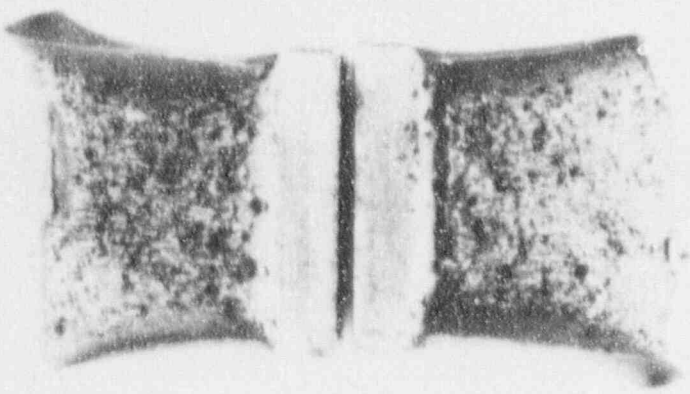

BASE: P1-26828
TEMP: 160°F
ENERGY: 110.5 ft-lb

MLE: 78
% SHEAR: 100

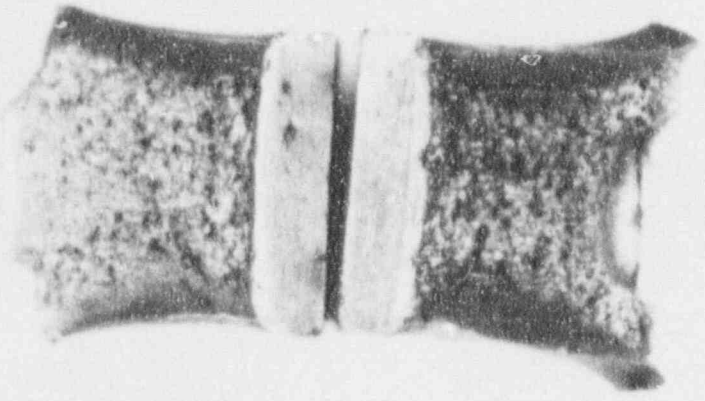

BASE: P1-26839
TEMP: 200°F
ENERGY: 107.0 ft-lb

MLE: 71
% SHEAR: 100

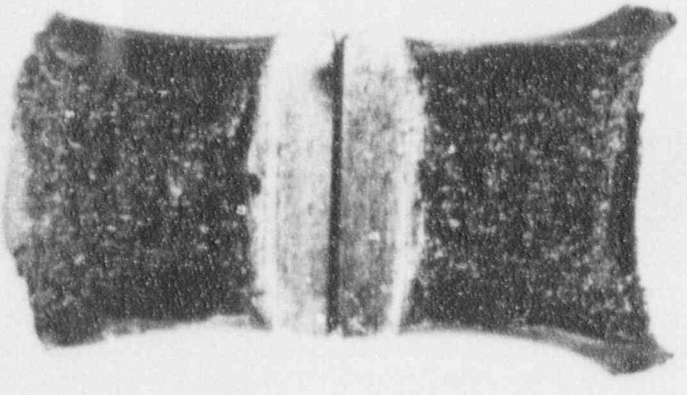

BASE: P1-26830
TEMP: 400°F
ENERGY: 119.0 ft-lb

MLE: 78
% SHEAR: 100

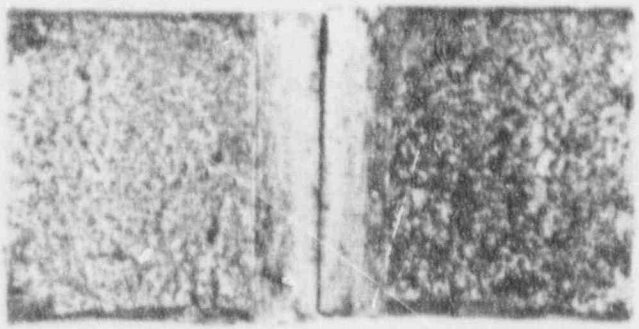

WELD: P2-26850
TEMP: -59°F
ENERGY: 5.5 ft-lb

MLE: 2
% SHEAR: 10

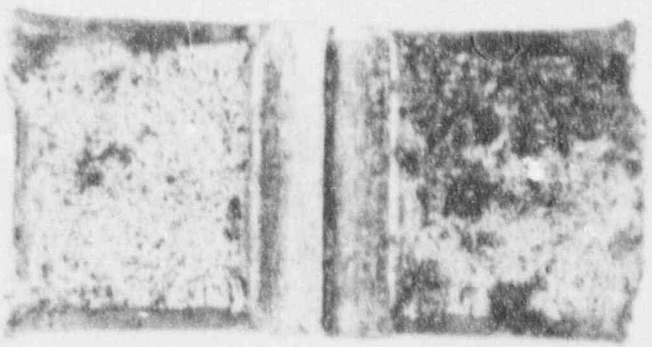

WELD: P2-26848
TEMP: -40°F
ENERGY: 21.5 ft-lb

MLE: 16
% SHEAR: 27

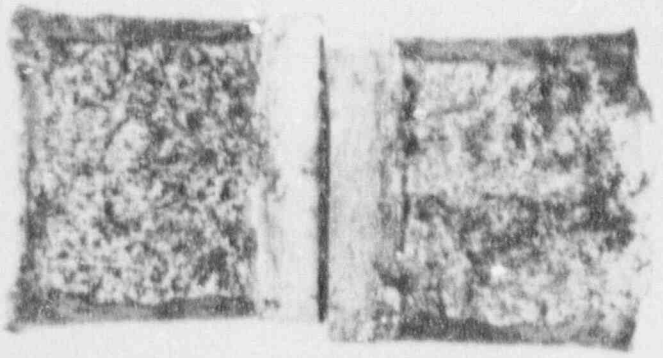

WELD: P2-26842
TEMP: −20°F
ENERGY: 24.0 ft-lb

MLE: 19
% SHEAR: 31

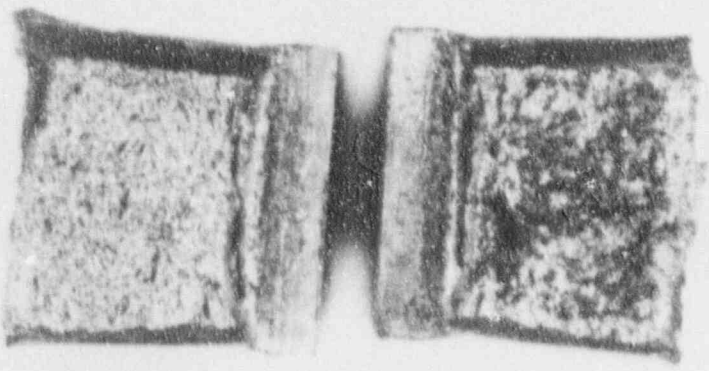

WELD: P2-26844
TEMP: −10°F
ENERGY: 38.0 ft-lb

MLE: 28
% SHEAR: 28

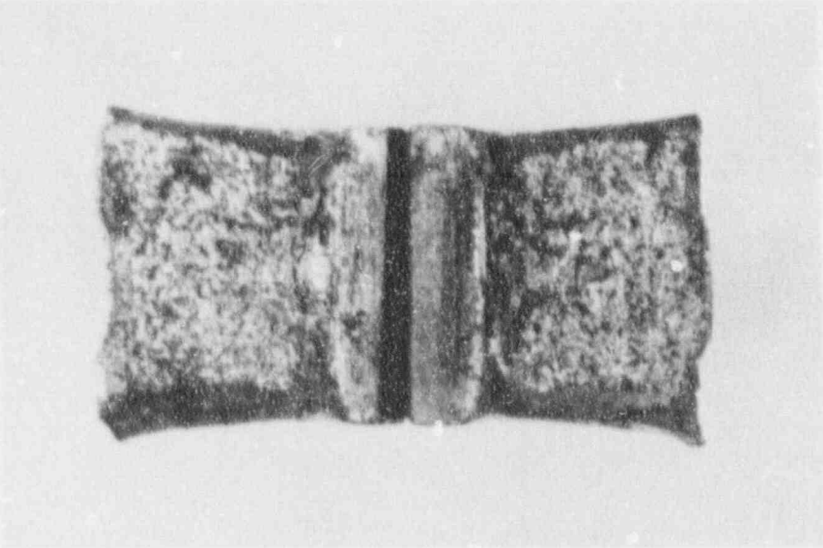

WELD: P2-26840
TEMP: 0°F
ENERGY: 61.0 ft-lb

MLE: 43
% SHEAR: 40

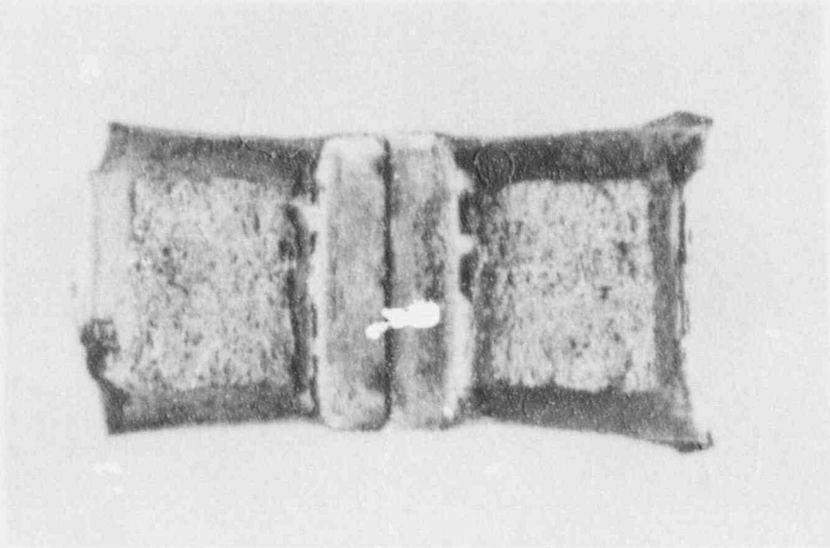

WELD: P2-26841
TEMP: 20°F
ENERGY: 62.5 ft-lb

MLE: 46
% SHEAR: 56

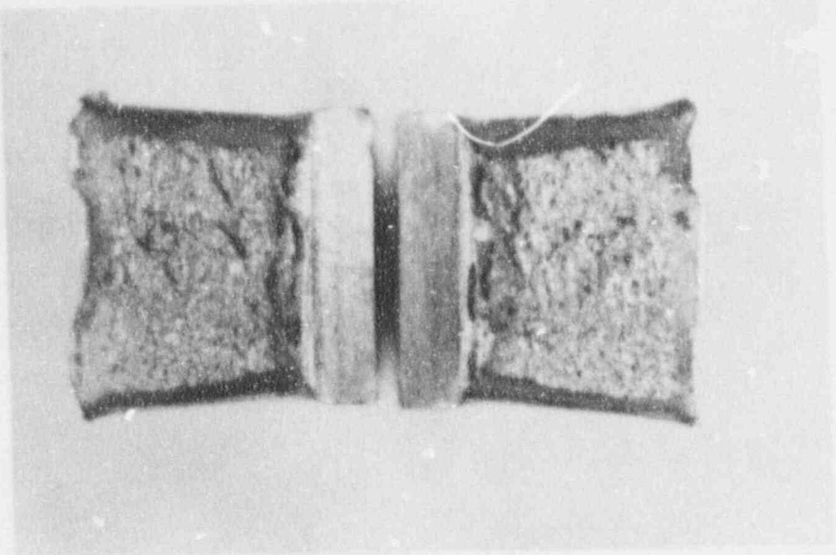

WELD: P2-26851
TEMP: 40°F
ENERGY: 50.5 ft-lb

MLE: 43
% SHEAR: 45

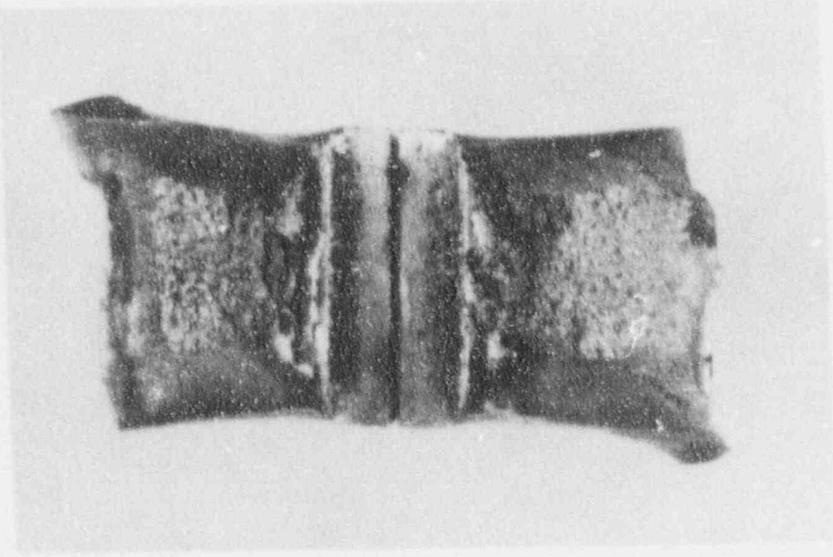

WELD: P2-26843
TEMP: 80°F
ENERGY: 101.0 ft-lb

MLE: 78
% SHEAR: 82

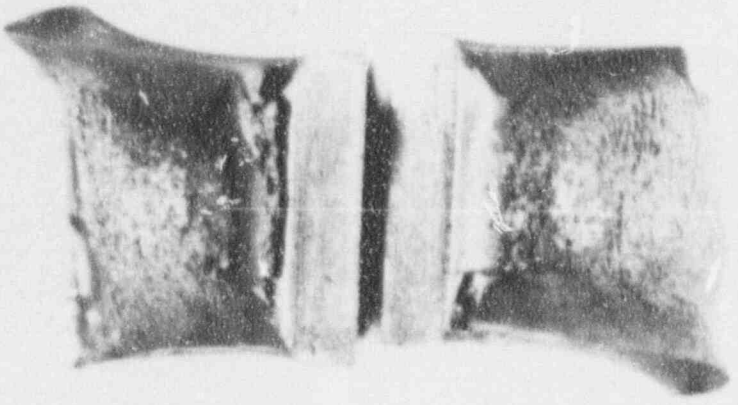

WELD: P2-26845
TEMP: 120°F
ENERGY: 122.5 ft-lb

MLE: 95
% SHEAR: 96

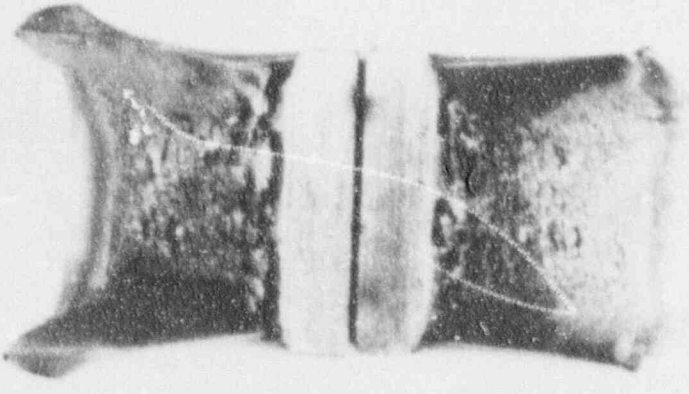

WELD: P2-26847
TEMP: 160°F
ENERGY: 111.0 ft-lb

MLE: 78
% SHEAR: 100

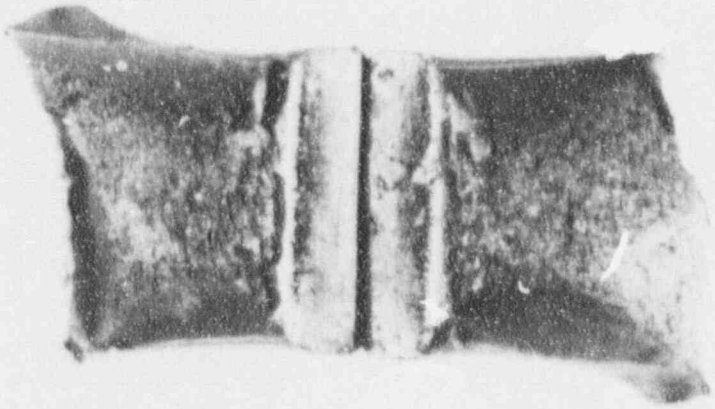

WELD: P2-26849
TEMP: 200°F
ENERGY: 126.0 ft-lb

MLE: 87
% SHEAR: 100

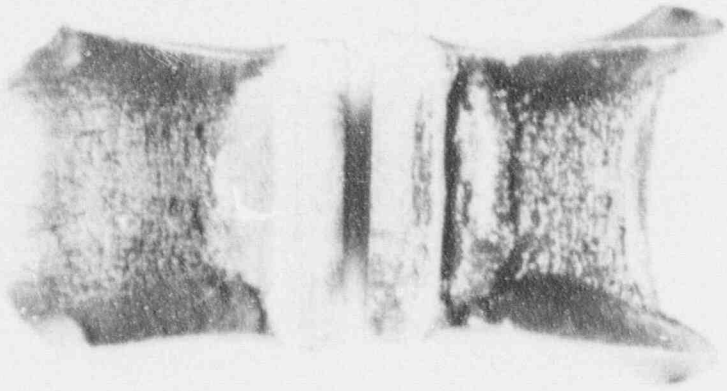

WELD: P2-26846
TEMP: 400°F
ENERGY: 117.0 ft-lb

MLE: 85
% SHEAR: 100

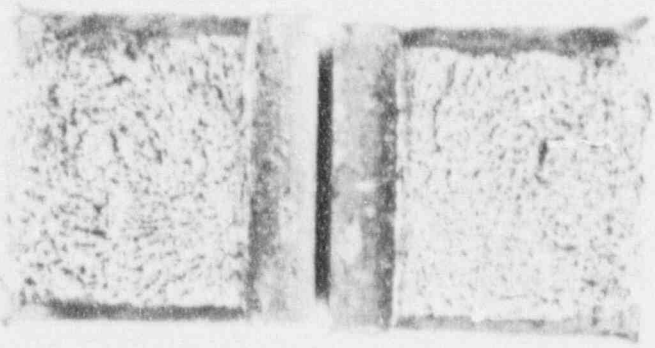

HAZ: P3-26860
TEMP: −60°F
ENERGY: 23.5 ft-lb

MLE: 17
% SHEAR: 21

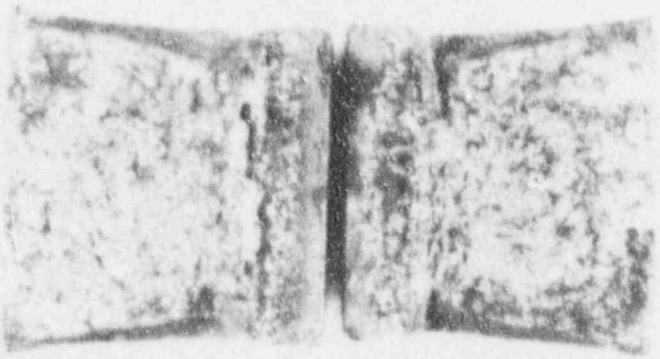

HAZ: P3-26862
TEMP: −60°F
ENERGY: 47.0 ft-lb

MLE: 31
% SHEAR: 27

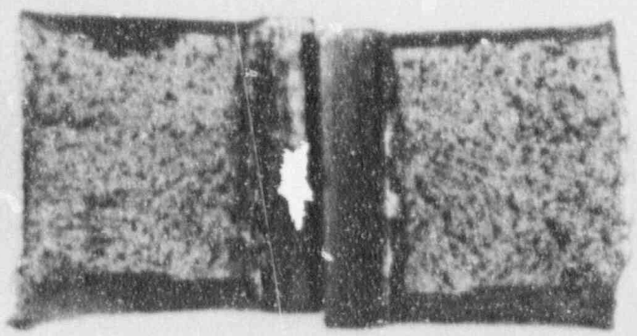

HAZ: P3-26855
TEMP: −40°F
ENERGY: 32.0 ft-lb

MLE: 23
% SHEAR: 26

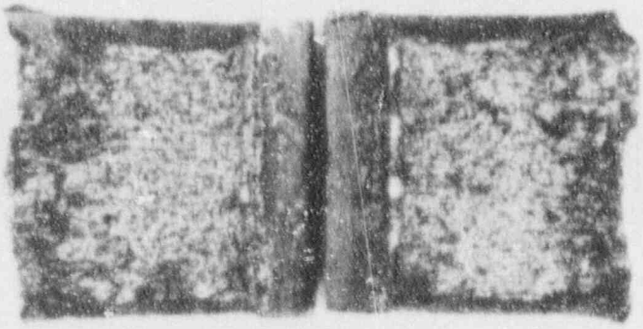

HAZ: P3-26861
TEMP: −20°F
ENERGY: 27.0 ft-lb

MLE: 22
% SHEAR: 24

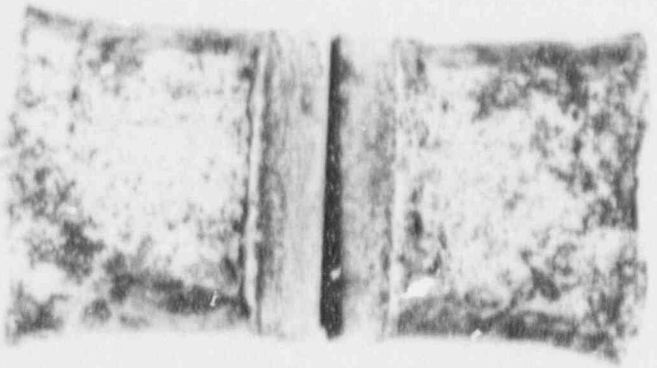

HAZ: P3-26854
TEMP: 0°F
ENERGY: 49.0 ft-lb

MLE: 34
% SHEAR: 57

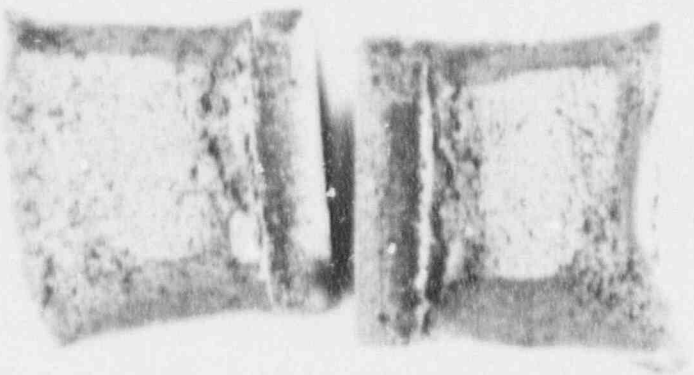

HAZ: P3-26853
TEMP: 20°F
ENERGY: 75.5 ft-lb

MLE: 54
% SHEAR: 62

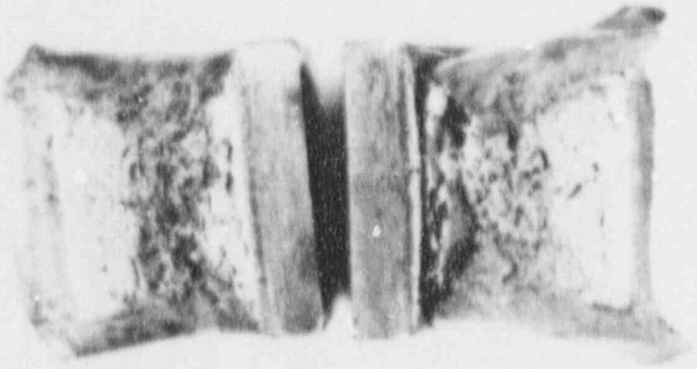

HAZ: P3-26859
TEMP: 40°F
ENERGY: 112.5 ft-lb

MLE: 73
% SHEAR: 73

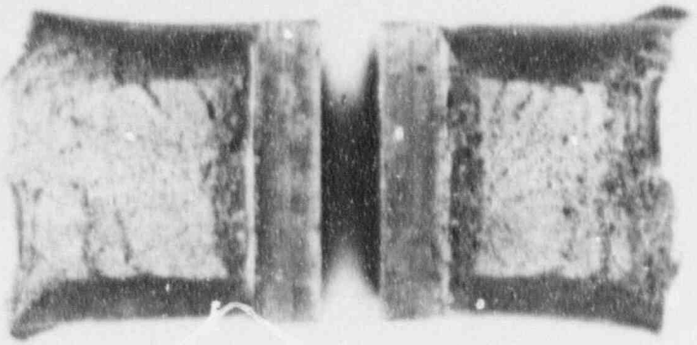

HAZ: P3-26863
TEMP: 80°F
ENERGY: 33.0 ft-lb

MLE: 48
% SHEAR: 65

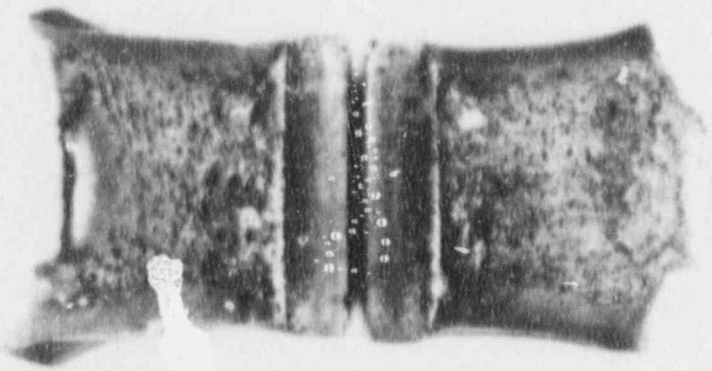

HAZ: P3-26856
TEMP: 120°F
ENERGY: 99.0 ft-lb

MLE: 68
% SHEAR: 100

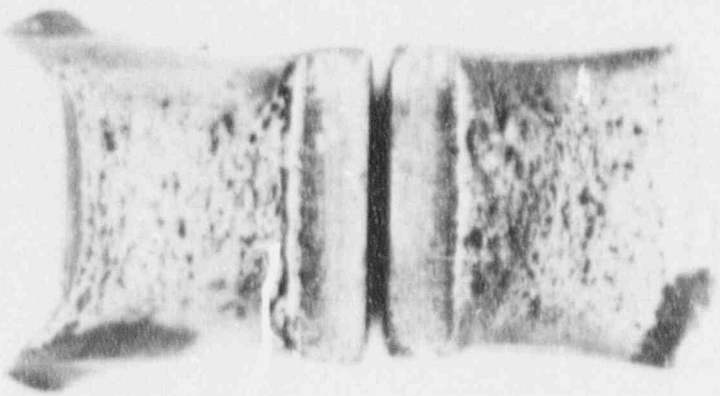

HAZ: P3-26852
TEMP: 160°F
ENERGY: 107.5 ft-lb

MLE: 74
% SHEAR: 100

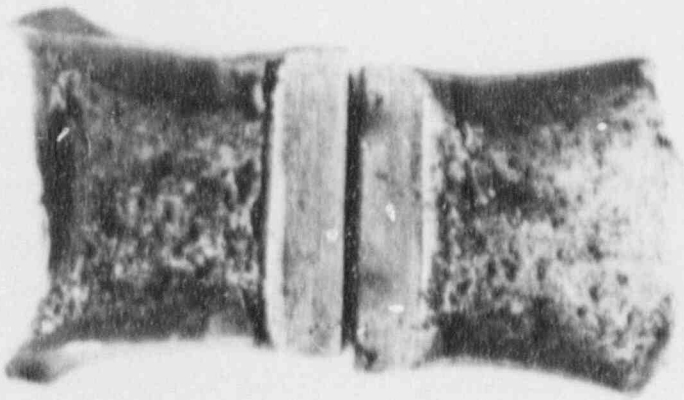

HAZ: P3 26857
TEMP: 200°F
ENERGY: 126.0 ft-lb

MLE: 80
% SHEAR: 100

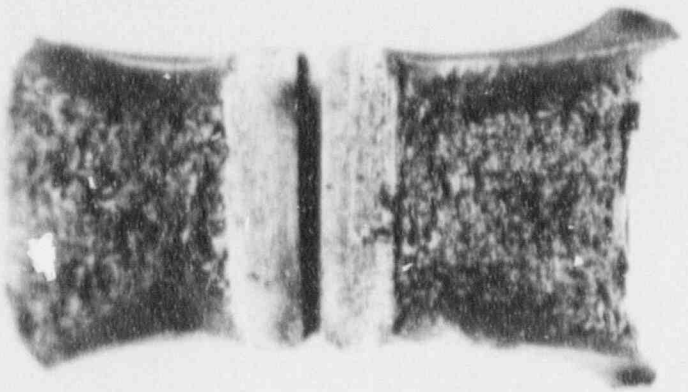

HAZ: P3 26858
TEMP: 400°F
ENERGY: 118.0 ft-lb

MLE: 85
% SHEAR: 100

APPENDIX B

BASIS FOR CONSERVATIVE RT_{NDT}

The values of initial RT_{NDT} used in this analysis were based on 30 ft-lb impact energy verification testing, with longitudinal Charpy specimens used for plate, as was standard practice at the time of vessel fabrication. The calculations of initial RT_{NDT} values in Section 3 are based on a GE procedure which establishes conservative values of RT_{NDT} from the fabrication test data. These RT_{NDT} values are expected to be conservative compared to results that would be obtained from current test methods.

For beltline materials, the methods of calculating adjusted RT_{NDT} in Rev 2 include a Margin term to be added to the calculated value, ΔRT_{NDT}. The Margin term includes a component for uncertainty in initial RT_{NDT}, σ_I. Rev 2 discusses determination of σ_I for two categories of initial RT_{NDT}, measured values and generic mean values. For generic mean values, σ_I is simply the standard deviation calculated for the data set used to compute the mean. For measured values, requirements for determination of σ_I are somewhat vague. Rev 2 states, "If a measured value of initial RT_{NDT} for the material in question is available, σ_I is to be estimated from the precision of the test method."[a] GE's position for RT_{NDT} values derived from measured data, as is the case for the Unit 2 beltline materials, is that σ_I is zero, as explained in the next paragraph.

---

[a] In the Rev 2 draft which was circulated <u>after</u> editing to incorporate public comments, the text stated, "σ_I, the standard deviation for the initial RT_{NDT}, may be taken as zero if a measured value of initial RT_{NDT} for the material in question is available."

The Charpy curves fit to surveillance data, which ultimately provided the ΔRT_{NDT} data for development of Rev 2, were best-estimate fits. An idealized example is provided as Curve 1 in Figure D-1. However, the ASME Code approach to determining RT_{NDT} is based on the lowest value of three specimens exceeding the required limits of impact energy and lateral expansion. A visualization of a Charpy curve drawn on the basis of the Code RT_{NDT} approach is shown as Curve 2 in Figure D-1. In comparing Curves 1 and 2, it is clear that Curve 2, which is based on the lowest value rather than the mean value, provides a conservative estimate of initial RT_{NDT}. Therefore, the current ASME Code method of determining RT_{NDT} from measured data is conservative. Since the method used in Section 3 to calculate RT_{NDT} values is conservative compared to current ASME methods, $\sigma_I = 0°F$ is appropriate.